AN ENGINEERING APPROXIMATION OF MATERIAL CHARACTERISTICS FOR INPUT TO HEAT, AIR AND MOISTURE TRANSPORT MODEL SIMULATIONS

Yu Huang

A Thesis

in

The Department

of

Building, Civil and Environmental Engineering

Presented in Partial Fulfillment of the Requirements
for the Degree of Master of Applied Science at
Concordia University
Montreal, Quebec, Canada

April 2003

Your file Votre référence
ISBN: 0-612-83858-7
Our file Notre référence
ISBN: 0-612-83858-7

ABSTRACT

An Engineering Approximation of Material Characteristics for Input to Heat, Air and Moisture Transport Model Simulations

Yu Huang

To avoid material damage and risk associated with mold growth or poor indoor air quality one needs to understand and predict moisture transport through building materials. While many heat, air and moisture (HAM) transport models have recently been developed, a state-of-the-art review shows that their application is limited by lack of the reliable material data. Towards this end, an alternative approach to material characterization, called an Engineering Model of material characteristics is examined in this thesis.

Series of moisture transport experiments were carried out on two building materials: aerated autoclaved concrete (AAC) and Portland cement plaster (exterior stucco). The experiments were to measure material characteristics, and to provide benchmark for the HAM model calculation. Furthermore, a ruggedness study was conducted on the factors that may have influence on the water absorption coefficient test.

This thesis introduces the concept of a platform with a minimum number of measured points for the input to heat, air and moisture transport models. From the current knowledge, HAM model requires the following material properties: material porosity, capillary saturation, liquid water diffusivity, water vapor permeability, and moisture

retention curve defined by two points on the sorption isotherm and two points in the over-hygroscopic region of the moisture retention curve. The proposed concept of engineering model was validated with an advanced HAM model, DELPHIN4, Grunewald (1997).

This thesis also presents results of parametric study conducted on the wetting and drying behavior of AAC, with respect to parameter variations and their interaction effects, including such parameters as capillary saturation, capillary liquid conductivity, water absorption coefficient, and moisture storage factor.

It was found even though the material structure of AAC and stucco are different, both can be approximated by the proposed material characteristics. This has been validated in HAM model simulations. Moreover, it was found that precisions of the Engineering Model can be improved by applying both the wetting and drying tests in the HAM model simulation.

ACKNOWLEDGMENTS

I would like to express my greatest gratitude to my supervisors **Dr. M. Bomberg** and **Dr. F. Haghighat** for their continuous and patient guidance, their constant support and encouragement in the course of this work, without which this thesis would not be finished.

My sincere appreciation and thanks are due to all the members of the Exterior Moisture Control research consortium for their financial support, including Canada Mortgage and Housing Corporation(CMHC), Du Pont Inc., Fortiber Corporation, Hal Industries, HPO – BC, DMO Associates, Louisiana Pacific Corporation and EJLB Foundation as well.

Special thanks are due to Dr. J. Grunewald for providing DELPHIN program; Dr.Qiu for providing his experimental data; and Mr. Heiko Fechner, Mr. Max Funk for their fruitful discussions on the model simulation.

I would also like to extend my appreciations to Dr. GQ Zhang, and Mrs. Xiaoxian He for their help on the way of my growth, and all those who have ever touched me deep in my heart.

Last, but not the least, I would like to give my deepest thanks to my parents, and my girlfriend Yi Huang, for their unconditional love, support, understanding and encouragement. I love them from the bottom of my heart.

TABLE OF CONTENTS

LIST OF FIGURES

CHAPTER 1

CHAPTER 2

CHAPTER 3

CHAPTER 4

CHAPTER 5

CHAPTER 6

APPENDIX B

APPENDIX C

LIST OF TABLES

CHAPTER 3

CHAPTER 4

CHAPTER 5

CHAPTER 6

APPENDIX A

APPENDIX B

APPENDIX C

NOMENCLATURE

English Letters

Aw	water absorption coefficient [$kg/m^2s^{0.5}$]
ce	specific heat capacity [J/kg K]
D	moisture diffusivity [m^2/s]
D_T	thermal moisture diffusivity [kg/m·s·K]
Dv	vapor diffusivity [m^2/s]
e	moisture storage factor
e_w	moisture storage factor determined by wetting
g	gravity acceleration [m/s^2]
H	height of the specimen [cm]
Js	surface inflow [kg/m^2]
K	moisture conductivity [s]
Kcap	capillary water conductivity [s]
KcSat	saturated liquid water conductivity [s]
K_L	liquid water conductivity [s]
Kr	relative liquid water conductivity [s]
M_{dry}	weight of the oven dry sample [g]
N	the number of test conducted
Opor	porosity [m^3/m^3]

P_C	capillary pressure [Pa]
Pv	partial vapor pressure [Pa]
Ps	saturated vapor pressure [Pa]
q	rate of moisture flow [$kg/m^2 \cdot s$]
Rv	gas constant for water vapor [461.5 J/K·kg]
RH	relative humidity [%]
S_A	surface area of the specimen [cm^2]
T	temperature [K]
t	t-value of a factor under evaluation
W	moisture content [kg/m^3]
Wcap	capillary moisture content [kg/m^3]
x	distance [m]

Greek symbols

μ	differential permeability [kg·m/Ns]
φ	relative humidity Pv/Ps [%]
ρw	water density [kg/m^3]
ρ	density of the specimen [kg/m^3]

Subscript

T	temperature
V	vapor

L	liquid

Glossary

AAC	aerated autoclaved concrete
MRC	moisture retention curve
pdf	phase dividing function
WVT	water vapor transmission

CHAPTER 1 INTRODUCTION

The rapidly changing building technologies, e.g., materials and interior building environment, have created higher expectations for the design of healthy and energy efficient buildings. In turn, this requires the use of computer based hygrothermal analysis tools, namely heat, air and moisture (HAM) transport models, to simulate and predict the performance of both the structural system and the service (HVAC) systems of a building.

1.1 Introduction to HAM modeling

The goal of using HAM models is the evaluation of the temperature and moisture conditions that might prevail across and within the building enclosure over time. The scope of the hygrothermal analysis can be identified as design, assessment, and research, of which the most important is to learn how to conduct a HAM analysis at design stage. Research is an extension of this basic need and because of the complexity of this purpose, more accurate and more complex mathematical models may be necessary.

Although the physics of moisture transport and moisture storage in construction materials are well understood, predicting moisture and temperature performance is never a straightforward task: It requires knowledge of geometry of the enclosure, boundary conditions, and material properties that are congruent with the thermodynamics used in the model. Material properties can exhibit wide variations depending on the information source, manufacturing technique used for a product and conditions during their

application. In turn, all these factors influence HAM model predictions. As we review later how the material characteristics are determined, this chapter will first describe physics of HAM modeling.

1.2 Review of HAM models

This review includes analysis of driving potential and material characteristics used in HAM models.

1.2.1 Driving potentials for moisture transport

There are a variety of variables used to describe the moisture driving potential. HAM models use partial vapor pressure, capillary pressure, or moisture content and temperature. One approach is to choose such a driving potential that can combine all flow mechanisms and produce one moisture diffusivity function. Another approach is to separate them into single flow e.g., separate the vapor diffusion from the liquid transport. Eq (1-1) illustrates the use of moisture content and temperature as driving potentials, while in Eq (1-2), capillary pressure and temperature are used to drive moisture flow (Bomberg 1973).

$$q = -(D\frac{\partial W}{\partial x} + D_T\frac{\partial T}{\partial x}) \tag{1-1}$$

$$q = -\left(K\frac{\partial P_C}{\partial x} + D_T\frac{\partial T}{\partial x}\right) \tag{1-2}$$

Where q = density of moisture flux (kg/m^2·s); x = distance (m);

W = moisture content (kg/m^3); D = moisture diffusivity (m^2/s);

P_C = capillary pressure (Pa); K = moisture conductivity (s);

T = temperature (K); D_T = thermal moisture diffusivity (kg/m·s·K)

As a driving potential, temperature is easy to measure. Temperature gradient, however, induces thermally driven vapour diffusion. While temperature is the only potential used for heat transfer, there is a great choice of possible potentials for moisture transport. Each possible potential has its advantages and disadvantages. Vapour pressure is easy to measure, however, the argument against it is that it drives only vapour phase, and hence is not typically used alone. The disadvantage of using moisture content, otherwise physically correct approach, is that it is discontinuous at material interfaces and hence it requires recalculating the moisture content into another driving potential at the boundaries between different layers, adding the need for knowing the relation between moisture content and the potential and thereby related mathematical calculations. Capillary pressure is likewise a continuous function, but it is not easy to measure, especially when the relative humidity exceeds 98%. Relative humidity does not actually drive liquid or vapour flow, hence it is not a driving potential, but may be considered for continuity conditions across the interfaces in the assembly, it has sometimes been applied as a tool for calculations of moisture redistribution within a porous material.

With proper transformation, one may use different potential description, because all of potentials can be recalculated to one another. However, the derivation of transport equations to fit into a model, using for example moisture content and temperature as potentials, entails among other problems of numerical errors and uncertainty of material characteristics. So, these descriptions of the moisture potential which are not primary

driving forces, or which are not continuous in a multi-layer building component are considered to be not appropriate. To facilitate the modeling task, the driving potentials should be widely known quantities, which are relatively easy to measure.

1.2.2 Moisture transfer mechanism and detailed HAM model review

Moisture can migrate in porous material either as vapor or liquid. The transport mechanism for vapor is molecular diffusion or effusion. The relevant driving force for vapor diffusion is the vapor pressure gradient. Conversely, liquid transport is induced by surface diffusion or capillary flow. Surface diffusion takes place in the absorbed water layer in the hygroscopic moisture range, whereas capillary flow becomes important when moisture content is high enough or when the material gets into contact with water. In both cases, the liquid driving force is capillary pressure, which in turn is related to relative humidity.

A state of the art review (Straube 2001) shows that Knudsen diffusion (effusion) is explicitly ignored by all HAM models used in building technology, because some models define lower limit of moisture content for the calculation. In this way the effect of the smallest pores is eliminated.

In most of the HAM models, liquid conductivity is included as a function of moisture content (Straube 2001). One model (WUFI) includes different functions for wetting and redistribution, although it may be possible to implement multiple sets of data for each material in the models, the accurate prediction requires defining regions of application for

these different material characteristics. The moisture content must be related to the suction curve to avoid the erroneous calculation of liquid flow in the over-hygroscopic region particularly when the moisture content is applied as a driving potential (Straube 2001).

For the accurate modeling of certain types of walls and some conditions, such as rain penetration, gravity-driven liquid flow may be also very important, because liquid water not instantaneously absorbed in the pores of capillary materials will cling to surfaces until gravity forces overcome the surface tension and the drainage flow initiates. This surface water can be modeled by assuming a surface material layer with certain moisture storage properties. Most of the models that include drainage assume perfect drainage after a certain amount of moisture is deposited on a surface.

In some of the most comprehensive models, convective vapour transport, i.e., air leakage, is accounted for. For some types of building, especially lightweight framed enclosure with incorrectly installed or low density insulation, the proper modeling of convective airflow and its effect on moisture transport is very important. However, accounting for mixed convection (i.e. involving both thermal and air flow effects) is even more difficult to model than diffusive and capillary moisture transport. The limitation lies in the following fact we need to model actual flaws in the "perfect" design (Straube 2001). Therefore, any model that does include air leakage effects must deal with the fact that the results are only as accurate as the estimate of these flaws in the control of airflow (air

barrier system). However, these models that do include air leakage component have been shown to be useful as research tools.

A Finite Difference Nodal Model developed by Cunningham (1990) took a simplified approach and used vapour pressure as the only driving potential, illustrated by Eq (1-3). Vapour diffusion and convection are assumed to be the only moisture transport mechanisms.

$$q = -D_V \frac{\partial P_V}{\partial x} \tag{1-3}$$

In this model, with knowledge of sorption isotherm, moisture content was coupled to vapour pressure, and a linearly vapour diffusion coefficient was used. The model was validated by simple lab tests (Cunningham 1994), and extensive in-service monitoring of wood-framed roof structures. However the scope of its application is limited to certain conditions in practice due to its extensive simplifications: on the one hand, the transport coefficient for vapour flow is never linear; on the other hand, it cannot deal with rain absorption, and situations where capillary active materials are above the critical moisture content, or where complex airflow is involved.

WALLDRY, a one-dimensional transient program (Schuyler *et al.* 1989), was initially used to model moisture transport in framed wall assemblies by decoupling heat, moisture, and airflow. Moisture transport is considered to be exclusively by vapor diffusion. Even though this model was valid in certain situations, it is unable to provide an accurate prediction of the drying process (Straube *et al.* 2001).

As a one dimensional hygrothermal model, MOIST (Burch 1997) takes into account both vapor diffusion and liquid flow, which is an advantage, compared with models that consider either vapor diffusion or liquid flow only. Moisture transport in this model is calculated as vapor flow driven by vapor pressure gradient and capillary flow driven by capillary pressure gradient. Vapor permeability and water conductivity are both given as functions of moisture content. The latent heat of phase changes is accounted for, as is the increased heat capacity provided by wet materials. The equation is shown as following:

$$q = -(D_V \frac{\partial P_V}{\partial x} + K_L \frac{\partial P_C}{\partial x} + D_T \frac{\partial T}{\partial x}) \tag{1-4}$$

The model has been validated with simple lab tests in the hygroscopic range (Burch 1995): the agreement between the calculation made by MOIST and measurement is good. However, the precision of model prediction depends on the number of nodes defined for each layer: MOIST allows only a number of equally spaced nodes in each layer. It loses accuracy at the interface between relatively thick and thin layers (Nofal *et al.* 2001).

Carsten Rode (1989) used both the sorption and water retention curves to define the moisture storage function in his one-dimensional model, MATCH. Sorption isotherm is used in the hygroscopic range, where there assumes vapor flow only. In the capillary range, the water retention curve is applied together with the hydraulic conductivity to model liquid flow. Some validation test has been carried out, but none of the work has involved driving rain absorption or similar natural exposure.

TRATMO (Transient Analysis Code for Thermal and Moisture Physical Behaviors of Constructions) developed by Kohonen (1984) used vapor pressure and temperature as driving potentials, which is illustrated by the following equation:

$$q = -(D\frac{\partial P_V}{\partial x} + D_T\frac{\partial T}{\partial x}) \tag{1-5}$$

In this model, liquid diffusivity and vapor permeability were constant, and surface diffusion was included as part of the vapor diffusion. However liquid diffusivity is highly dependent on the moisture content. The model is therefore restricted in its application.

WUFI (Germany), as well as WUFI ORNL/IBP (international version) is a windows-based program (Kuenzel, et al., 1997). The later one was jointly developed by Building Technology Center of Oak Ridge National Laboratory and Fraunhofer Institute for Building Physics. This one-dimensional transient hygrothermal model covers the whole range of relative humidity from oven dry to 100% RH. Both sorption isotherm and water retention curve are used in the model. It assumes that water vapor pressure and relative humidity are respectively the potentials of water vapor and liquid water transport. Important features of this model are its ability to incorporate driving rain deposition as part of the boundary conditions, and the use of different liquid diffusivities for wetting, and redistribution processes. However, there are a number of limitations in its scope of application: the model does not deal with air leakage and the associated heat and moisture flow; in addition, the assumption of constant water vapor resistance may not always be true (Straube 2001).

LATENITE, which was developed by Karagiozis and Salonvaara (1994), used a most complete moisture storage function. This model considers vapor and liquid transport separately, driven by vapor pressure and suction, respectively. Compared with other models, it takes into account the influence of airflow on the moisture transport. Vapor permeability and liquid diffusivity in this model are given as a function of moisture content. Surface diffusion is included in the liquid diffusivity, but it depends more on measurement technique. Airflow, gravity drainage, driving rain deposition, moisture sources (e.g., leaks), wind, and stack pressures can all be incorporated into a simulation of up to three dimensions if desired. Stochastic modeling can be used to assess the influence of inaccurate or variable material properties and boundary conditions. One, two, or three dimensions can be modeled, but only one- and two-dimensional calculation results have been presented.

Other HAM models such as TCCCD2 (Ojanen *et al.* 1989, Ojanen *et al.* 1994), FSEC (Keresteciogl u 1989), MOISTURE-EXPERT (Karagiozis 2001) and UMIDUS (Mendes *et al.* 1999, Mendes *et al.* 2001) are similar to one of the models reviewed.

1.3 Determination of material characteristics

The material properties required for hygrothermal analysis depends on the type of problem that needs to be solved and the analysis tool chosen to assist in the solution. There exist different models to describe moisture flow through porous building materials. Corresponding transport coefficients of each material that are used in the model vary from one to another. Even within the same specimens, the material properties may vary

significantly as a result of moisture condition, temperature condition, aging, as well as their chemical interactions with other materials. This initiates the need to review the manner in which material characteristics for HAM model input are generated.

1.3.1 Moisture retention curve

Moisture retention curve (MRC) shows the equilibrium moisture content in relation to the capillary suction P_C, at which this equilibrium was measured. Each moisture retention curve contains two fields: hygroscopic and over-hygroscopic fields of moisture content. The transition between the hygroscopic and over-hygroscopic fields is characterized by the limiting moisture content. Meanwhile, field of over-hygroscopic moisture content can be further divided into two ranges: unsaturated capillary flow and saturated capillary flow fields. (The amount of moisture that flows into the porous material is influenced by the entrapped air inside the specimen: the flow process reaches only a certain degree of saturation restricted by the limit of unsaturated capillary flow. Unless air is removed by means such as vacuuming or boiling, the rate of further ingress of water is very slow. Region above the unsaturated capillary flow is realised by external force, and has been defined as saturated capillary flow field.)

The hygroscopic field is described by sorption isotherm, which shows the relation between equilibrium moisture content and relative humidity at which this moisture equilibrium was measured. For the sorption isotherm measurements, the materials were placed in decissitor with various relative humidities inside, ranging from dry to 98% RH.

The equilibrium moisture content plotted versus relative humidity gives the sorption isotherm.

Measurement of sorption isotherm can cover the range from entirely dry to 98% RH. It is however difficult to precisely measure both relative humidity and corresponding equilibrium moisture content when the relative humidity exceeds 98%. To circumvent this dilemma, pressure plate apparatus has been applied in the over-hygroscopic field to measure water retention curve, the relationship established between equilibrium moisture content and the corresponding capillary pressure. Water retention curve is therefore a supplementary to sorption isotherm when relative humidity exceeds 98%. It can be converted into sorption isotherm by Kelvin's equation: $Pv = -\rho w \cdot T \cdot R_V \cdot \ln(\varphi)$.

A typical moisture retention curve, defined with the help of extreme wetting and drying MRC, is shown in Figure 1-1. Extreme wetting MRC is the process of free water intake started with oven dry material till it reaches capillary saturation. While extreme drying MRC starts the drainage and /or drying process with vacuum saturated samples (absolute saturation).

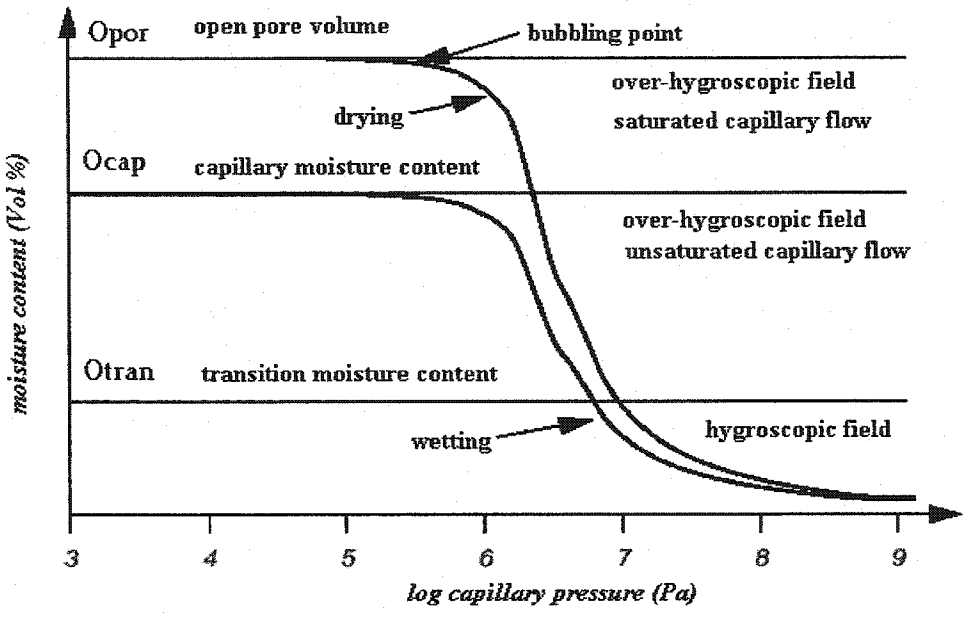

Figure 1-1. Definition of characteristic moisture storage parameters, Grunewald (2001)

1.3.2 Water vapor permeability

Water vapour permeability relates vapour diffusion flux to gradient of partial vapour pressure. Series of cup tests can be performed to determine the permeance of the material by measuring water vapour transmission through the specimen. These cup experiments are based on the ASTM test method 96-80 (ASTM, 1989). With knowledge of the specimen thickness, water vapour permeability can be calculated from permeance of the material.

However, the drawback of experimental determination of water vapor permeability is the difficulty to separate moisture transported as liquid from that transported as vapor. As a result, instead of water vapor permeability, some researchers proposed the use of average

moisture permeability, which combines vapor and liquid flows together. The term "average moisture permeability" $\overline{\mu}$ has been defined in such a way that it pertains to the varying humidity conditions along the moisture transmission pathway L. It is expressed as (Bednar 1999):

$$\overline{\mu} = \frac{1}{(\phi_2 - \phi_1)} \int_{\phi_1}^{\phi_2} \mu d\phi \qquad (1\text{-}6)$$

where ϕ_1, ϕ_2 is the relative humidity on both sides of the moisture transmission path. The prediction of average moisture permeability for any set of boundary conditions constitutes one of the central prerequisite for application of modeling techniques. It can be seen from Eq (1-6) that the average moisture permeability cannot be obtained directly, but it is possible to generate the function $\mu(\phi)$ from values of $\overline{\mu}$ measured from a series of cup test covering a wide relative humidity range. This property, even though it was called water vapor permeability, is not a true physical property, but is an apparent property that includes liquid phase contribution. Depending on the material and range of moisture content tested, different numerical relations have been used, e.g.

- $\mu = a + b\exp(c\phi)$ *Various researchers* (1990-1996)
- $\mu = \exp(a + b\phi)$ *Burch* (1996)
- $\mu = a + b\phi^C$ *Galbraith and McLean* (1992)
- $\mu = \exp(a + b\phi + c\phi^2)$ *Richard* (1996)

Non-linear regression technique can be used to provide curve fitting to determine parameters, such as a, b, and c for the average moisture permeability in the above proposed equations.

1.3.3 Liquid water diffusivity

Liquid transport exercises a particular influence on moisture behaviour. The amount of water it transports inside the building materials can be many times higher than that transported by diffusion. The correct determination of the transport coefficient for liquid flow is thus of great importance. Liquid diffusivity is however highly dependent on the moisture content, it cannot be measured directly. Researchers thus proposed different methods to determine the moisture diffusivity indirectly. Hensen (1993) estimated liquid diffusivity of aerated autoclaved concrete (AAC). In *Hensen's* approach, liquid diffusivity was determined from measurement of moisture content in a single point during water absorption process, and Boltzmann's transformation was used for calculation. This measurement of moisture content was made with Time Domain Reflectometry (TDR) equipment. Boltzmann transformation method used on transient moisture profiles measured with gamma ray or nuclear-magnetic resonance was also applied to determine the moisture diffusivity by Descamps (1997), NMR Gummerson et al. (1979), and Pel (1995). These methods are precise but time consuming and cost intensive. Martin, Andreas (1995) and some other researchers proposed approximation method for the liquid diffusivity of the wetting and drying process based on fundamental hygric parameters already known for most building materials or parameters from simple additional experiments, such as moisture absorption test and the drying behaviour

measurement. Listed below are mathematical models proposed for calculation of the liquid diffusivity:

- $D = a\left((b+1)\left(\frac{w}{w_{cap}}\right)^{\frac{1}{b}} - b\left(\frac{w}{w_{cap}}\right)^{\frac{2}{b}} \right)$ *Fechner* (1997)

- $D = 6.74 \cdot 10^{-3}\left(\frac{A}{w_{cap}}\right) e^{\frac{6.4}{w_{cap}} \cdot w}$ *Depraetere et al.* (1999)

- $D = 3.8 \cdot \left(\frac{A}{w_{cap}}\right)^2 \cdot 1000^{\frac{w}{w_{cap}} - 1}$ *Kunzel* (1995)

- $D = 10^{(a+b \cdot w)}$ *Bednar* (2000)

where A is water absorption coefficient; Wcap is capillary moisture content; w is moisture content; a, and b are parameters of the equations.

1.3.4 Water absorption coefficient

As discussed in the moisture retention curve, at the first stage of water inflow, air is in a continuous phase, and moisture flow is governed by the capillary force. At the secondary stage, however, air becomes discontinuous phase and further moisture inflow is prevented by the entrapped air inside the specimen. Therefore, the water intake process reaches only a certain degree of saturation. Unless air is removed by means such as solubility or diffusion, further ingress of water is stopped. The whole process of free water intake can therefore be divided into two stages. The first stage, which is governed by the capillary nature of the material, ends when the waterfront reaches the upper surface of the specimen. The secondary stage, typically involving a much lower rate of

water ingress is governed by the process of air and water redistribution within the specimen, and involves air dissolution or diffusion through the specimen, Bomberg, et al. (2001).

Capillary moisture content has been defined as the moisture content of the specimen at the transition from the first stage to the second stage during the 1-D character free water intake process. Capillary moisture content is usually measured together with the water absorption coefficient, namely A-coefficient, during the above mentioned one-dimensional free water intake process. A-coefficient has been defined as the slope of the first stage of the cumulative inflow curve into an oven-dry specimen, in relation to the square root of time. Figure 1-2 illustrates a typical water absorption process of red clay brick.

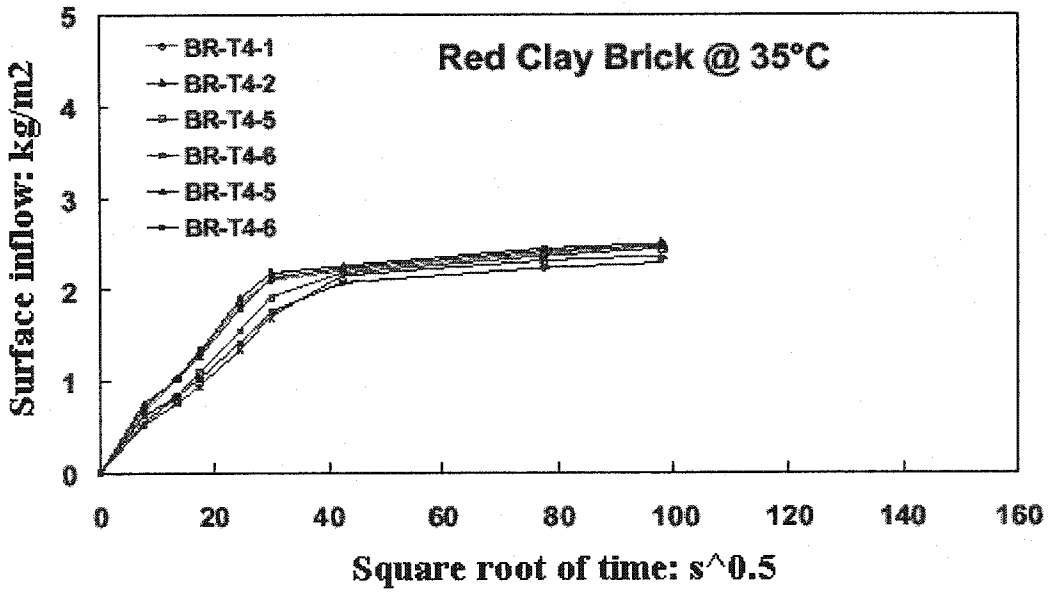

Figure 1-2. Water inflow curve of red clay brick (50 mm x 20 mm x 50 mm), Mukhopadhyaya, et al. (2002)

A-coefficient represents a combined material response to capillary force and resistance to unsaturated water flow. The proposed method depends on the assumption that the moisture front reaches the opposite side of the sample, the thickness of the sample has to be chosen in such a way that it is only a fraction of the maximum capillary height. There are still a number of problems associated with the present method. Descamps (1997) stated that conditions of air pressure on the free surface of the material would depend on the duration of the experiments and the length of the specimen. Furthermore, long experimental times will also increase the thickness of the boundary layer at the water ingress face. Finally, it was found that, for many materials, the A-coefficient, the slope of the cumulative moisture flux against the square root of time, changes with time. The question remains if one proposes the use of the initial slope or an average slope over 1-3 days of water imbibition process (Bomberg 2001). This necessitates research project dealing with following issues before consensus can be reached on how to determine A-coefficient precisely:

- To establish a relation between the water absorption coefficient and the moisture conductivity coefficient for a selected class of materials
- To establish the significance of factors affecting repeatability and reproducibility precision of a practical test method for determination of the water absorption coefficient.

1.3.5 Phase dividing function

There are interactions between liquid water and water vapour transport, as well as cross-linkage effects between heat and moisture transfer. Furthermore, there are interactions

between air and liquid flows as well as air and vapour flow. To circumvent some of these difficulties, transport coefficient is related to the thermodynamic potential of water and a phase dividing function is introduced by Grunewald (1997). It is defined as the liquid water flow divided by total moisture flow. Phase dividing function is therefore a ratio that changes with moisture content, starting at 0 and ending at 1. It's a continuously increasing function, with an S shape slope in between, for most materials. Figure 1-3 shows the phase dividing function of clay brick.

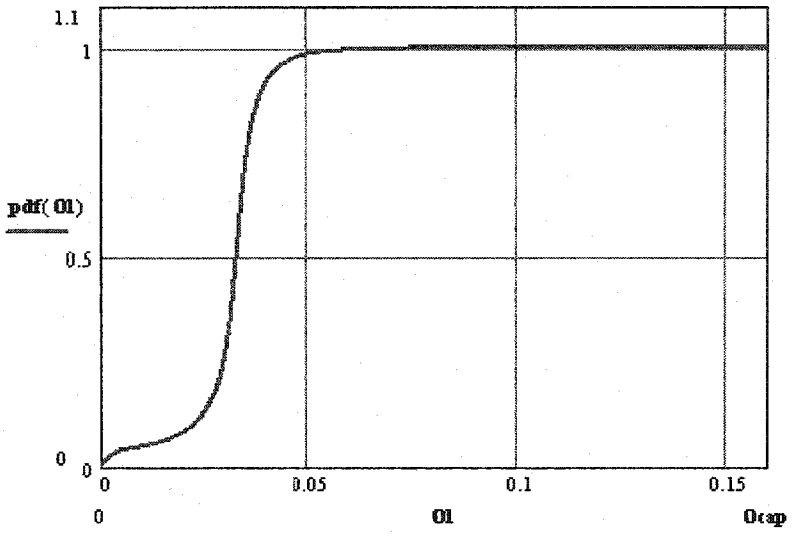

Figure 1-3. An example of phase dividing function calculated with Mathcad for a clay brick material, Grunewald (2001).

The phase dividing function can be used as one of the indicators for the goodness of a model. A local minimum or maximum in a phase dividing function indicates something wrong in the material model. Values below 0 or above 1 are never allowed, and indicate serious problems.

Determination of water vapour diffusion and liquid water transport coefficients can be realised by experimental methods. However, experimental methods do not allow a distinction between the different phase states of water. Therefore, the moisture flow is regarded either only as water vapour diffusion or only as liquid water advection, but this assumption is not valid for the unsaturated moisture range. Phase dividing function should thus be determined by non-isothermal moisture and energy transport experiments.

1.3.6 Bubbling point

The air bubble cannot pass through a fully saturated water field unless it has a pressure high enough to break all menisci that the air bubble would encounter on the way through the specimen as shown in Figure 1-1. The minimum air pressure required to pass air bubbles through such a specimen is defined as the bubbling pressure (Bomberg 2000). Capillary moisture content is known to be associated with the process of wetting of the material, the bubbling point is similar in concept, but determined when the drying process starts from vacuum saturation. It is the moisture content on the extreme drying moisture retention curve corresponding to the bubbling pressure. Bubbling point on the extreme drying curve would denote the moisture content, where air pressure is high enough to end region of saturated capillary conductivity and initiate the region of unsaturated moisture conductivity. In other words, it is equal to the maximum capillary moisture content.

Determination of the bubbling point is needed to define the upper limit in the preferential pore filling function. This function describes a pattern of pore filling under actual conditions of moisture flow into the control volume. As yet, with exception of soil

science, it appears to be no test method to measure moisture content in equilibrium at bubbling point.

1.4 Need to introduce Engineering Model of material characteristics

The state-of-the-art review indicates existing HAM models are restricted in their scope of application because of problems such as continuity across the interface of an assembly or the problem of hysteresis. But a more common and severe problem encountered is the determination of transport coefficients: on the one hand these transport coefficients are either over-simplified as constant or not clearly defined in each flow mechanism; on the other hand, experimental determination of these material properties requires highly developed laboratory and expertise, which is time-consuming and cost-intensive. Therefore, precisions of HAM model prediction are greatly influenced by the material properties used in the model, and their range of application selected.

Then how to select simulation tool among the existing HAM models? What properties are easy to determine in each of the model selected? Having taken all these factors into account, a paradigm can be developed to classify hygrothermal models into two levels. **Practical HAM models** use moisture content gradient as driving force, and in doing so utilises secondary moisture characteristics. **Research HAM models** are based on the water pressure gradient. At this level, primary transport coefficients are individually measured over the full range of moisture content.

For the practical HAM model, despite the fact that it is easy to use in the engineering practice, the need to analyse different forces driving moisture when assessing physical and mechanical effects, such as freeze-thaw resistance, shrinkage, and crack development, warrants the use of research HAM model. However, hygrothermal models at research level require a large effort to measure material characteristics and are difficult to handle for most practitioners. Research HAM model therefore serves only as a reference tool, and is not likely to become widely used by architects, civil engineers, and HVAC industry.

Practical HAM models are more likely to become tools for designers and manufactures of construction materials. For this to happen, however, both correct basis of physics and adequate consideration of material characteristics are necessary. Material characteristics must fulfil two requirements: describe well the moisture response of the material, and be congruent with the hygrothermal model. This initiates the need to introduce **Engineering Model of Material Characteristics.**

Hygrothermal material properties of Engineering Model allow an easy-to-handle generation of material functions that can be used by external groups and are based on the research level of modeling. Engineering model thus helps bridge practical and research HAM models. The introduction of material characteristics at such an engineering level can support transformation of scientific knowledge into practice, providing a higher degree of utility of HAM models. Only through the implementation of Engineering Model, material characteristics can well describe the moisture response of the material

and be congruent with the hygrothermal model. Engineering Model is therefore an assumption important for a fruit work together between research and practice in the field of building construction and building climatology.

1.5 Objective of the research

Despite a large number of existing HAM models, the lack of reliable material characteristic data, and the complexity of measurement techniques, prevented any model from being universally accepted. To better understand the moisture transfer mechanisms, to facilitate the use of moisture simulation tool, as well as to support technology transfer from research to practice, an engineering approximation of material characteristics based on the description of porosity is thereof proposed with the following objective:

- To establish a platform for HAM model input, with adequate material characterizations
- To reduce the number of measured points to a minimum and these measurements must be relatively easy to perform.
- To verify the HAM model simulation with experimental data from two building materials: stucco and AAC.

To satisfy the first objective of the thesis, we follow the approach developed by Haupl and Grunewald et al. (2001), where the material transport characteristics are derived from the pore size distribution. Yet while we use the same type of material characteristics as proposed by Grunewald et al (2003), we do not start from measurements of the porosity

but from the assumed minimum of 6 points on the moisture retention curve. The number and the choice of these points are explained later.

Furthermore, it is postulated that performing two simple benchmarking tests (wetting and drying) can be used to improve precision of the estimated MRC curve. These two hypotheses will be verified with the HAM model simulation using experimental data determined in this thesis and Qiu (2002). Two construction materials selected for this purpose were: Portland cement plaster (exterior stucco) and aerated autoclaved concrete (AAC).

1.6 Thesis organization

The thesis consists of the collection of quantitative data for the evaluation of Engineering Model. Since during the literature review it was found that the precision of determination of the water absorption coefficient is questionable, in addition to the verification of the assumed hypothesis, experimental evaluation (ruggedness test) was performed on factors that may influence the measurement of water absorption coefficient. Parametric studies were also carried out to analyze the initial input parameters that may have impact on the precisions of HAM model predictions. The thesis is organized as follow:

Part 1. State-of-the-art review

Chapter 1 reviews the fundamentals of heat and moisture transport through porous building materials, the material characteristics that are used in the hygrothermal models, and postulates the need for Engineering Model of material characteristics.

Chapter 2 presents the formulation of Engineering Model for calculations of material characteristics.

Part 2. Experimental study

Chapter 3 presents the experimental results used to characterize material properties for model control.

Chapter 4 presents a ruggedness study on the factors that may have influence on the water absorption coefficient test.

Part 3. Numerical calculation and parametric study

Chapter 5 presents HAM model predictions with input from Engineering Model, and compare them with benchmark test.

Chapter 6 presents a parametric study on the input parameter to the HAM model, and discusses how the input is controlled for a precise model prediction.

Part 4. Summary and conclusions

Chapter 7 summarises the finding of the present study and makes suggestions for the future work.

CHAPTER 2 ENGINEERING MODEL FOR MATERIAL CHARACTERIZATION

This chapter is to provide a background necessary for formulating research on improved methods of material characterization proposed by Grunewald, et al., (2001) for use in heat, air, and moisture (HAM) transfer models.

2.1 Introduction

HAM models are available with a high degree of user-friendliness. Yet the main difficulties preventing a broader use of these simulation tools are insufficiency of hygrothermal material characterization for the majority of building materials. The determination of hygric material functions at the fundamental level is, however, time-consuming and requires highly developed building material laboratory and specialists. This initiates the need to introduce an engineering level material characterization for input into HAM model simulation.

By referring to the fundamental level of material characterization, it means free use of any mathematical method or function to describe the material properties within the required accuracy. In this way, fundamental level material characterization allows an "individual description" of material properties: different models can be alternatively used to express the dependence of a property on a state variable, such as moisture content, temperature or capillary pressure etc. However, material characterization at engineering level means describing the hygrothermal material properties by a minimum number of

input information, which requires the use of only one set of material functions for all materials, and the materials are characterized by their parameters: only the parameters differ from material to material, while the functions to describe the materials remain the same. The hygrothermal material functions generated from the input parameters take into account the inter-relation between moisture storage and moisture transport, and the relation between liquid water and water vapor transport as well.

A transformation rule can be established between the engineering level and fundamental level of material characterization so that materials available at the fundamental level are also available at the engineering level at the same time. The introduction of such an engineering level material characterization therefore helps link research and practice in the field of building construction and building climatology, and thereof, allows the transformation of scientific knowledge into building practice.

At the fundamental level, different analytical expressions can be used to describe the same property of different materials. This requires the model to support a set of analytical functions for each single material property so that users can choose the most suitable one when evaluating the measurement. The most difficult part of hygrothermal material characterization is the modelling of moisture storage and transport. Different from fundamental levels, engineering level material characterization has predetermined type of MRC, and the following hygrothermal material properties are needed:

1. Material parameters

- Open porosity
- Density (volume divided by oven dry mass)
- Specific heat capacity (of the dry material)
- Capillary moisture content

2. Material functions
   - Moisture retention curve (MRC) under extreme wetting and drying loops (MRC describes the storage of moisture under specified conditions of moisture flow)
   - Phase dividing function (the ratio of liquid water flux to the total moisture flux)
   - Liquid water diffusivity (describes a transient flow in the liquid phase)
   - Water vapour permeability (describes a vapour flow caused by a vapour pressure gradient)

2.2 Engineering Model for material characterization

2.2.1 Assumptions for engineering level material characterization

Different from material characterization at fundamental level, the engineering level model makes the material characterization easier but provides not the same degree of accuracy like the fundamental level, and a loss of potential accuracy can be expected. The basic criteria for material modelling at the engineering level are:

- Material characterization based on thermodynamics
- Reduction of the required input to HAM models to a minimum
- Overall goodness of fit for the description of required material functions
- Easy-to-measure input parameters for practitioners

To meet the criteria mentioned above, material characteristics at the engineering level should be restricted to the following two requirements:

- Describe well the moisture response of the material
- Be congruent with the model simulation.

Assumptions (Grunewald 2002) were then made for the engineering level material characterization:

- Engineering model is related to material structure: it assumes that the characteristic moisture contents are determined by the peak position in the pore size distribution curve (see Figure 2-1 for peak position).
- Engineering model has a pre-determined type of hygrothermal material function: in this case the Gauss probability distribution is used to describe porosity distribution.
- Engineering model includes the following simplifications
    1) Assume that WVT (water vapour transmission) at low end is that of dry cup measured at 25% RH.
    2) Assume that the maximum WVT is at the point of transition moisture content: Otran (see Figure 1-1 for transition moisture content)
    3) Assume a specific type of function for WVT that is calculated from parallel flow/serial flow considerations. (Grunewald 2002)
    4) Assume that total moisture conductivity is defined by saturated Darcy flow (at vacuum saturation).

5) Assume that the storage component (relation between diffusivity and conductivity) is uniquely based on the derivative of the moisture retention curves. (Grunewald 2002)
6) Assume that the character of the change in the total moisture conductivity is represented by a specific model of porosity.

A brief explanation of some nomenclatures used in the assumption is given below:
Parallel flow means vapour diffusion and liquid flow happens simultaneously during the whole range of MRC; series flow means the vapour diffusion and liquid flow are separate from each other: each flow takes place in different ranges of MRC and they do not interact with each other; storage component refers to moisture storage factor expressed as a ratio of moisture conductivity to liquid diffusivity.

2.2.2 Implementation of the Engineering Model

In this section, a case study on clay brick (Grunewald 2001) is shown to help understand the application of Engineering Model for material characterization, and how these points are chosen. Material characteristics from calculation could then be used as input to HAM model simulations.

Implementation of the Engineering Model starts with definitions of some general parameters. Iso-barometric conditions are assumed, vapour diffusion constant is calculated at the given reference temperature, and transformations between transport coefficients are done at constant temperature as well.

General parameters:

Density of water (kg/m^3)	$\rho w = 1000$
Water vapour gas constant (J/kg K)	$R_v = 462$
Reference temperature (K)	$T = 293.15$
Gravity constant (m/s^2)	$g = 9.81$
Reference saturation pressure of vapour (Pa)	$ps = 2338$
Vapour diffusion constant in air (m^2/s)	$D(T) = 2.3 \cdot 10^{-5} \cdot \left(\frac{T}{273.15}\right)^{1.81}$

General material parameters for clay brick:

Density (kg/m^3)	$rho = 2350$
Specific heat capacity (J/kg K)	$ce = 1050$
Porosity (m^3/m^3)	$Opor = 0.2$
Capillary moisture content (m^3/m^3)	$Ocap = 0.16$

The pore volume distribution is the starting point of construction of the Engineering Model. A normal distribution of the pore volume as function of logarithmic capillary pressure is assumed: Equation (2-1) gives the pore volume distribution of the Engineering Model (Grunewald 2001).

$$\frac{dOl(pC)}{dpC} = \sum_{i=0}^{N-1} \frac{O_i}{S_i \cdot \max pC\sqrt{2\pi}} \cdot \exp\left[\frac{-(pC - PC_i)^2}{2(S_i)^2 \cdot \max pC^2}\right] \qquad (2\text{-}1)$$

where N is modality (modality is determined by pore structure measurement, and it is the number of peaks in the pore size distribution curve); pC is defined as logarithmic positive capillary pressure; S is the standard derivation of the peaks; Ol is moisture content; O_i is characteristic moisture content.

Modality, the characteristic pC-value and their corresponding partial pore volumes are the minimum input information; standard derivation of the peaks is the additional input information: they are additional parameters of the curve, which can be determined when more measured points are available (Grunewald 2001).

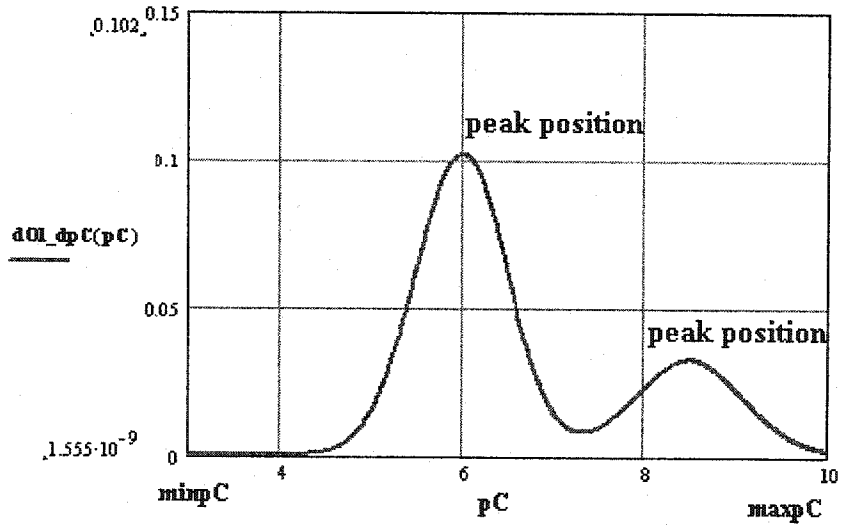

Figure 2-1. Pore size distribution curve of clay brick (the value of modality is 2) (Grunewald 2001)

Moisture retention curve can be obtained by numerical integration of Equation (2-1). Results of sorption curve and water retention curve are given in Figures 2-3 and 2-3.

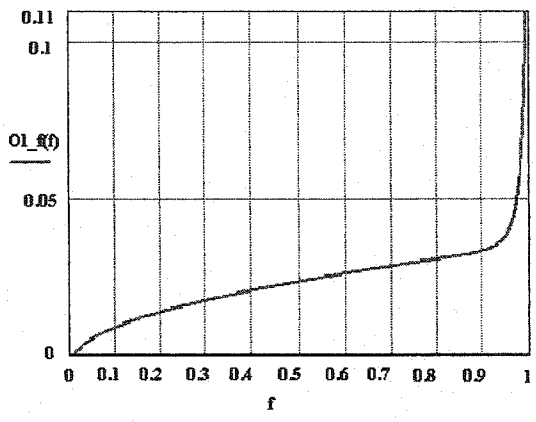

Figure 2-2 Sorption curve of clay brick

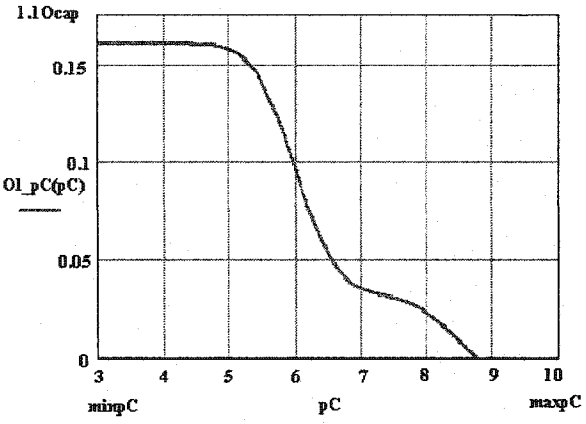

Figure 2-3 Water retention curve of clay brick

Introducing the pressure height $h = pC/(g \cdot \rho w)$, reverse functions for the water retention curve and sorption isotherm can be determined from Figure 2-2 and 2-3. Results are shown in Figure 2-4 and Figure 2-5.

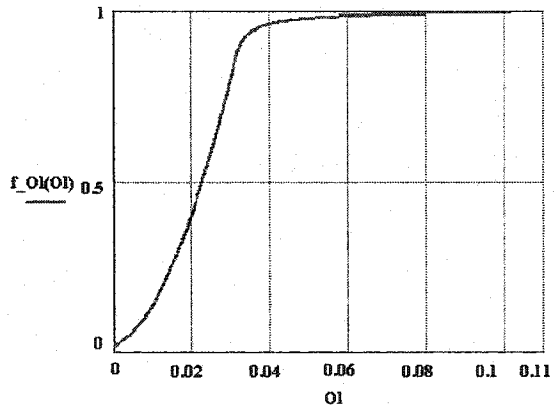

Figure 2-4. Reverse sorption curve

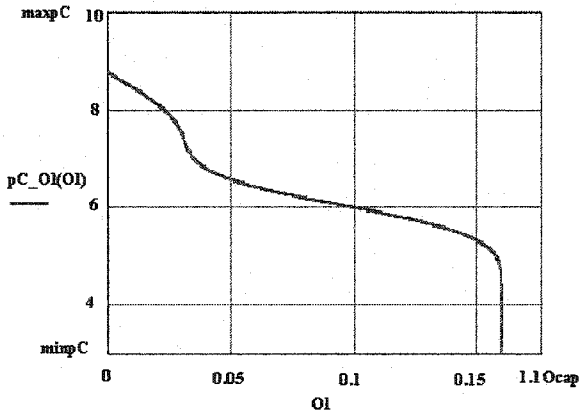

Figure 2-5. Reverse water retention curve

Numerical integration of reverse pressure height as a function of moisture content: h (Ol) gives liquid water conductivity Kc(Ol), which is illustrated by:

$$Kc(Ol) = \int_0^{Ol} \left(\frac{1}{h(Ol)} \right)^2 dOl \qquad (2\text{-}2)$$

Saturated liquid water conductivity: $KcSat = Kc(Ocap)$ $KcSat = 1 \cdot 10^{-10}$ (s)

Absolute liquid water conductivity can be related to its saturation value, and generate only a relative conductivity function (Grunewald 2001), it is expressed by the following equation:

$$Kr(Ol) = \frac{Kc(Ol)}{KcSat} \tag{2-2}$$

$$Kl(Ol) = Kr(Ol) \cdot KcSat \tag{2-3}$$

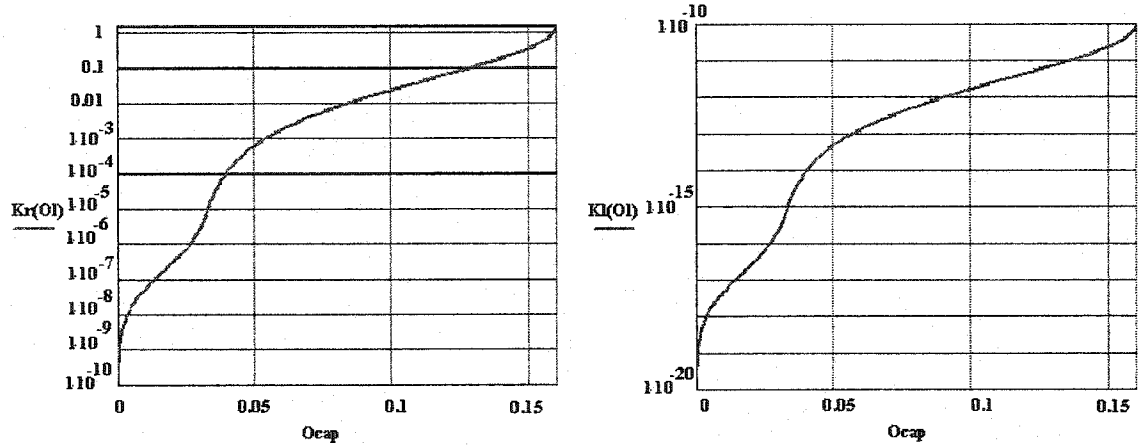

Figure 2-6. Relative liquid water conductivity and absolute liquid water conductivity of clay brick (Grunewald 2001)

Water vapour permeability is the next material function to be determined. It relates a vapour diffusion flux to a vapour pressure gradient. The parameters of the vapour permeability are the vapour diffusion resistance factor at low relative humidity (myDry=dry cup value) and the transition moisture content: Otran. The transition moisture content determines the maximum point of vapour permeability that matches the maximum value of the derivative of the phase dividing function. A functional approach of the vapour permeability is given by Eq (2-4), and its graph is shown in Figure 2-7.

Assuming a homogeneous and isotropic porous medium, Eq (2-4) can be derived by taking into account mixed parallel and serial transport of liquid water and water vapour. Parameter P is the volume fraction in which parallel transport dominates. Serial transport takes place in the volume fraction 1-P. This approach divides the vapour permeability into two regions.

$$D_v(Ol) = \frac{D(T)}{myDry} \cdot \frac{1 - \frac{Ol}{Ocap}}{(1-P)\cdot(1-\frac{Ol}{Ocap})^2 + P} \tag{2-4}$$

where myDry=5; Otran=0.04. The transition moisture content determines the maximum point of vapour permeability that matches the maximum value of the first derivative of the phase dividing function.

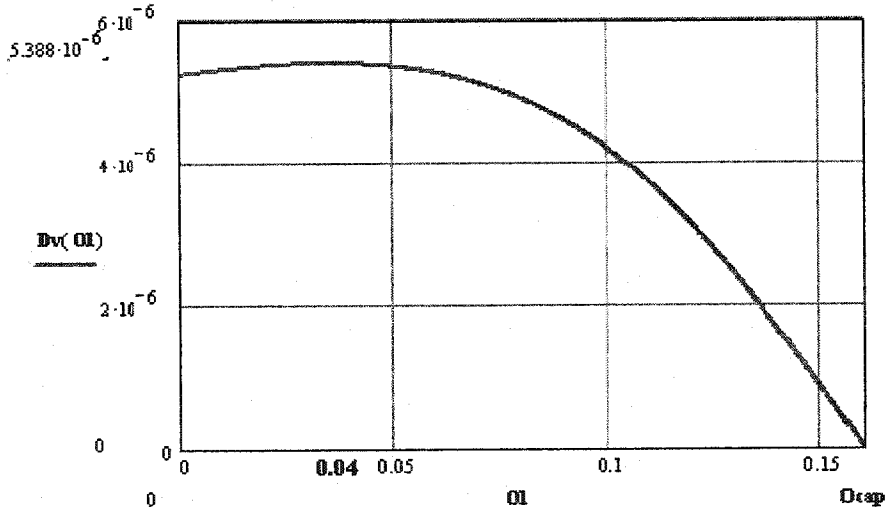

Figure 2-7. Water vapour permeability of clay brick (Grunewald 2001)

With knowledge of liquid water conductivity Kl(Ol) and water vapour permeability Dv(Ol) from previous calculation, one can calculate two moisture conductivities: the hygroscopic moisture conductivity Kh(Ol) and capillary moisture conductivity Kc(Ol).

The relation between hygroscopic and capillary moisture conductivity is the reverse relation between vapour and capillary pressure gradients: the density ratio of liquid water to water vapour. The density of vapour in the gaseous phase has been defined as function of relative humidity at reference temperature. Hygroscopic moisture conductivity at the dry end of MRC (*Khdry*) and that at the capillary saturation (*Khsat*) are introduced. These two variables can be calculated from input parameters, and are used to define the hygroscopic and capillary moisture conductivity, Kh(Ol) and Kc(Ol) respectively.

Dry hygroscopic moisture conductivity: $$Khdry = \frac{D(T)}{myDry \cdot Rv \cdot T}$$

Saturated hygroscopic moisture conductivity: $$Khsat = \frac{\rho w}{\rho v} \cdot KcSat$$

With the general parameters of both water and clay bricks defined at the beginning, Khdry and Khsat can be calculated, and their values are given below:

$Khdry = 3.86 \cdot 10^{-11}$ (s); $Khsat = 5.793 \cdot 10^{-6}$ (s)

$$Kh(Ol) = Kr(Ol) \cdot (Khsat - Khdry) + Khdry \tag{2-5}$$

$$Kc(Ol) = Kl(Ol) + \frac{D_v(Ol)}{R_v \cdot T} \frac{\rho v(f(Ol))}{\rho w} \tag{2-6}$$

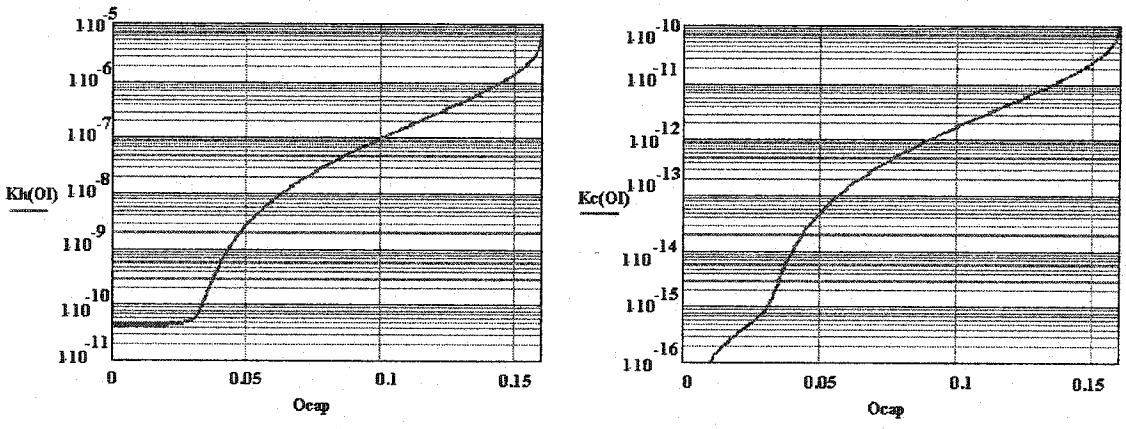

Figure 2-8. Hygroscopic moisture conductivity and capillary moisture conductivity

The liquid water flux divided by total moisture flux is a ratio that changes with moisture content. It can be introduced as phase dividing function according to Eq (2-7). (Grunewald 2001). It starts at 0 and ends at 1. In between is a continuously increasing function, with an S shape slope for most materials. The phase dividing function can be used as one of the indicators for goodness of a model. The graph for phase dividing function is given in Figure 2-9.

$$pdf(Ol) = \frac{Kl(Ol)}{Kc(Ol)} \tag{2-7}$$

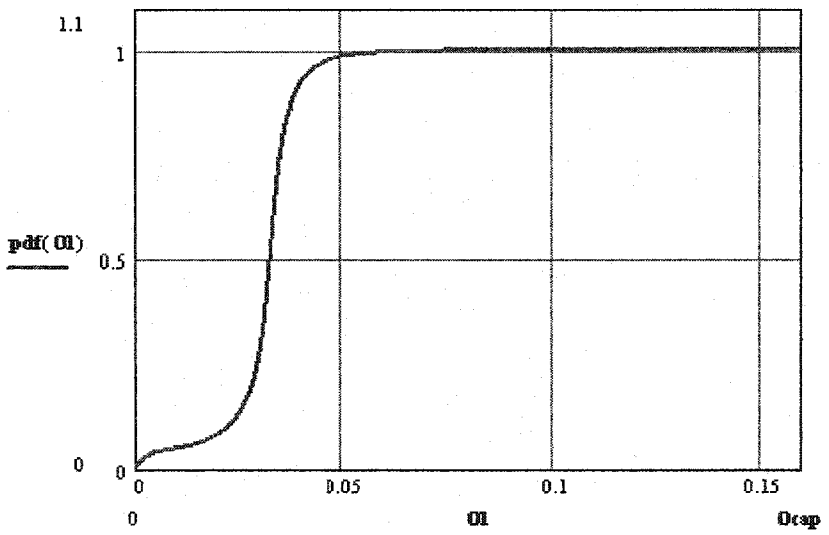

Figure 2-9. Phase dividing function of clay brick (Grunewald 2001)

The first derivative of the phase dividing function can be used to identify the point of maximum changing rate of the liquid water flux/total moisture flux ratio. This point indicates the transition from moisture flow dominated by water vapour transport to moisture flow dominated by liquid water transport. The derivative of the phase dividing function is given by Eq (2-8), and shown in Figure 2-10.

$$\frac{dpdf(Ol)}{dOl} = \frac{\frac{d}{dOl}Kl(Ol)}{Kc(Ol)} - \frac{Kl(Ol)}{Kc(Ol)^2}\frac{d}{dOl}Kc(Ol) \tag{2-8}$$

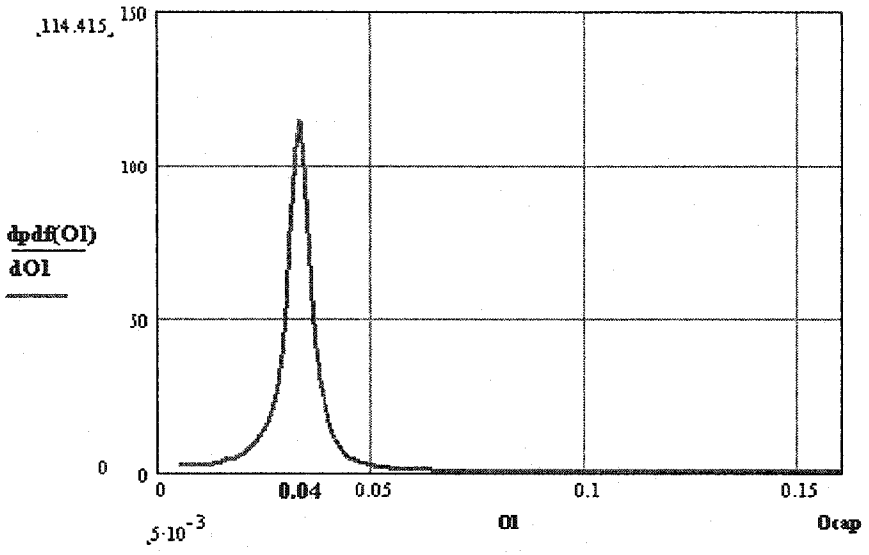

Figure 2-10. Derivative of phase dividing function of clay brick (Grunewald 2001)

The transition moisture content can be identified (4 Vol%) at the peak position of the derivative of phase dividing function. This is the same value as given for the parameter of the vapour permeability as shown in Figure 2-7. A change of this parameter (transition moisture content) would influence the location of the maximum in the curve shown in Figure 2-10 slightly. The transition moisture content can be determined in 2 or 3 iterations with a reasonable initial guess.

2.2.3 Discussions on input to HAM model

Grunewald (2000-2002) and Haupl (2001) highlighted that the most correct approach to material characteristics should be based on material structure, and pore size distribution is important to define material response to moisture flow. According to Haupl and

Grunewald et al. (2001), for an N-modality material, 3N parameters have to be known. While minimum input information is required to determine MRC, additional points can be used to optimize MRC.

In the present study, two peaks are assumed. This postulates 6 points to define the MRC, including a point at 25%RH (for the dry end), 2 points from hygroscopic range, 2 points from over-hygroscopic range, and a bubbling point. Also required are transport coefficients at both ends of the MRC. They are water vapour permeability (D_L) at 25% RH and liquid water conductivity at the bubbling point (Kcap). In this way, the input to HAM model simulation requires knowledge of two transport coefficients and 6-point-defined MRC. Since the two transport coefficients are at both ends of MRC, which coincides with the two extreme points used to define the MRC, the total number of input is therefore reduced to 6. In brief, the following parameters are selected for input to HAM model:

- Equilibrium moisture content and water vapor permeability (D_L) at 25%RH
- Equilibrium moisture content and liquid water conductivity (Kcap) at capillary saturation
- Equilibrium moisture content at bubbling point
- 2 points from sorption isotherm and 2 points from over-hygroscopic range

Material characterization at the engineering level should be validated for practical purposes. Towards this end, Delphin4, an advanced HAM model developed by Grunewald (1997), will be used to provide a platform for input of engineering level material characterization. This HAM model is to be benchmarked by comparing the

results from simulation with that from measurements: wetting and drying behaviour of two commonly used building materials-- AAC and stucco. This benchmark serves two purposes: check the material characteristics used in the HAM model as well as a check of the scope of HAM model application. Therefore, analysis of proposed material characterization, model benchmarking and the manner in which material characteristics are introduced into DELPHIN, constitutes the core of the present study.

2.3 Conclusions

At the fundamental level, the hygrothermal material characterization of porous building materials for input to HAM model simulation is generally not available now. To determine respective material functions requires highly developed building physical laboratories for selected materials. Therefore, modelling the material characterization at the fundamental level serves only the research purposes, and is not likely to become widely used in practice.

To support technology transfer from research to practice, material characterization at engineering level has been introduced (Grunewald 2001). Based on thermodynamics, the respective Engineering Model is backed by the fundamental material modelling. Through the Engineering Model of material characteristics, the required input to HAM models has been reduced to a minimum (standard parameters only), and a reasonable description of required material functions is given. Additional information (more measured points) can be used to improve the goodness of fit for the material characterization.

CHAPTER 3 EXPERIMENTAL DETERMINATION OF THE MATERIAL PROPERTIES

3.1 Re-calculation of A-coefficient into the liquid diffusivity

3.1.1 General

A literature survey lists different methods to determine liquid diffusivity from measurement of moisture content profile (Janz, 2000). There are as many as 10 different methods of measuring moisture content, including slice-dry-weigh-method, neutron radiography, gamma-ray attenuation, nuclear magnetic resonance etc. The majority of these methods to determine the liquid diffusivity are based on the calculation from the moisture profile measured at various times after start of water uptake or start of moisture redistribution. Two of the most commonly used calculation methods are the Boltzmann transformation method, and the profile method. These experimental methods involving the use of expensive testing facilities are generally unavailable to engineers. They are also time-consuming and complicated in operation. Hence, methods to calculate liquid diffusivity based on simple moisture properties are proposed: it has been suggested that water absorption coefficient together with capillary saturation moisture content can be used to calculate a constant liquid diffusivity (Krus and Kunzel, 1993; de Wit and van Schindel, 1993).

In this chapter, water absorption coefficient of two commonly used building materials, i.e., stucco and AAC, were measured from a series of absorption tests. The constant liquid diffusivity value is determined from the water absorption coefficient as described in the following section. Liquid diffusivity will also be determined in the present study as

a function of the moisture content of the specimens. The value of liquid diffusivity obtained from the calculations and that from the experiment will be used as input to HAM model for a comparative study. The comparison will be addressed in details in Chapter 5.

3.1.2 Test method for capillary moisture content

Capillary moisture content is usually measured together with the water absorption coefficient from the one-dimensional free water uptake experiment. It has been defined as the moisture content of the specimen at the transition from the primary stage to the secondary stage during the 1-D character free water uptake process. To ensure the 1-D character, the specimen is sealed on its five sides by applying paraffin wax or epoxy resin. The bottom side of the specimen is then immersed into water to a depth of 2 ± 1mm.

This protocol does not require samples to be initially oven dry, nor does it specify the number of periodic measurements, nor dimensions of the specimen. It may be valid for material with a single pore size distribution that contains a significant fraction of micro-pores, such as ceramic-bricks where the capillary suction is not significantly affected by the gravity if water already accumulated in the specimen. However, this may not be the case for all materials, e.g. aerated autoclaved concrete (AAC). A whole range of capillary moisture contents can be listed from 180 kg/m^3 up to 340 kg/m^3 according to Bomberg (2002). Uniform moisture content in the imbibition test is seldom available, and the test

result is affected by a number of factors, such as thickness of the specimen, history of wetting and drying.

Another way (Bomberg 2001) defines capillary moisture content as the uniform moisture content corresponding to the capillary suction equal to zero. Yet using this approach and determining moisture profiles, there is also a whole range of local moisture contents.

The capillary moisture content of Savonniers limestone was found by Roels (2000) to vary between 129 kg/m^3 and 241 kg/m^3 in terms of two different subgroups of pores. Based on his experiment, Roels concluded that higher capillary moisture content corresponds to a higher water absorption coefficient, but the correlation remained poor. While the water absorption coefficient and the rate of water transport may be correlated with each other, however, it is not strongly related to the mechanism of pore filling.

A survey (Bomberg 2001) of existing open literature indicates there is no common agreement on how to determine the capillary moisture content. Towards this end: to deal with the practical issue of capillary moisture content definition, a specific moisture flow experiment that would produce a good and reproducible descriptor for the material should be selected. Capillary moisture content should, on the one hand, be considered as the apparent measure of air entrapment under given conditions of moisture flow into the porous system. On the other hand, a practical test to characterize this property under carefully selected and predetermined flow conditions is preferred.

In the present study, capillary moisture content of the specimens was determined together with the water absorption coefficient during the free water uptake process. Results are shown in Table 3-1 and 3-2. But a thorough understanding of capillary moisture content should be based on the following researches:

- To establish a general relation between the capillary moisture content and the rate of moisture inflow to the control volume as well as the history of moisture content in the specimen (hysteresis). This actual flow condition may be quite different from that taking place under 1-D character free water intake process.
- To establish the rate in the increase of the capillary moisture content at the material boundary exposed to water inflow.
- To establish the significance of factors affecting repeatability and reproducibility precision of a practical test method for determination of the capillary moisture content.

3.1.3 A-coefficient and liquid diffusivity

3.1.3.1 Experimental determination of A-coefficient for AAC and stucco

Specimens were shaped to the specific size from a material block. Before starting the test, specimens were put in the oven (temperature was set at 105°C) for several days until the weight of each specimen did not change. The exact weight and size of the specimens were recorded at this stage. Rosin and wax were mixed at a ratio of 4: 6 to seal the five surfaces of the specimens. After sealing the specimens, they were clamped and hung in a position where free surface was in continuous contact with the water. The experimental

setup is shown in Figure 3-1. During the water absorption process, care was taken to ensure that no air bubbles were entrapped at the interface between the water and surface of the specimen by observing and keeping the water level in the tank. Time was recorded immediately after the specimen surface came in contact with the water. At periodic intervals, weight changes of each specimen were monitored and recorded. The whole process of measurement lasted three to four days until the weight change of each specimen was less than 0.5%. Six specimens were tested each for AAC and stucco. Temperature and relative humidity in the laboratory were also monitored (see Appendix A and B).

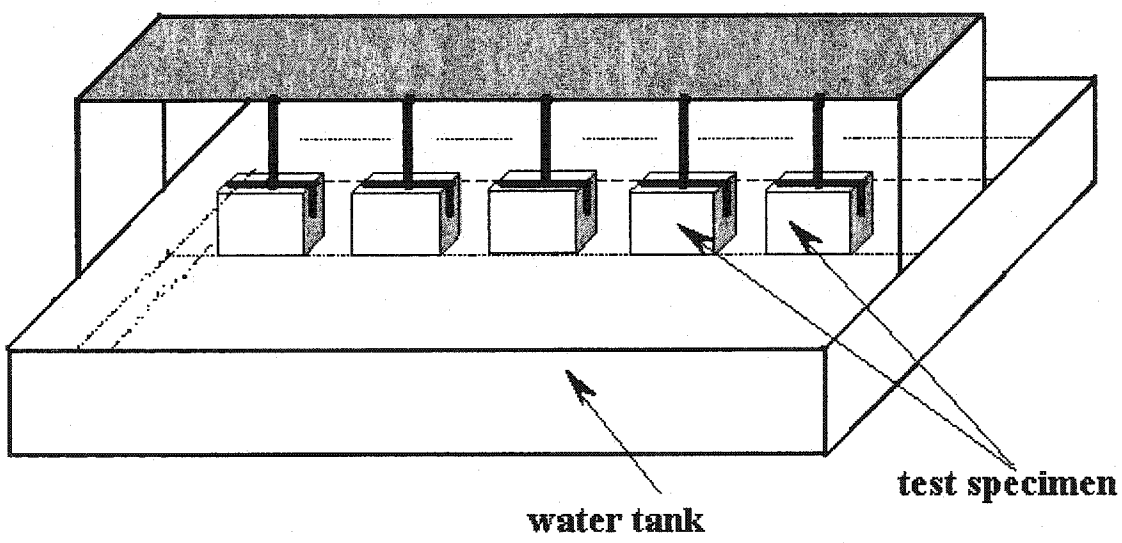

Figure 3-1. Schematic diagram of experimental setup for measuring surface water inflow for the calculation of A-coefficient and capillary moisture content

Test results (plots of surface inflow versus square root of time) for AAC and stucco are shown in Figure 3-2, 3-3 respectively.

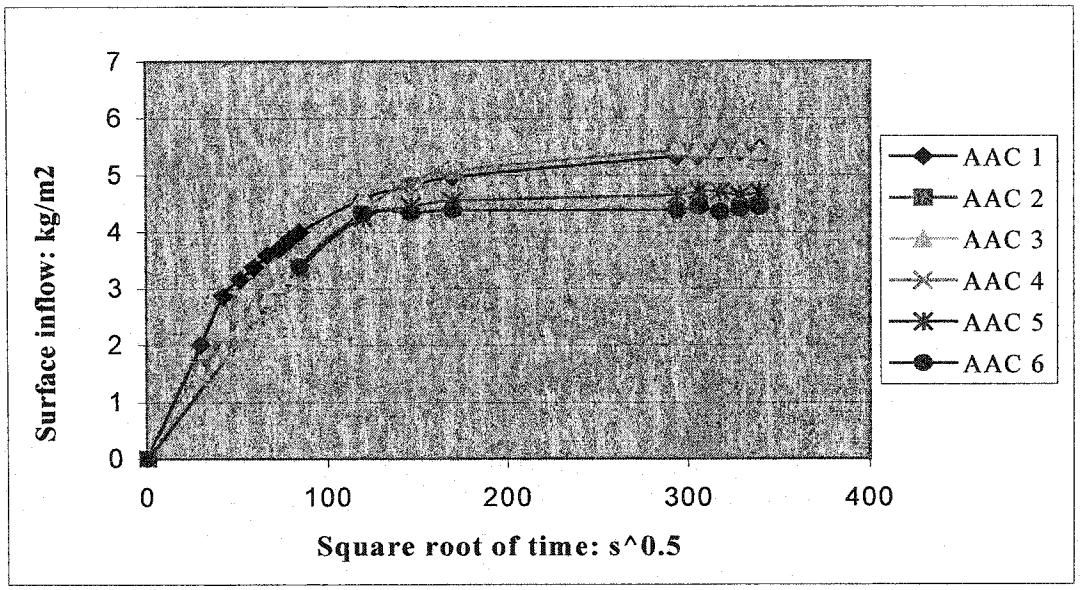

Figure 3-2. Instantaneous surface influx of water to the specimen of AAC (50 mm x 50 mm x 50 mm)

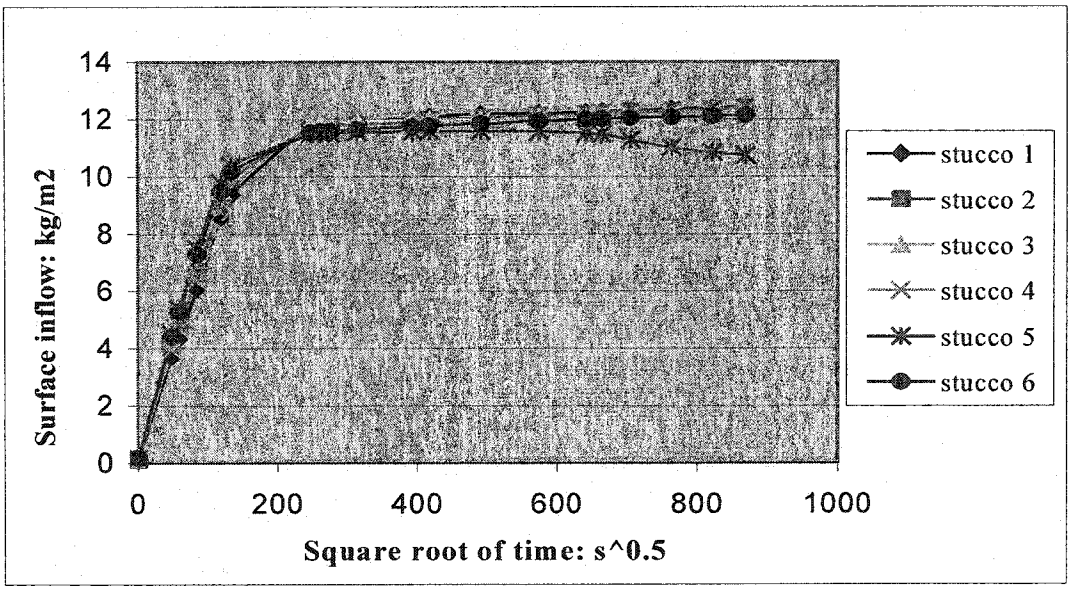

Figure 3-3. Instantaneous surface influx of water to the specimen of stucco (50 mm x 50 mm x 50 mm)

It should be noticed from Figure 3-3 that two curves at the end of the surface water inflow measurement show experimental errors: they are stucco 3 and stucco 5.

3.1.3.2 Determination of constant liquid diffusivity

Krus and Kunzel (1993) calculated constant liquid diffusivity based on a relationship established between water absorption coefficient (A_w) and capillary moisture content (W_{cap}). It is expressed as:

$$D_L = \frac{\pi}{4}\left(\frac{A_w}{w_{cap}}\right)^2 \tag{3-1}$$

Eq (3-1) is used in this study to derive a constant liquid diffusivity D_L over the range from completely dry to over-capillary saturation.

Water absorption coefficient (A_w), and capillary moisture content (W_{cap}) can be calculated from previous experiment of surface water inflow (See Figure 3-2, Figure 3-3). With knowledge of these two variables, constant liquid diffusivity using Eq (3-1) for AAC and stucco can be obtained, and they are shown in Table 3-1, and Table 3-2.

Table 3-1. Constant liquid diffusivity of AAC

Specimen Number	Density (kg/m^3)	Aw ($kg/m^2s^{1/2}$)	Wcap (kg/m^3)	D_L (m^2/s)
AAC 1	444.88	0.0453	273.43	2.16E-08
AAC 2	445.61	0.0324	266.90	1.16E-08
AAC 3	440.01	0.0345	272.03	1.26E-08
AAC 4	491.17	0.0313	250.20	1.23E-08
AAC 5	463.89	0.0361	273.09	1.37E-08
AAC 6	478.66	0.0366	285.48	1.29E-08
Average	**460.70**	**0.0360**	**270.19**	**1.41E-08**
Stdev	20.82	0.0050	11.54	3.71E-09

Table 3-2. Constant liquid diffusivity of stucco

Specimen Number	Density (kg/m^3)	Aw ($kg/m^2s^{1/2}$)	Wcap (kg/m^3)	D_L (m^2/s)
Stucco 1	1830.07	0.0475	214.36	3.86E-08
Stucco 2	1776.20	0.0465	216.61	3.62E-08
Stucco 3	1983.71	0.0463	226.40	3.28E-08
Stucco 4	1988.12	0.0444	223.06	3.11E-08
Stucco 5	1936.24	0.0452	219.18	3.34E-08
Stucco 6	1980.37	0.0452	216.89	3.41E-08
Average	**1915.79**	**0.0459**	**219.42**	**3.44E-08**
Stdev	90.85	0.0011	4.51	2.64E-09

It should be noted that constant liquid diffusivity could be used as a guideline for understanding the physical significance of moisture transport: the magnitude of the constant liquid diffusivity can be used to estimate the time for specimens to reach capillary saturation. According to Mukhopadhyaya et al. (2002), a magnitude of 10^{-7} indicates the specimens come close to the capillary saturation within hours while constantly in touch with liquid water, 10^{-8} indicates within a day, and 10^{-9} indicates within a few days while constantly in touch with liquid water.

Water absorption test in the present study gives an average liquid diffusivity with a magnitude of 10^{-8} for both AAC and stucco, which means specimens come close to the capillary saturation within a day while constantly in touch with liquid water. This agrees with observations of the experiment: for both AAC and stucco, the waterfront reaches top surface of the specimen within a day.

From water absorption measurement, the capillary moisture content for AAC is found to be in a range of 247.04 to 330.12 kg/m^3; for stucco it ranges from 200.68 to 237.48

kg/m^3. It can also be noticed that the knick point (defined by Bomberg (2000) as the crossing point of two tangential lines respectively drawn from primary stage and secondary stage of water inflow curve) for AAC is not very clear: it is in a transition region, whereas the knick point for stucco is uniform in distribution, which is reflected by measurements. (See Figure 3-2, 3-3)

3.1.3.3 Determination of liquid diffusivity as a function of moisture content

While constant liquid diffusivity derived from Eq (3-1) serves as a reference value for moisture transport, the liquid diffusivity coefficient is actually a function of the moisture content. The following empirical equation proposed by Kunzel (1995) is used to calculate D_L from the water absorption coefficient. The knowledge of capillary moisture content is necessary for this calculation.

$$D_L = 3.8 \cdot \left(\frac{A}{w_{cap}} \right)^2 \cdot 1000^{\frac{w}{w_{cap}}-1} \qquad (3\text{-}2)$$

Results of calculated liquid diffusivity using Eq (3-2) for AAC and stucco are shown in Figure 3-4, and 3-5, respectively.

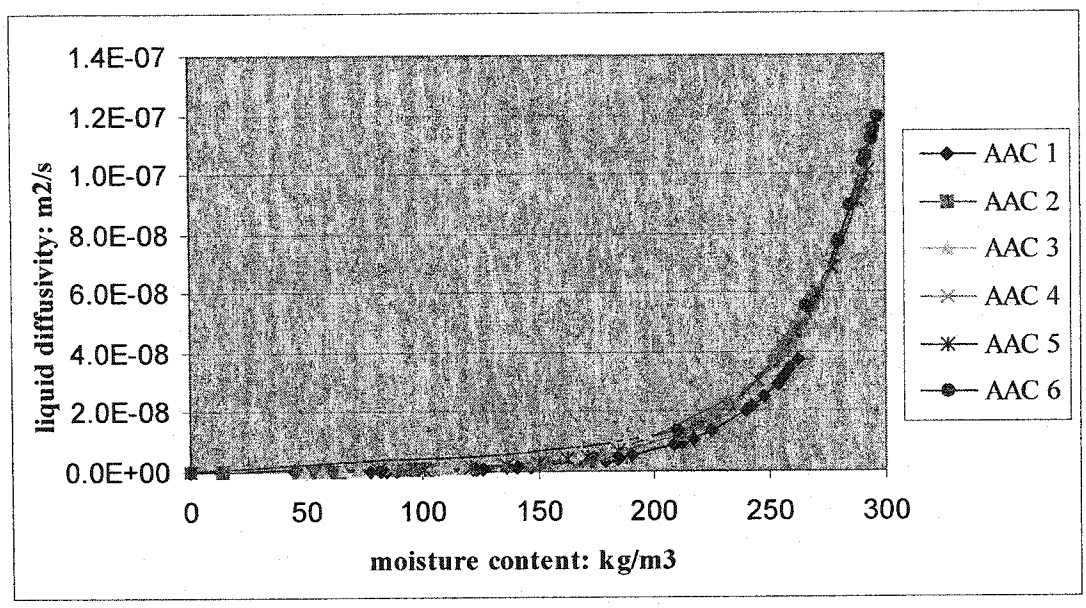

Figure 3-4. Calculated liquid diffusivity of AAC

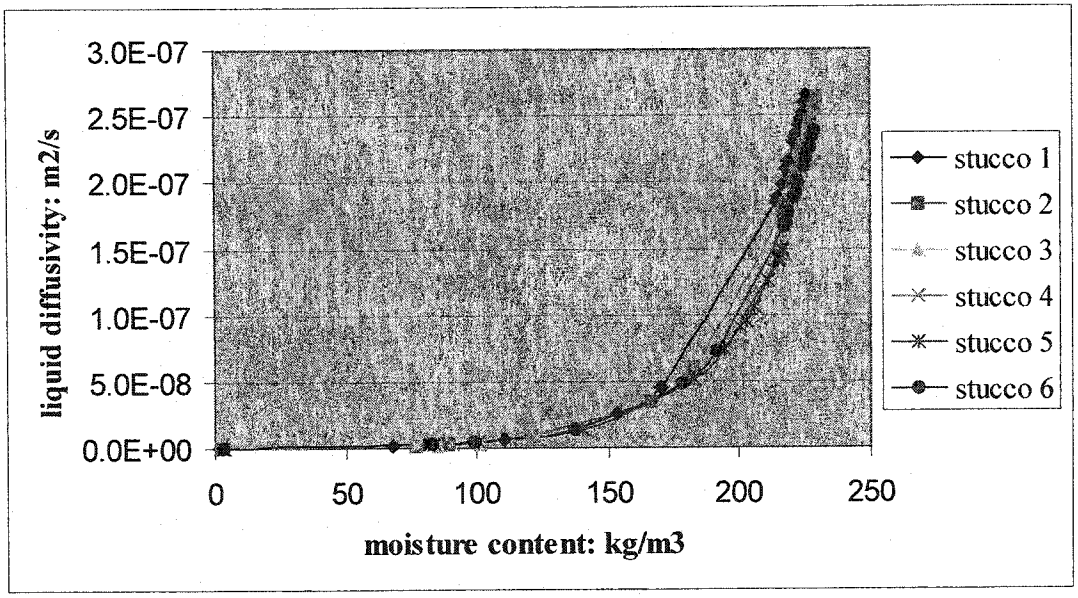

Figure 3-5. Calculated liquid diffusivity of stucco

It should be noted from Figures 3-4 and 3-5 that the liquid diffusivity calculated for AAC ranges from 3.75E-08 to 1.72E-07 m^2/s; and for stucco, it ranges from 9.02E-08 to 2.66E-07 m^2/s. The comparative study concerning the liquid diffusivity obtained from water absorption coefficient calculation and that from direct measurement will be addressed in Chapter 5 in details.

3.2 Material properties for HAM Model input

The implementation of Engineering Model requires a minimum of 6 material properties (See Chapter 2 for details). The following is a list of material properties required as input for the model:

- Total open porosity of the material (Opor),
- Capillary saturation (Ocap; i.e., porosity attainable under free water intake process),
- Liquid water diffusivity (D_W) as a function of moisture content,
- Water vapor permeability (WVP) as a function of moisture content,
- Moisture retention curves under extreme wetting and drying. As the minimum to this end, one needs two points from sorption curve (equilibrium moisture content at selected RH) and two points from over-hygroscopic region of MRC

3.2.1 Material properties of AAC

For AAC, all the required material properties are available: they are either obtained from measurement performed in this thesis or taken from Qiu (2002). These material properties are given below:

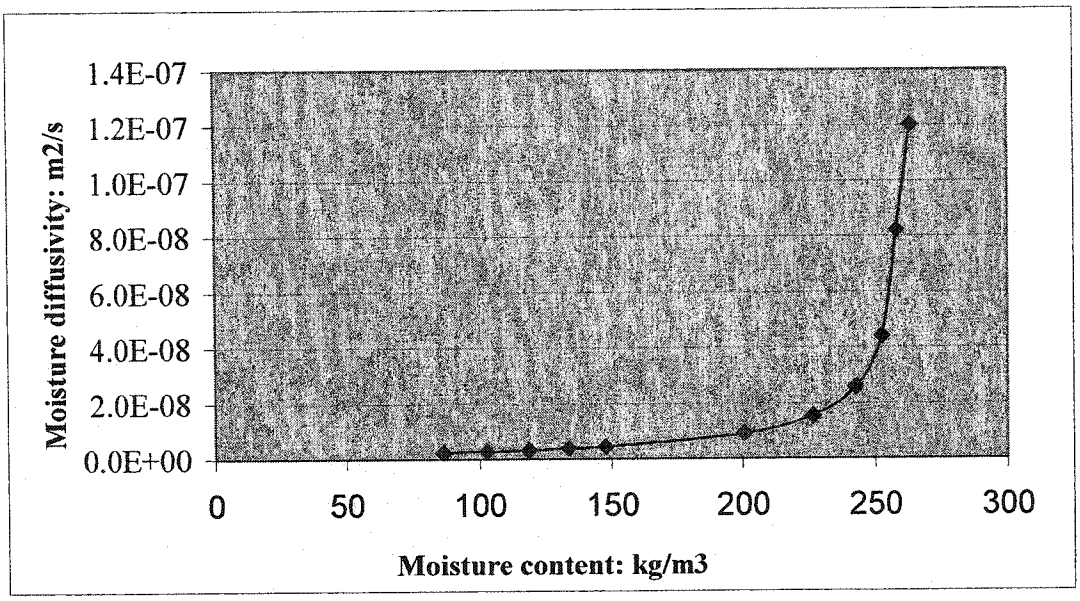

Figure 3-6. Liquid diffusivity calculated from gamma ray measurement (Qiu. 2002)

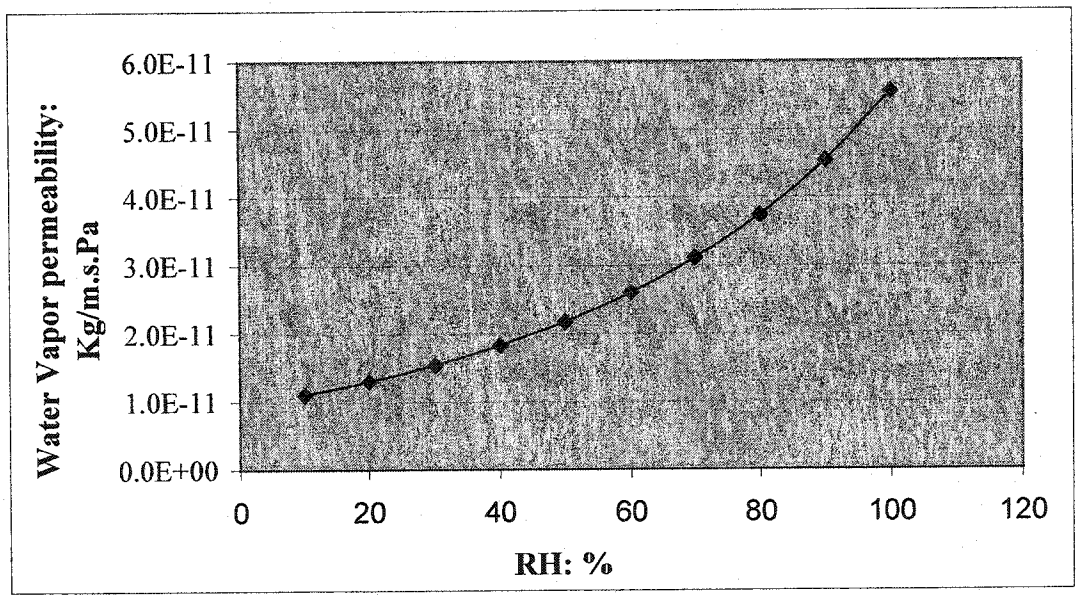

Figure 3-7. Water vapor permeability of AAC (Qiu. 2002)

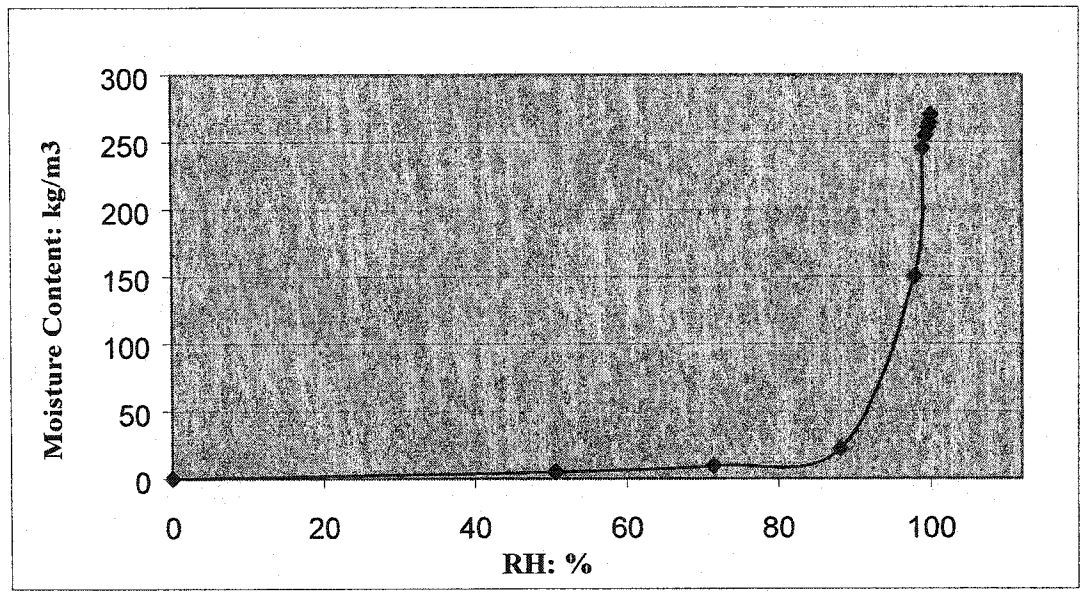

Figure 3-8. Sorption isotherm curve of AAC (Qiu. 2002)

According to measurement conducted by Qiu (2002), material porosity of AAC is 75%, and capillary saturation is 26.2%.

3.2.2 Material properties of stucco

For stucco, the total open porosity was estimated as 26% material porosity from the analysis of the existing hygrothermal databases, while other properties were measured at Concordia University, and are given below:

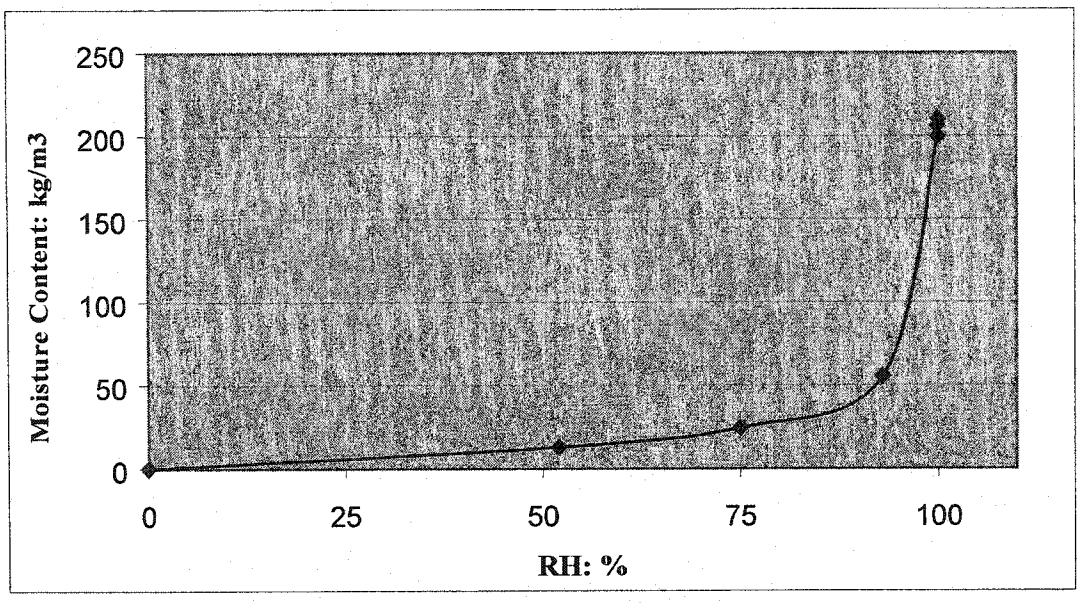

Figure 3-9. Sorption isotherm curve of stucco measured by pressure plate apparatus

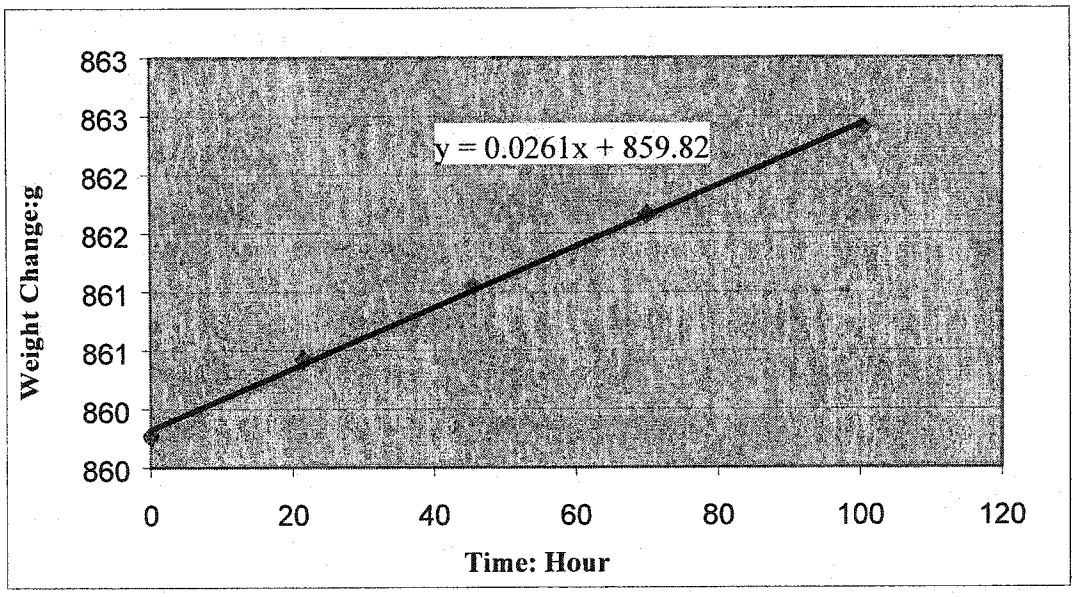

Figure 3-10. Water vapor transmission at 75% RH measured by dry cup test: stucco A

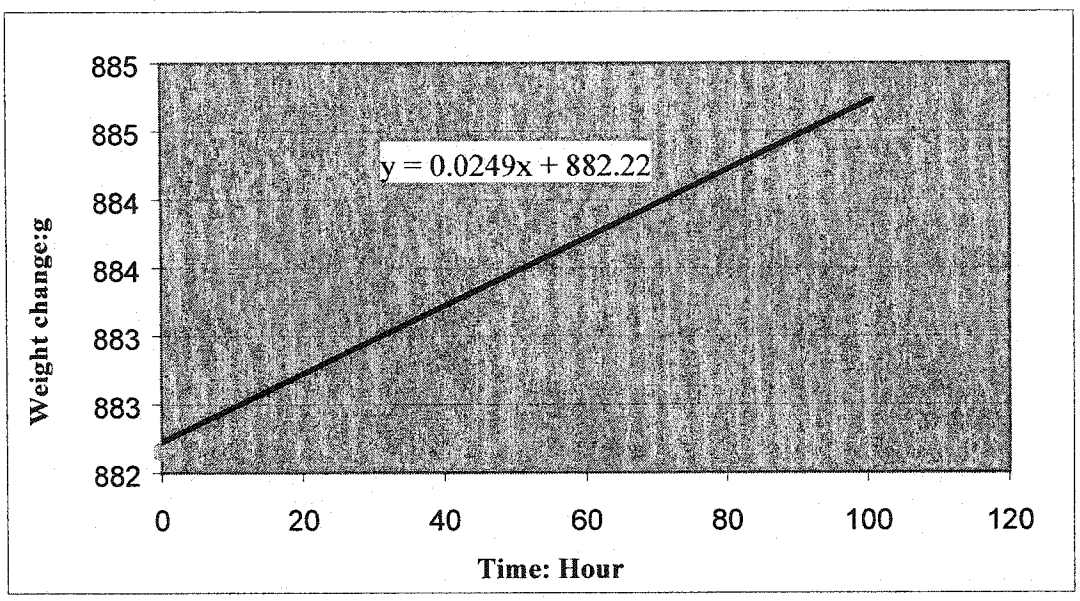

Figure 3-11. Water vapor transmission at 75% RH measured by dry cup test: stucco B

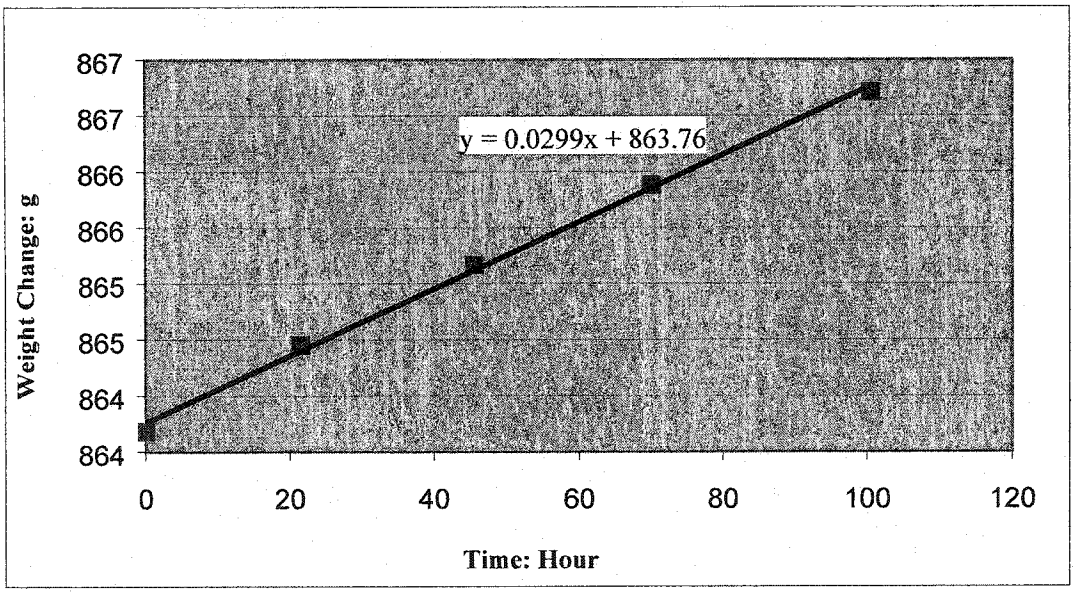

Figure 3-12. Water vapor transmission at 75% RH measured by dry cup test: stucco C

Water vapor permeability of stucco measured at 75% RH for Specimen A, B, C are 6.92E-12, 7.10E-12, and 8.35E-12 respectively.

Material properties of both AAC and stucco obtained in this Chapter will be used as input to HAM Model. Results from calculation will then be compared with benchmark test in Chapter 5.

CHAPTER 4 A RUGGEDNESS STUDY OF A COEFFICIENT ON AAC

4.1 General

Water absorption coefficient is defined as slope of the cumulative, one-directional water inflow into a specimen versus the square root of period from the beginning of the water inflow process. Water absorption coefficient represents a combined material response to capillary force and resistance to water flow (Bomberg 2000), and because of the nature of simplification in its definition, it should be measured during the initial stage of the water inflow into a dry specimen (Bomberg 2000). The proposed method assumes that the moisture front does not reach the opposite side of the sample, the thickness of the sample has to be chosen in such a way that it is only a fraction of the maximum capillary height (Bomberg, 2002). However, a number of problems are associated with the present method, e.g., conditions of air pressure on the upper surface of the material would depend on the duration of the experiments (Descamps, 1997) and the length of the specimen; Long experimental times will also increase thickness of the boundary layer at the water ingress face (where the moisture content exceeds the capillary moisture content); For many materials, the slope of the cumulative moisture flux against the square root of time changes with time: no consensus has been reached on the existing methods to measure the A-coefficient.

To better understand water absorption coefficient, a ruggedness test has been initiated to study significance of factors affecting repeatability and reproducibility precision of a

practical test method for the determination of this variable. The purpose of this ruggedness test is to find experimental factors that strongly influence the measurements provided by the test method, and to determine how closely these factors need to be controlled. Worthy of mention is ruggedness test do not determine the optimum conditions for the test method (Robert, et al., 1986).

4.2 Experimental design

The experimental design most often used in the ruggedness test is the "Plackett-Burman" design, namely PB design (ASTM 1994). To examine the relative importance of different factors affecting test precision, effect of each factor is tested at two extreme levels: a high and a low setting. The selection of factors and the range of their variation are arbitrary: it is based entirely on the experience of researchers. Yet, with a sufficient number of comparative tests evenly split between the high and low settings, one may distinguish the relative significance of factors affecting the precision of the test method.

The design requires the simultaneous change of the levels of all the variables, and allows the determination of the separated effects of each of the variables on the measured results. Easy to use, P-B design is efficient in developing the information needed for improving test methods. Two levels for each variable are set so as not to be greatly different. For such situations, the calculated effect for any given variable is generally not greatly affected by changes in the level of any of the other variables (Wernimont, et al., 1977).

Experimental evaluation of A-coefficient, reported in this Chapter, is made up of two series. Each series comprised 7 factors. The first series examined parameters of the specimen surface condition, initial condition, and parametric model for data analysis as well, while the second series compared results obtained from different specimen size, thickness, and test procedures.

4.2.1 The first series of test

4.2.1.1 Description of selected factors and settings

The following factors are selected in the first test series conducted for evaluation:

A. **Side protection:** The size of the specimens in the first series is mostly around 5cm·5cm·5cm. The water absorption process was maintained as one-dimensional by sealing the specimen on its five surfaces. The high setting chosen for this factor was wax sealing and the low setting was duct-tape sealing.

B. **Immersion depth:** The bottom surface of the specimen was put in contact with water. In this series, immersion depth of the specimen into the water was chosen as a factor. High setting for this factor was 3 ± 1mm immersion depth, while 1 ± 0.5mm was chosen for low setting.

C. **Drying the wet surface:** When specimen was taken out from the water tank, there are water dews on its contact surface. To dry the wet surface with paper towel was chosen for the high setting, while to drain water from the wet surface naturally was for the low setting.

D. **Initial moisture content of specimen:** To test the influence of initial moisture content of specimen on the water absorption coefficient, initial oven dry specimen

was used for the high setting. Low setting was made for specimens, which were placed for 21 days in a desiccator containing saturated salt solution that provides 75% RH inside. The specimens were then tested to have an initial moisture content around 13 kg/m^3.

E. **Time lapse for weighing:** Weighing the specimen immediately or sometime after it was taken out would be one of the factors influencing the test result. High setting for this factor was made by weighing the specimen immediately, while low setting was weighing the specimen 5 minutes after it was taken out.

F. Roughness of the immersed surface: Specimen surface was in direct contact with the water during the absorption process. Different surface conditions present different contact areas. Smooth surface was made for the high setting in this factor, while grooved surface was for the low setting.

G. **Calculation model:** Water absorption coefficient was calculated with either 1 or 2 parameter model. Different models would induce different results. How the parametric model influence the calculation result constitutes one of the factors into our consideration. 2-parameter model was chosen for the high setting, while 1-parameter model was for the low setting.

$$J_s = A \cdot \sqrt{t} \qquad \text{1-parameter model} \qquad (4\text{-}1)$$

$$J_s = A_0 \cdot \sqrt{t} + A_1 \left[1 - \left(\frac{1}{t+1} - 1 \right)^2 \right] \qquad \text{2-parameter model} \qquad (4\text{-}2)$$

Table 4-1. Summary of evaluated parameters for the first series

Factor	Evaluated parameters	Settings	
		Low (-)	High (+)
A	Side protection	Duct tape	Wax
B	Immersion depth	1 ± 0.5mm	3 ± 1mm
C	Drying the wet surface	Naturally	Paper towel
D	Initial moisture content	75% RH	Initial dry
E	Time lapse for weighing	After 5 min	Immediately
F	Roughness of the immersed surface	Grooved	Smooth
G	Calculation model	1P model	2P model

The first series of P-B design for seven factors (A through G) and eight measurements is given in Table 4-2. This design is suitable for use whenever an independent estimate of measurement variability is available. Note that each column of the design contains an equal number of plus (+) and minus (-) factor settings. A (+) for a given factor sets at the high level, and a (-) indicates the factor is to be at the low level. All seven factors are set for each measurement (test result). The eighth measurement is a dummy made in such a way that the requirement for the ruggedness test is satisfied: the same number of plus (+) as minus (-). The design is constructed in such a way that the four A (+) and the four A (-) terms will each be associated with an equal number of B (+) and B (-) terms. The A effect is orthogonal to the B effect, that is, it is not affected by the B effect. In this way, all main effects (columns) are orthogonal to all other main effects (columns). This orthogonality of the main effects and the acceptance of possible contamination of estimates for the main effects (by the interactions) are the major characteristics of ruggedness test.

Table 4-2. P-B design for the first series of test

Exp.	Factors Tested						
N	A	B	C	D	E	F	G
1	+	+	+	-	+	-	-
2	-	+	+	+	-	+	-
3	-	-	+	+	+	-	+
4	+	-	-	+	+	+	-
5	-	+	-	-	+	+	+
6	+	-	+	-	-	+	+
7	+	+	-	+	-	-	+
8	-	-	-	-	-	-	-

Specimens in the first series of test were therefore arranged in accordance with parameter settings in Table 4-1 and P-B design in Table 4-2. The arrangement is shown in Table 4-3.

Table 4-3. Test set-up for first series

	Factors						
Test set-up	Side protection (A)	Immersion depth (B)	Drying the surface (C)	Initial condition (D)	Contact break (E)	Absorption surface (F)	Parametric model (G)
1	Wax	3 ± 1mm	Paper towel	75% RH	Immediately	Grooved	1 P model
2	Duct tape	3 ± 1mm	Paper towel	Dry	After 5 min	Smooth	1 P model
3	Duct tape	1 ± 0.5mm	Paper towel	Dry	Immediately	Grooved	2 P model
4	Wax	1 ± 0.5mm	Naturally	Dry	Immediately	Smooth	1 P model
5	Duct tape	3 ± 1mm	Naturally	75% RH	Immediately	Smooth	2 P model
6	Wax	1 ± 0.5mm	Paper towel	75% RH	After 5 min	Smooth	2 P model
7	Wax	3 ± 1mm	Naturally	Dry	After 5 min	Grooved	2 P model
8	Duct tape	1 ± 0.5mm	Naturally	75% RH	After 5 min	Grooved	1 P model

4.2.1.2 Water intake process of the first series

Result of water intake for two typical specimens in the first series is shown in Figure 4-1. Detailed graphic presentations of water intake for all the specimens in the first series are given in Appendix A.

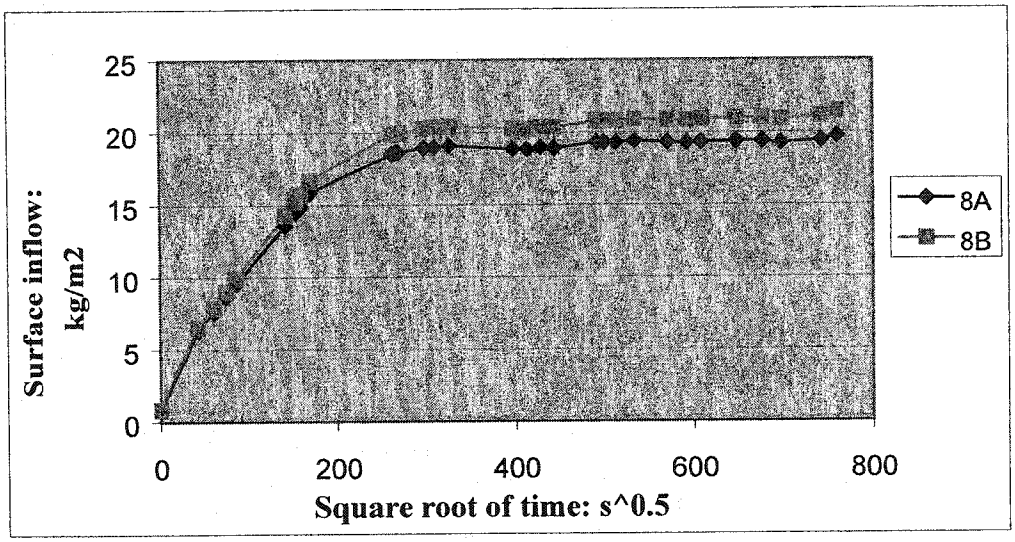

Figure 4-1. A typical representation of water absorption process in the first series of ruggedness tests. The size of the specimen was 50 mm x 50 mm x 50 mm.

Test results of water absorption coefficient for the first series are given in Table 4-4.

Table 4-4. A-coefficient for the first series

set-up	set: A	set: B
1	0.0200	0.0220
2	0.0561	0.0511
3	0.0670	0.0680
4	0.0343	0.0324
5	0.0880	0.0850
6	0.0310	0.0360
7	0.0350	0.0370
8	0.0680	0.0728

4.2.1.3 Calculation for the first series of test

The effect of a factor, such as A, is calculated as the average of the measurements made at the high level minus the average of the measurement made at the low level, and is given by the following equation (ASTM 1994):

$$Effect A = \frac{\sum A(+)}{N/2} - \frac{\sum A(-)}{N/2} = (\frac{2}{N})[\sum A(+) - \sum A(-)] \quad (4\text{-}3)$$

The significance of the effect of varied settings for each factor was determined, using a *t-test*. Since two sets of test (set A and set B) were conducted each having eight set-ups, the t-value for each factor was calculated from the average of the two t-values obtained for each effect with the following formula (ASTM 1994):

$$t_{N-1} = \frac{Effect_{average} A}{2\sqrt{[\sum d^2/(N-1)](N/8)}/\sqrt{2N}} \quad (4\text{-}4)$$

Where N is the number of test conducted (in this series, N=8)

d is the difference between effect values calculated from two sets of data

Data below shows the *t-value* calculated using Equation (4-4) for the average effect obtained from two sets of results.

Table 4-5. Calculated *t-value* for the averaged effect of each factor under evaluation

Factor	Level	First Data Set		Second Data Set		difference between effect		average effect	t-value
		average	effect: E1	average	effect: E2	d=E1-E2		(E1+E2)/2	
A +	Wax	3.01E-02		3.19E-02		d	d^2		
A -	Duct-tape	6.98E-02	-3.97E-02	6.92E-02	-3.74E-02	-2.32E-03	5.41E-06	-3.85E-02	**-30.12**
B +	3 ± 1mm	4.98E-02		4.88E-02					
B -	1 ± 0.5mm	5.01E-02	-3.00E-04	5.23E-02	-3.52E-03	3.22E-03	1.04E-05	-1.91E-03	**-1.49**
C +	Towel	4.35E-02		4.43E-02					
C -	Natural dry	5.63E-02	-1.28E-02	5.68E-02	-1.25E-02	-2.75E-04	7.56E-08	-1.27E-02	**-9.90**
D +	Initial dry	4.81E-02		4.71E-02					
D -	75% RH	5.18E-02	-3.65E-03	5.40E-02	-6.83E-03	3.17E-03	1.01E-05	-5.24E-03	**-4.09**
E +	Immediately	5.23E-02		5.19E-02					
E -	After 5 min	4.75E-02	4.80E-03	4.92E-02	2.63E-03	2.18E-03	4.73E-06	3.71E-03	**2.90**
F +	Smooth	5.24E-02		5.11E-02					
F -	Grooved	4.75E-02	4.85E-03	5.00E-02	1.18E-03	3.68E-03	1.35E-05	3.01E-03	**2.35**
G +	2 P model	5.53E-02		5.65E-02					
G -	1 P model	4.46E-02	1.07E-02	4.46E-02	1.19E-02	-1.28E-03	1.63E-06	1.13E-02	**8.82**

4.2.2 The second test series

4.2.2.1 Description of selected factors and settings

The following factors are selected in the second test series that were conducted for evaluation:

H. **Material thickness:** The thickness of the material may be one of the factors affecting the absorption coefficient. A specimen with thickness of approximately 50 mm was the high setting, and a specimen with a thickness of approximately 20 mm was the low setting.

I. **Initial period of testing:** Including the initial period of test was the high setting while excluding the initial period of test was the low setting. Including the initial

period indicates it was linear at the beginning, while excluding indicates it was not linear at the beginning.

J. **Stability of water level:** Ensuring constant water supply to maintain the water level was the high setting, while putting the water in the tank naturally was the low setting.

K. **Period of testing:** A short period of test was the high setting while the long period of test was the low setting. Despite the difference in the test period, number of measurements was used in both cases the same.

L. **Top surface:** An open top surface was the high setting, while a wrapped top surface with polyethylene foil was the low setting. This factor is to study the influence of moisture evaporation on the water absorption coefficient when the top surfaces are in different situations: exposed or wrapped.

M. Number of readings: taking 5 points for A-coefficient measurement was the low setting, while taking 3 points was the high setting for A-coefficient.

N. Surface area of the specimens: the surface area can be one of the factors influencing the test result. A surface area with 50mm x 50mm was the high setting, while an area of 100mm x 100mm was the low setting.

Table 4-6. Summary of evaluated parameters for the second series

Factor	Evaluated parameters	Settings	
		Low (-)	High (+)
H	Material thickness	<2cm	> 5cm
I	Initial period of testing	Excluding	Including
J	Stability of water level	Naturally	Constant level
K	Period of testing	Long	Short
L	Top surface	Closed	Open
M	Number of readings	5 points	3 points
N	Surface area	10cm x10cm	5cm x5cm

The principles in the P-B design that were applied to the first series of test were applied to the second series. Table 4-7 shows the P-B design for the second series of test.

Table 4-7. P-B design for the second series of test

Exp.	Factors Tested						
N	H	I	J	K	L	M	N
1	+	+	+	-	+	-	-
2	-	+	+	+	-	+	-
3	-	-	+	+	+	-	+
4	+	-	-	+	+	+	-
5	-	+	-	-	+	+	+
6	+	-	+	-	-	+	+
7	+	+	-	+	-	-	+
8	-	-	-	-	-	-	-

Specimens in the second series of test were therefore arranged in accordance with parameter settings in Table 4-6 and P-B design in Table 4-7. It is shown in Table 4-8.

Table 4-8. Test set-up for 2nd series

	Factors						
Test set-up	Material thickness (H)	Initial period of testing (I)	Stability of water level (J)	Period of testing (K)	Top surface condition (L)	Number of readings (M)	Specimen surface size (N)
1	>5cm	Included	Constant	Long: 24hr	Open	5 points	10cm x10cm
2	<2cm	Included	Constant	Short: 1-2hr	Closed	3 points	10cm x10cm
3	<2cm	Excluded	Constant	Short: 1-2hr	Open	5 points	5cm x5cm
4	>5cm	Excluded	Natural	Short: 1-2hr	Open	3 points	10cm x10cm
5	<2cm	Included	Natural	Long: 24hr	Open	3 points	5cm x5cm
6	>5cm	Excluded	Constant	Long: 24hr	Closed	3 points	5cm x5cm
7	>5cm	Included	Natural	Short: 1-2hr	Closed	5 points	5cm x5cm
8	<2cm	Excluded	Natural	Long: 24hr	Closed	5 points	10cm x10cm

4.2.2.2 Water intake process of the second series

Result of water intake for two typical specimens in the second series is shown in Figure 4-2. Detailed graphic presentations of water intake for all the specimens in the second series are given in Appendix B.

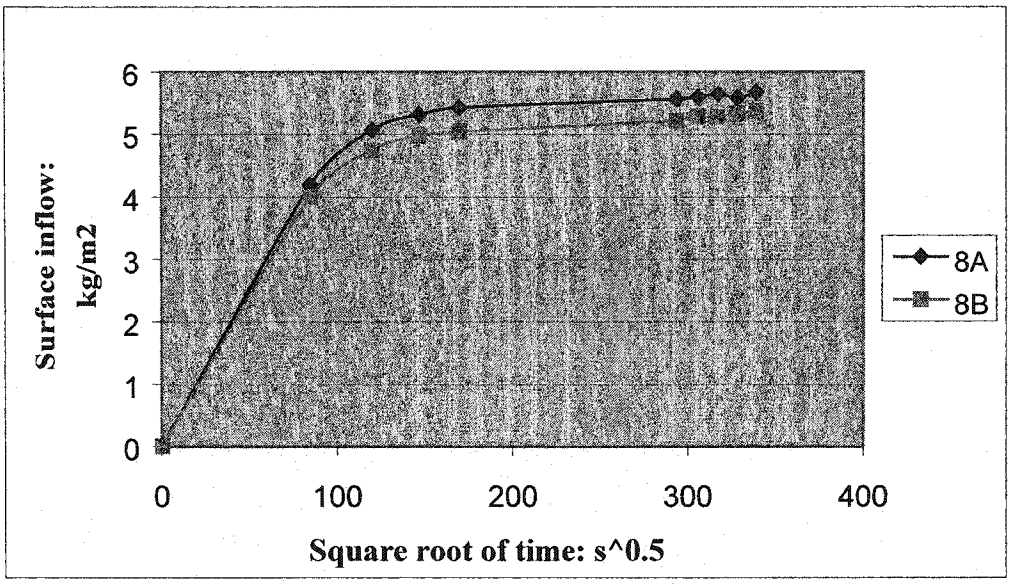

Figure 4-2. A typical representation of water absorption process in the second series of ruggedness tests. The size of the specimen was 10 mm x 10 mm x 20 mm.

Test results of water absorption coefficient for the first series are given in Table 4-9.

Table 4-9. A-coefficient for the second series

set-up	set: A	set: B
1	0.0463	0.0480
2	0.0701	0.0738
3	0.0415	0.0429
4	0.0479	0.0410
5	0.0367	0.0372
6	0.0410	0.0303
7	0.0609	0.0535
8	0.0329	0.0306

4.2.2.3 Calculation for the second series of test

Principles in the P-B design calculation that were applied to the first series of test were applied to the second series of test. Table 4-10 shows the *t-value* calculated using Equation (4-4) for the average effect obtained from two sets of results for the second series of test.

Table 4-10. Calculated *t-value* for the averaged effect of each factor under evaluation

Factor	Level	First Data Set		Second Data Set		difference between effect		average effect	t-value
		average	effect: E1	average	effect: E2	d=E1-E2		(E1+E2)/2	
H +	> 5cm	4.90E-02		4.32E-02		d	d^2		
H -	< 2cm	4.53E-02	3.73E-03	4.61E-02	-2.93E-03	6.65E-03	4.42E-05	4.00E-04	**0.22**
I +	Including	5.35E-02		5.31E-02					
I -	Excluding	4.08E-02	1.27E-02	3.62E-02	1.69E-02	-4.25E-03	1.81E-05	1.48E-02	**8.02**
J +	Constant	4.97E-02		4.88E-02					
J -	Natural	4.46E-02	5.13E-03	4.06E-02	8.18E-03	-3.05E-03	9.30E-06	6.65E-03	**3.60**
K +	Short	5.51E-02		5.28E-02					
K -	Long	3.92E-02	1.59E-02	3.65E-02	1.63E-02	-4.00E-04	1.60E-07	1.61E-02	**8.71**
L +	Open	4.31E-02		4.23E-02					
L -	Closed	5.12E-02	-8.13E-03	4.71E-02	-4.77E-03	-3.35E-03	1.12E-05	-6.45E-03	**-3.49**
M +	3 points	4.89E-02		4.56E-02					
M -	5 points	4.54E-02	3.53E-03	4.38E-02	1.83E-03	1.70E-03	2.89E-06	2.68E-03	**1.45**
N +	5cm x5cm	4.50E-02		4.10E-02					
N -	10cmx10cm	4.93E-02	-4.27E-03	4.84E-02	-7.38E-03	3.10E-03	9.61E-06	-5.83E-03	**-3.15**

4.3. Evaluation of test parameters using "ruggedness study" result

4.3.1 Comparison with statistics table

To determine the statistical significance for each of the main effects under evaluation, the 5% critical *t-value* associated with 7 degrees of freedom obtained from statistics table was compared to the calculated *t-value*. From *Moore and McCabe (1993)* the value was established to be 1.90. The effect of any factor with a t-value less than 1.90 is determined to be statistically insignificant.

In the first series of test, the observed t-effect absolute values for factors A, C, D, E, F and G are 30.12, 9.90, 4.09, 2.90, 2.35 and 8.82 respectively, which are larger than the significance level of 1.90. This means that the following factors had a significant effect on the precision of the test method:

- Side protection
- Ways to dry the wet surface
- Initial moisture content of the specimen
- Time lapse for weighing
- Roughness of immersed specimen
- Parameter model for the regression analysis

For factor B, the *t-effect* value was 1.49, which is less than the significance level of 1.90. This means factor B "*immersion depth* " was found statistically insignificant on the precision of the test method.

In the second series of test, the observed t-effect absolute values for factors I, J, K, L, and N are 8.02, 3.60, 8.71, 3.49, and 3.15 respectively, which are larger than the significance level of 1.90. This means the following factors in the second series of test had significant influence on the precision of the test method. Listed below are influential factors in the second series:

- Initial period of testing
- Stability of water level
- Period of testing
- Top surface condition
- Surface size of the specimen

For factors H, and M, the *t-effect* value was 0.22 and 1.45 respectively, less than the significance level of 1.90. This means factor H "*Material thickness*" and " Numbers of reading" were statistically insignificant on the precision of the test method.

4.3.2. Discussion on factors indicated as significant in the ruggedness study

4.3.2.1 The first series of test

In the first series of test, the t-value for factor A "*side protection*" is the largest one: 30.12. One possible explanation for this large value might be the fact that for the duct-tape applied specimens, when moisture content increased to a certain level, the finite volume of AAC cannot hold more water. However, water is continuously coming into the specimen, which then expands the duct-tape around. As a result, the volume that can contain water increases. Furthermore, there is an air space between the duct-tape and

AAC specimen once the tape is expanded. This air space when small enough may act as capillary pores, which induces capillary flow into the specimen. In comparison, for wax-applied specimens, because of the inflexibility of wax, the volume that can contain water does not change, and wax does not expand either. So for the duct-tape-applied specimens, capillary flow into the air space between the tape and the specimen is involved, apart from the normal water intake process. For the wax-applied specimens, however, there's only water intake into the specimens. The mechanisms involved for the two kinds of side protection are essentially different. This explains why the side protection factor has the largest t-value in the first series of test. And this explanation agrees with the observation from the experiment. The use of duct-tape to seal the specimen is therefore not recommended.

According to the ruggedness study in the first series, the immersion depth does not influence the test result. This is in agreement with the assumption that water intake is a one-dimensional process. Once the absorbing surface was fully immersed into the water, and the four sides were well protected by sealing, the immersion depth does not spell much difference, be it 3mm or 1mm: water comes into the specimen only though the absorption surface one dimensionally.

The way to dry the wet surface is also a factor into our consideration. Leaving the wet surface to dry naturally, moisture in the form of vapor inevitably evaporates from inside the specimen into the environment due to the moisture content difference. Drying the wet surface with wet paper towel can, however, prevent vapor inside the specimen from

evaporating. Drying the wet surface immediately or 5 minutes after it was taken out from the water encounters the same problem: during the 5 minutes, vapor inside the specimen may evaporate. This calls for our concerns about ways and interval to dry the wet surface during the measurement process.

The difference between the grooved and smooth surfaces lies in the surface area that is directly in contact with water. Grooved specimen has large surface area than that of the smooth specimen. The surface is directly responsible for the water absorption. That is why the grooved surface and smooth surface give different test result, and influence the test precision.

It was found in the first series of test that initial moisture content of the specimens also influences the test precision on water absorption coefficient. An experimental study conducted by Schwarz (1972), and Gosele, et al. (1971) on AAC to determine the relation between initial moisture content and water absorption coefficient does not indicate any significantly higher variations in the water absorption coefficient at low initial moisture content. Another similar experiment conducted by Janz (1995) indicates the water absorption coefficient vary strongly when the initial moisture content ranges from 0 to 20 kg/m^3. But the material used by *Janz* was sedimentary calcareous sandstone, named Uddvide. One possible explanation given by *Janz* is that *"water is blocking critical passages in the pore system when the moisture content W_{in} = 20 kg/m^3 is reached. The water is then forced to detour and the capillary water transport decreases."*

In the present study, the average initial moisture content of the specimens, 13 kg/m^3 was found to have an impact on the water absorption coefficient compared with initially over dry specimens. Since systematic measurements concerning the water absorption coefficient and initial moisture content are not carried out in the present test, instead of giving a precise relation between the two variables, and defining how they interact with each other, it can only be concluded that initial moisture content has an impact on the test precision of water absorption coefficient compared with those initial over dry specimens, and further study conducted with different initial moisture contents is required before consensus can be reached.

AAC is a multi-phase system, and its pore size distribution is different from that of stucco. The study in this series indicates the use of different parametric models has an impact on the final test results since the t-value for "*Factor G*" is 8.82 exceeding the reference value of 1.90. As discussed in Chapter 3, the knick point of AAC is in a transition region, and its capillary moisture content is not uniformly distributed (See Figure 3-1), therefore, the use of 2-paremeter model is more precise in defining the water absorption coefficient for AAC, and can help adjust the initial stage of water inflow curve.

4.3.2.2 The second series of test

In the second series of test, the t-value for factor H "*thickness of the specimen*" 0.22 is far from the reference level, which means thickness of the specimen was found to be statistically insignificant.

Factor K and I have a t-value exceeding 1.90. "*Initial period of test*" influences the intercept of the trend-line: including the initial period of test, the intercept was set at zero, however, excluding the initial period of test set the intercept at a value above zero. Thus the trend-line goes in different styles. "*Period of testing*" also influences the slope of the trend line for regression analysis: longer period tends to increase the thickness of the boundary layer at the water ingress face. The slope of the cumulative moisture influx against square root of time also changes with the time. Thus long period of testing tends to have a slope different from that obtained from short period of testing. These two factors are therefore significant in affecting repeatability and reproducibility precision of the practical test method for the determination of the water absorption coefficient.

Factor L "*top surface condition*" has a t-value –3.49: its absolute value exceeds 1.90, which means top surface condition influences the test result. When the top surface is open to the environment, moisture that comes into the specimen tends to evaporate once the moisture content gradient between the specimen and the environment develops: moisture comes in from the bottom, and evaporates out from the top surface. Compared with specimens, whose top surface was closed, there's no moisture flow out of the specimen, moisture content inside the specimen increases steadily. This explains why at the end of absorption process, moisture content of specimen tends to decrease for those whose top surface is open.

Worthy of mention is factor N "*surface area of the specimen*". The test indicates it influences the final result. However water absorption coefficient was tested at one-

dimensional flow condition, and surface area is not supposed to have influence on the test result. So, the t-value in the ruggedness study for factor N is not compatible with the one dimension assumption, and this requires further examination of the effect of surface area on the water absorption coefficient.

The level of water in the tank is also an influential factor since its t-value of 3.60 exceeds the reference value of 1.90. Keeping a constant water level or leaving the water in the tank naturally are not supposed to influence the test result, since it's a one-dimensional process. One possible explanation for this controversy might be the fact that water in the tank keeps evaporating. When water is not maintained at constant level, it may evaporate to such an extent that leads the absorption surface not in full contact with the water. As a result, water is not continuously absorbed into the material once the water level in the tank is lower than the bottom surface of the specimen. It is therefore important to maintain a constant water level during the whole process of the measurement so that the surface responsible for absorption is completely immersed into the water.

The number of points (Factor M) selected to calculate water absorption coefficient is found statistically insignificant. This however requires that points are selected from the first stage of the intake process, and points are evenly distributed in the linear range.

4.4 Concluding remarks

Ruggedness test based on P-B design was used to study 14 factors that may have influence on the test precision of water absorption coefficient measurement. From the two series of tests conducted in the present chapter, it was found that:

- The following three factors are statistically insignificant on the test precision:
    1. Immersion depth
    2. Thickness of the specimen
    3. Number of points required for calculation
- The following eleven factors have significant impact on the repeatability and reproducibility of the test result:
    1. Side protection
    2. Ways to dry the wet surface
    3. Initial moisture content of the specimen
    4. Time lapse for weighing
    5. Roughness of immersed surface
    6. Parameter model for the regression analysis
    7. Initial period of testing
    8. Stability of water level
    9. Period of testing
    10. Top surface condition
    11. Surface area of the specimen

The measurement reported in this Chapter was conducted in the lab condition. It should be noted that ruggedness test studies experimental factors that may influence the measurements provided by the test method, but interactions between each factor are not taken into account. There are also other concerns inherent to the test method. But the majority of results from two series of ruggedness studies agree with the assumptions made for water absorption coefficient. Since the measurements were not precise enough, much work has to been done on the limitation for water absorption coefficient, and more detailed test, i.e., experimental factorial design, based on the present study is recommended to find interactions between each factor, and how these interactions affect the test precisions.

Detailed experiment data is reported in the Appendix A and B.

CHAPTER 5 BENCHMARKING TESTS AND CALCULATION

5.1 General

The precision of HAM model prediction depends on the adequacy of material characteristics that are used as input for the model calculation. To address precision in the HAM model predictions, one needs to perform:

- Benchmarking test of the HAM model
- Parametric analysis of climate and material properties

The present chapter deals with benchmarking test of HAM model. Material properties taken from either literature or from Engineering Model are used as input for HAM model calculation. Measurements of water inflow of AAC and stucco are then compared with HAM model predictions.

In the present study, two commonly used building materials, namely AAC and stucco, were selected for the benchmarking tests. AAC product delivered for testing was manufactured in Florida, United States: it had an average density of 450 kg/m^3. Stucco used for testing was prepared in a laboratory environment, with an average density of 1884 kg/m^3. Stucco was composed of cement, lime and sand, at a ratio of 1: ½: 4.5. Material porosity and liquid water diffusivity of AAC were taken from Literature (Qiu 2002). It should be noted however that AAC specimen tested in this thesis was the same material block tested by Qiu (2002). Material porosity of stucco was estimated from the analysis of the existing hygrothermal databases.

5.2 Application of HAM model to simulate AAC free water intake

5.2.1 The first series

An AAC specimen was taken as a benchmark and compared with results calculated by Delphin4. The material properties taken from Qiu (2002) were used as input to HAM model calculation, and are listed in Table 5-1. For simulation, two different boundary conditions were applied to the bottom surface respectively, namely rain density and constant moisture content. Results from model calculation versus benchmarking test are shown in Figure 5-1.

Table 5-1. List of material properties as input to HAM model calculation

Material porosity	Opor	75%
Capillary saturation	Ocap	26%
Liquid diffusivity	Dw (max)	1.28E-7 m^2/s
Water vapor permeability	WVP	1.449E-11 kg/m·s·pa
Capillary moisture conductivity	Kcap	5.64E-10 s

Note: Kcap is the product of Dw and moisture storage factor e at extreme of wetting MRC. And moisture storage factor e is the derivative of MRC, which is defined by the 6 points discussed in Chapter 2.

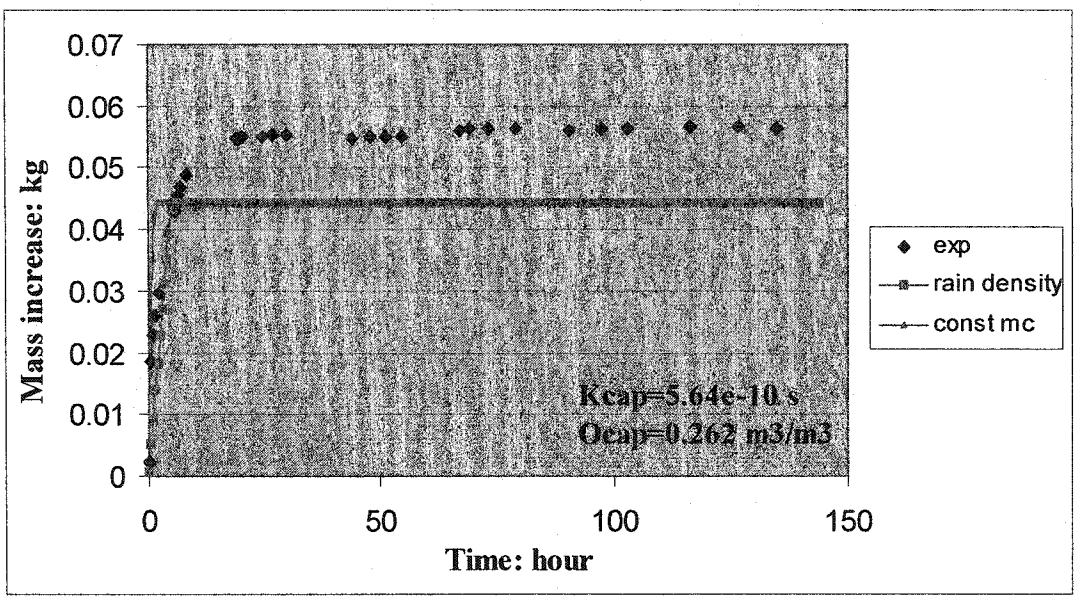

Figure 5-1. Free water intake of AAC (55 mm x 55 mm x 55 mm), material properties taken from Qiu. (2002)

The capillary saturation of 26% from Qiu (2002) was measured in such a way that the water inflow went only somewhere higher than capillary saturation without reaching the vacuum saturation. In this case, region of over saturated capillary flow was neglected in the measurement, where in real life scenario this region is significant in addressing problems of material durability and drying performance of building envelopes. So, the gammy ray measurement of capillary saturation from Qiu (2002) does not agree with the benchmark test in the present study.

Also noticeable is the use of rain and constant moisture content as boundary condition gives the same result during the secondary stage of water inflow. This indicates driving rain when properly defined can replace constant moisture content as boundary condition

during the simulation. A further study is assumed in the present chapter, which deals with issues of rain density applied simulation of free water intake.

5.2.2 The second series

In this series of calculation, while liquid diffusivity (Dw=3.86E-08 m^2/s) and capillary saturation (Ocap=33%) were obtained from the water absorption experiment (*Chapter 3*), the other input parameters were the same as those listed in Table 5-1. Results from model calculation are compared with measurement. They are illustrated in Figure 5-2.

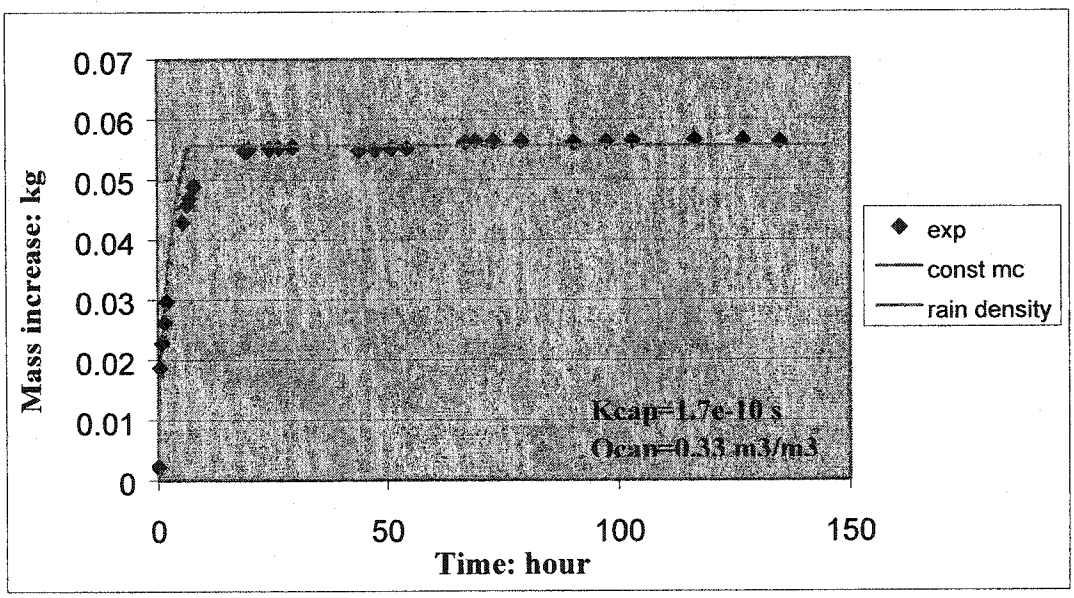

Figure 5-2. Free water intake of AAC (55 mm x 55 mm x 55 mm), calculated curve is based on material properties derived from measurement discussed in Chapter 3.

In the second series, results from HAM model simulation fit the measured inflow curve better than that in the first series. The discrepancy that occurs in the first series (see

Figure 5-1) between the simulation and measurement at the secondary stage does not exist any more (see Figure 5-2). As Dw and Ocap are the only changing factors between the two series of simulation, it can be concluded that liquid diffusivity and capillary moisture content as input are responsible for the control of model predictions.

5.3 Rain intensity based simulation of free water intake

Constant moisture content when applied as boundary condition imposes a water flux to the boundary domain of the problem. Possible applications of the boundary condition "constant moisture content" are direct water contact of underground building constructions and the simulation of water absorption experiments. However, in engineering practice, driving rain is also an important source of accumulated moisture in the building envelopes.

In this section, series of simulation of water absorption experiment were carried out. Instead of applying constant moisture content as boundary condition to the bottom surface of the specimen, driving rain was used in the simulation. Driving rain is quantified by rain intensity and rain exchange coefficient, which represent the amount of rain applied to a unit surface area at a unit time, and the amount of rain absorbed by a unit surface area at a unit time respectively. In this case, the influence of rain intensity and rain exchange coefficient on model predictions are taken into account in the simulation.

5.3.1 The influence of rain intensity on simulation result

When driving rain is applied as boundary condition, the two influential factors in the simulation are rain intensity and rain exchange coefficient. In the first series, the influence of rain intensity is studied while exchange coefficient is kept constant. The values of rain intensity applied to the boundary condition are 8E-4 l/m^{2}s, 8E-5 l/m^{2}s, and 8E-6 l/m^{2}s (2.88 kg/m^{2}h, 0.288 kg/m^{2}h, and 0.0288 kg/m^{2}h). Results from simulation are shown in Figure 5-3, and are compared with water absorption experiment conducted on a 55 mm x 55 mm x 55 mm AAC specimen.

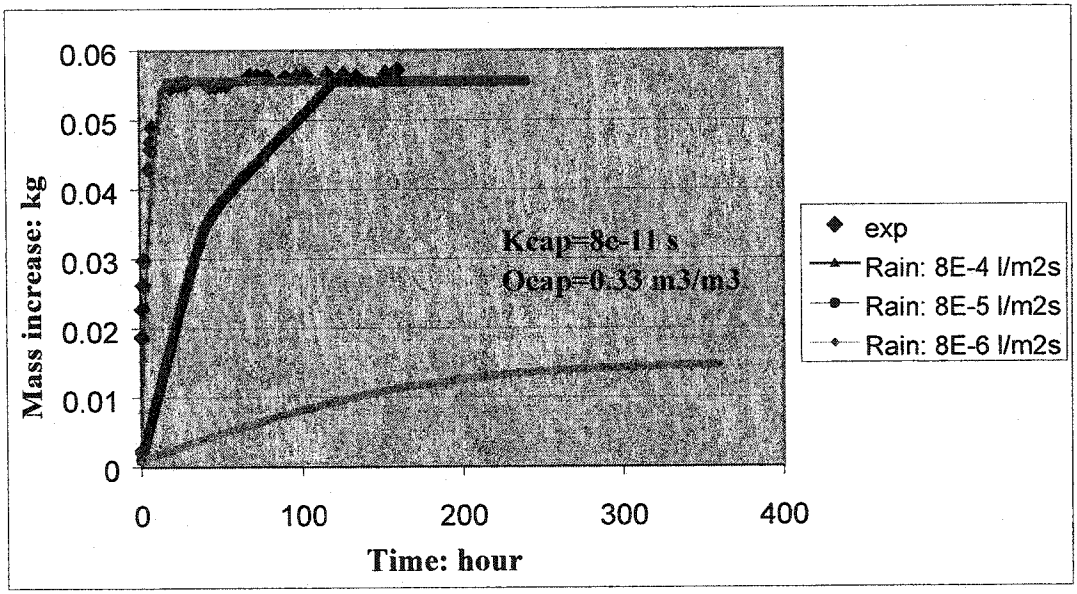

Figure 5-3. Simulation of driving rain on AAC (55 mm x 55 mm x 55 mm), calculated curves are based on constant rain exchange coefficient

From the result above, it can be seen with the increase of the rain intensity, the time for material to reach the capillary saturation decreases. In other words, the larger the rain

intensity is, the faster the specimen goes through the initial stage. However, there is a practical limit to define the rain intensity: it is compared with a maximum water flux that can be taken up by the surface. If the rain intensity exceeds the maximum water flux, then it is limited to the maximum water flux (Grunewald 1998).

5.3.2 The influence of rain exchange coefficient on simulation result

In the second series, the influence of rain exchange coefficient is studied while keeping rain intensity at constant value. Results from simulation are compared with water absorption experiment conducted on the same specimen as the one in 5.3.1.The comparison of simulation and measured inflow curve are shown in Figure 5-4.

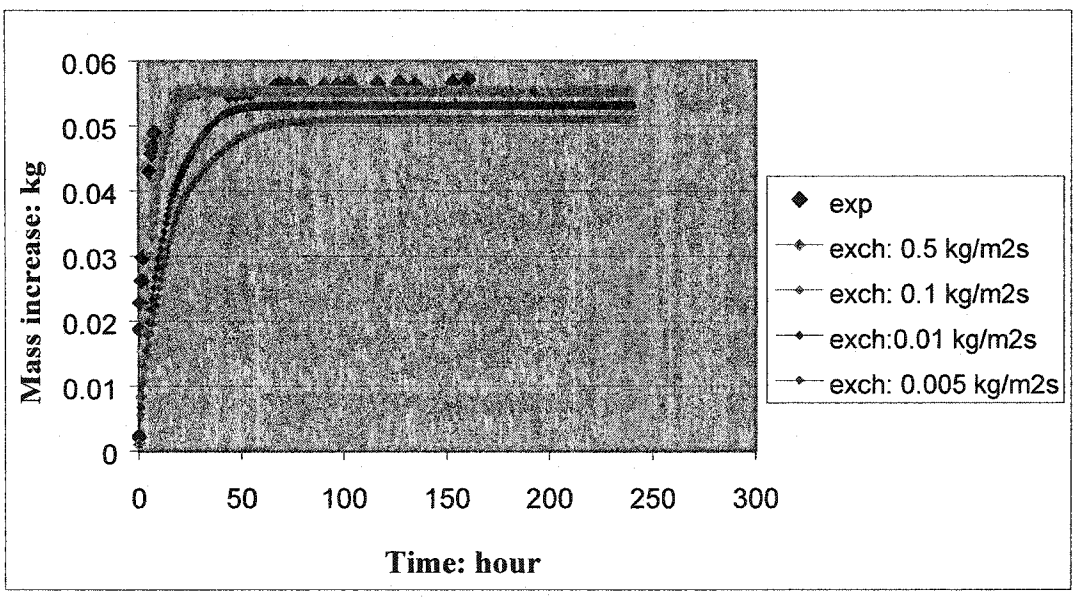

Figure 5-4. Simulation of driving rain on AAC (55 mm x 55 mm x 55 mm), calculated curves are based on constant rain intensity

It should be noted that an increase of rain exchange coefficient leads to the decrease of time to reach capillary saturation, and increased capillary moisture content. Compared with rain intensity, however, exchange coefficient has an impact that is relatively small: rain intensity has more significant influences on the moisture accumulation, in terms of both time to reach the capillary saturation, and the quantity of moisture that can be stored.

5.4 Case study on representative specimens

The measurement of free water intake gives series of water absorption coefficients, ranging from 0.02 to 0.086 $kg/m^2s^{0.5}$, and corresponding capillary moisture content ranging from 0.26 to 0.34 m^3/m^3. In Chapter 4, water absorption experiment was carried out on 32 AAC specimens (see Append A and B). According to the distribution of water absorption coefficients in these 32 measurements, representative specimens were taken as benchmark, and compared with results from simulation. The selected specimens have an Aw of 0.027, 0.057 and 0.086 $kg/m^2s^{0.5}$ respectively, which represents the minimum, medium and maximum value of absorption coefficients in the 32 measurements. Some basic parameters of the specimens are given in Table 5-2. Initial input parameters and results are shown in Figure 5-5. It can be seen the simulation and measurement agree with each other.

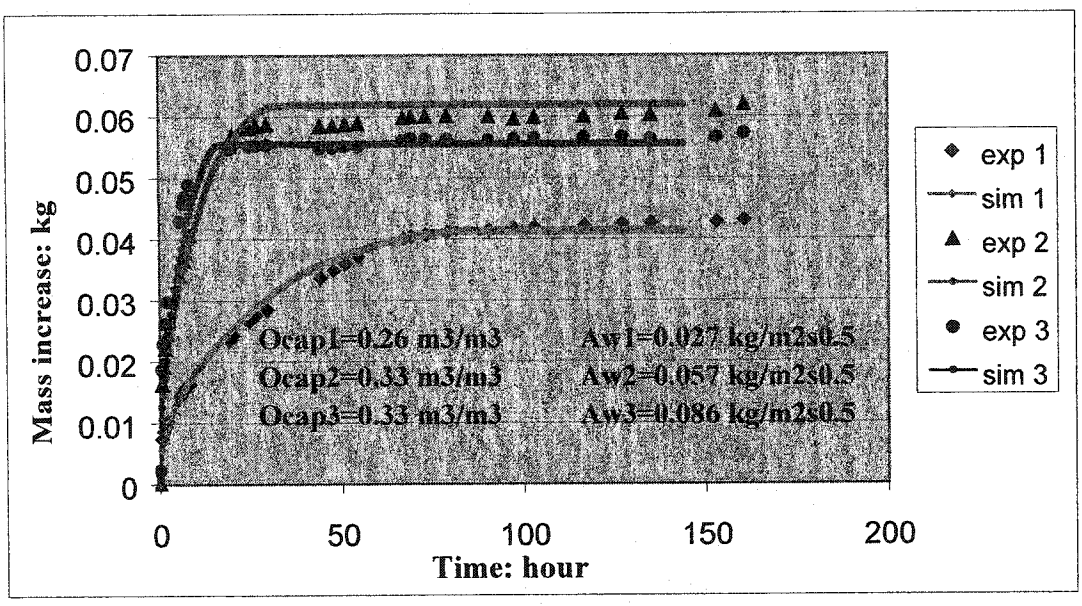

Figure 5-5. Case study on representative AAC specimens with minimum, medium and maximum water absorption coefficient.

In the case study presented above, constant moisture content at the bottom surface was applied as boundary condition. Kcap used for simulation was 1.50E-11s, 8.00E-11s, and 1.72E-10 s for specimen 1, 2, and 3 respectively.

Table 5-2. Basic parameters of the AAC specimen in the case study

AAC	1	2	3
H: cm	5.70	5.65	5.49
S_A: cm2	27.92	33.50	30.72
A_w: kg/m2s0.5	0.027	0.057	0.086
ρ: kg/m3	440	459	445

5.5 Application of HAM Model to simulate stucco free water intake

Engineering Model is related to material structure, and it assumes that the characteristic moisture contents are determined by position of peak in the pore size distribution curve. Compared with AAC, stucco has different material structure: the density of stucco is much larger. Moreover, the water absorption coefficient and capillary moisture content of stucco are more uniformly distributed, as reported in the experimental study from Chapter 3. In this section, two specimens were taken as benchmark and compared with results calculated by Delphin4. Some basic parameters of the specimens are given in Table 5-3. Initial input parameters and result from HAM model calculation are shown in Figures 5-6 and 5-7.

Table 5-3. Basic parameters of stucco in the case study

Stucco	**1**	**2**
H: cm	5.4	5.5
S_A: cm2	23.64	26.01
A_w: kg/m2s0.5	0.0468	0.0475
ρ: kg/m3	1888	1789

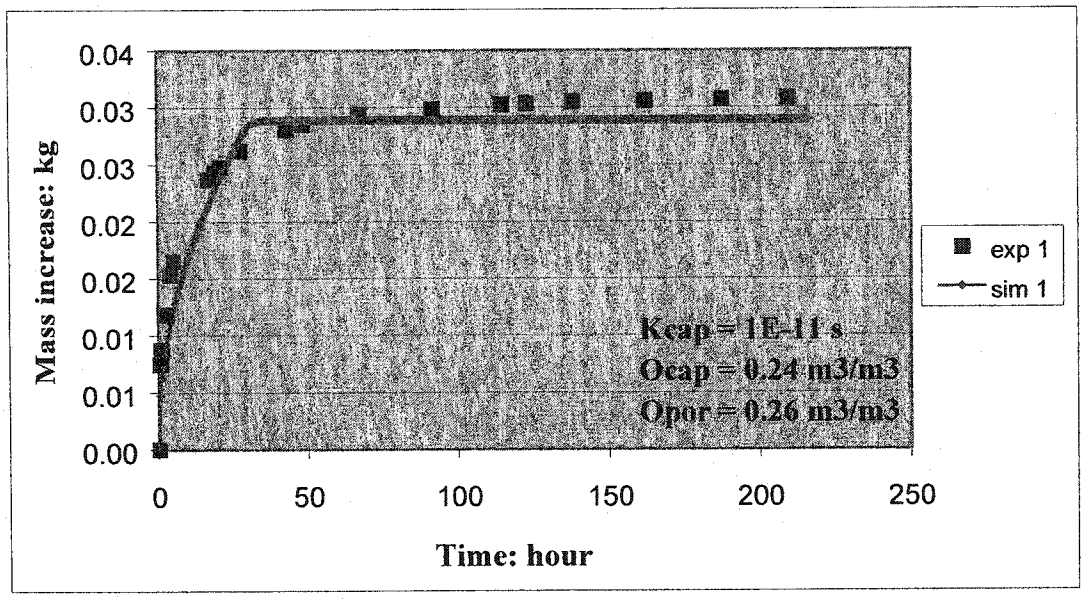

Figure 5-6. Case study on the water absorption process of stucco (Specimen size: 49mm x 54mm x 49mm)

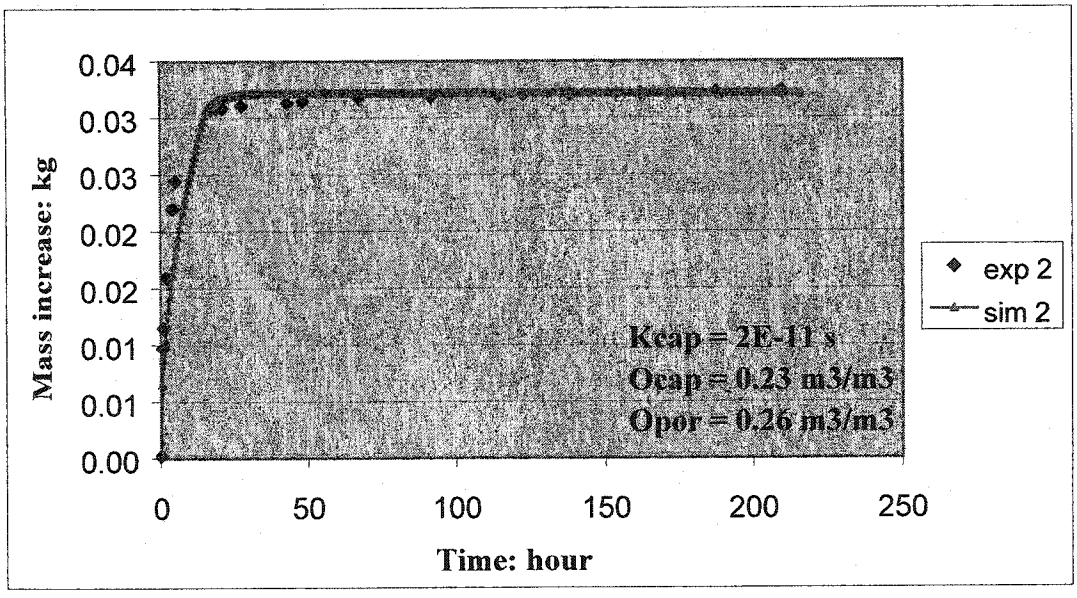

Figure 5-7. Case study on the water absorption process of stucco (Specimen size: 51mm x 55mm x 51mm)

The results shows the input parameters to simulate free water intake of stucco gives good agreement with the inflow curve from measurement. Furthermore, from the simulation, it can be seen, the initial input parameters for stucco are more uniformly distributed, and their range of deviation is smaller than that of AAC. This basically validates the fact that the structures of AAC and stucco are different in nature: while AAC has a multiphase pore structure, and is microscopically heterogeneous; stucco is more uniform in the distribution of pore size, which in turn supports the assumption that Engineering Model is related to material structure.

5.6 Conclusions

In this Chapter, based on the measurement of free water intake of two commonly used building materials: AAC and stucco, series of benchmarking test and calculation are carried out. The study leads to the following conclusions:

- An adequate material characterization and material properties, when appropriately defined, can be used as input for the HAM Model calculation. The number of required input to the HAM Model is reduced to a minimum, and these measurements are relatively easy to perform. The assumption that input for the HAM Model includes a minimum of 6 material properties is validated by the simulation, and agrees with the experiment.

- A comparison between measurement and simulation shows that for AAC, a whole range of capillary moisture content can be listed from 0.26 to 0.34 m^3/m^3 (see

Figure5-1); while for stucco, the capillary moisture content is more uniformly distributed. This indicates material structures for AAC and stucco are essentially different, and characteristic moisture contents are determined by the pore size distribution. This is in agreement with the assumption made for Engineering Model: structure related.

- Simulations of driving rain, an important source of moisture stored in building envelopes, are carried out. Results from calculation indicate rain intensity and rain exchange coefficient are important factors that affect moisture accumulation in building envelopes. A comparative study shows that an increase of either factor leads to the decrease of time to reach capillary saturation, and increased capillary moisture content. Moreover, compared with rain exchange coefficient, rain intensity has more significant impact on the moisture accumulation, in terms of both time to reach the capillary saturation, and the quantity of moisture that can be stored.

- Case study on representative specimens of AAC and stucco shows that for AAC, instead of being a constant value, the input parameters for Engineering Model are distributed in a range, where some of the parameters are responsible for the precision of model predictions; for stucco, the initial input parameters are more uniform. This postulates the need to conduct parametric studies on material properties for AAC so that a precise control of model prediction can be achieved.

CHAPTER 6 PARAMETRIC STUDY

6.1 Introduction

The use of hygrothermal model depends on the adequacy of material characterization and selection of appropriate material properties. Therefore, easy to use and precision in the predictions are the priority concerns for HAM model. The number of initial input parameters has already been reduced, and measurements of these initial parameters are in fact relatively easy to perform. So the next step for the spread for HAM Model is the precisions in the model prediction. As stated in Chapter 5, for some material, the initial input parameters are distributed in a certain range, while others are comparatively uniform in the distribution. Thereof, in this chapter, a parametric study is carried out on AAC wetting and drying, with respect to parameter variations and their interaction effects, including capillary saturation (Ocap), capillary liquid conductivity (Kcap), sorption coefficient (Aw), material porosity (Opor), and storage factor (e).

6.2 Parametric study on capillary saturation

As previously stated capillary saturation may vary over the wide range. The specimen selected for the case study has a dimension of 5.5cm·5.5cm·5.5cm. While capillary saturation (Ocap) changes at three different levels, the other five input parameters are kept at constant value. Figure 6-1 shows the case of Ocap set at three different values: 0.26 m^3/m^3, 0.30 m^3/m^3 and 0.33 m^3/m^3 respectively.

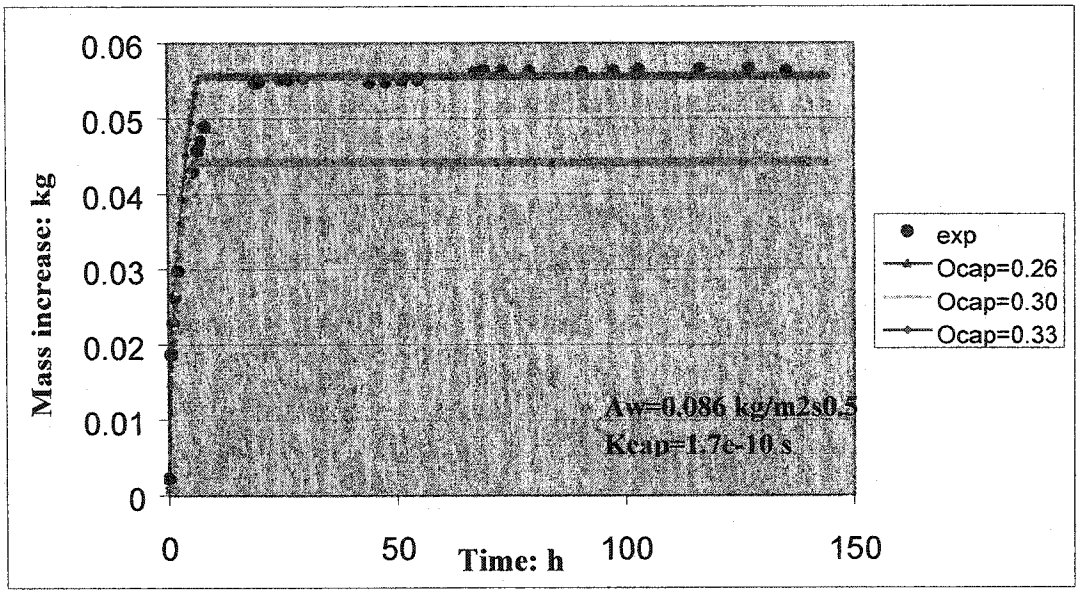

Figure 6-1. Parametric study on capillary saturation (Ocap) of AAC

It should be noted with the increase of capillary saturation, secondary stage of the inflow curve goes up constantly, while the initial stage of the inflow curve does not change, or changes only slightly. Results of the simulation are predictable by limiting the capillary saturation (Ocap) in the input data.

6.3 Parametric study on capillary liquid conductivity

Capillary liquid conductivity (Kcap), as one of the input parameters, can be experimentally measured. Yet, with the knowledge of moisture storage factor, it can be calculated from liquid diffusivity, which comes either from direct measurement, such as gamma ray attenuation, nuclear magnetic resonance, or indirectly calculated from free water intake experiment. The value of Kcap in the present study covers a range from 1.5E-11s to 1.7E-10 seconds, which is calculated from knowledge of storage factor and

free water intake measurement. Kcap of 5.6E-10 s (Dw=1.23E-7m2/s; e=4.6E-3 Qiu. 2002) is calculated from direct measurement of moisture content profile by gamma ray. Simulation results versus measured inflow curve are given in Figure 6-2.

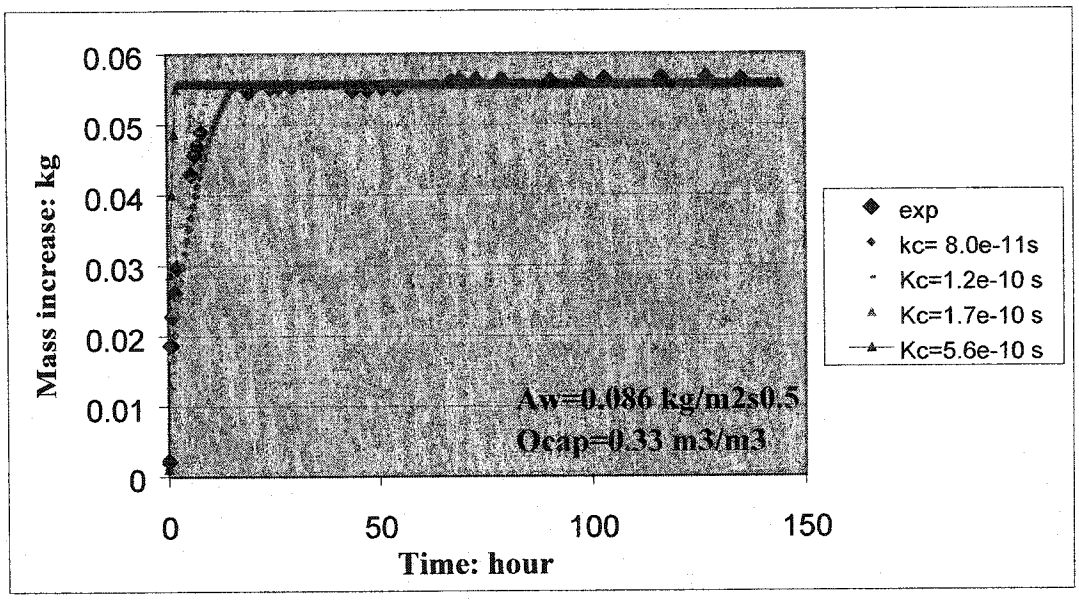

Figure 6-2. Parametric study on capillary liquid conductivity (Kcap) of AAC (Specimen size: 55 mm x 55 mm x 55 mm)

While capillary liquid conductivity is the only changing factor in this case study, the other five input parameters are kept constant. A comparison of different input Kcap values indicates the larger the capillary liquid conductivity, the quicker the material passes through the initial stage of the water inflow, and reaches the capillary saturation faster. From the simulation results, it can be seen the change of Kcap value only influences the time to reach capillary saturation, but does not influence the value of the capillary saturation. It can therefore be concluded that capillary liquid conductivity is

responsible for the control of the initial stage of the inflow curve: it determines the time for material to reach the capillary saturation.

6.4 Parametric study on the relation between Aw and Kcap

Three specimens with different water absorption coefficient values were selected for the case study. The selected sorption coefficient values represent the minimum, medium, and maximum value from the whole range. Results from simulation versus measurement are shown in Figures 6-3, 6-4 and 6-5.

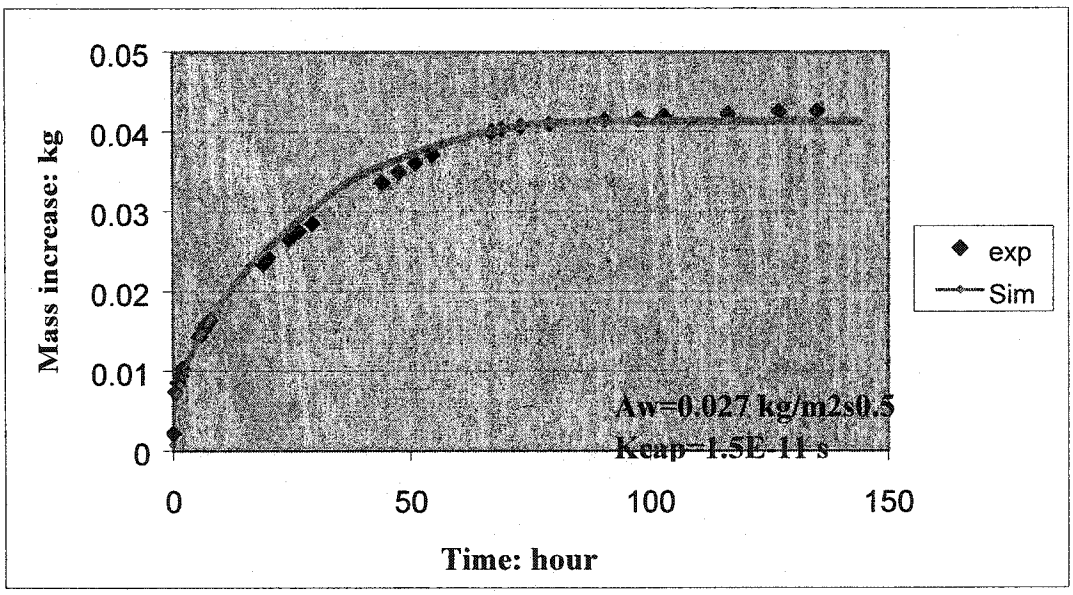

Figure 6-3. Case study on AAC with minimum Aw

(Specimen size: 53mm x 57mm x 53mm; Ocap=0.26 m^3/m^3, Opor=0.75 m^3/m^3)

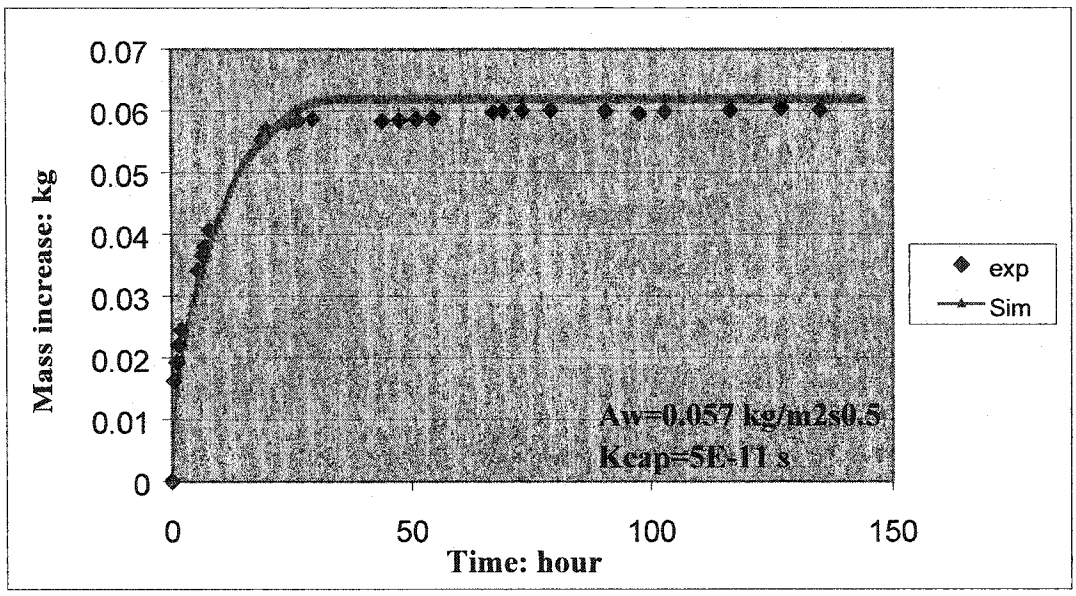

Figure 6-4. Case study on AAC with medium Aw

(Specimen size: 58mm x 57mm x 58mm; Ocap=0.33 m^3/m^3, Opor=0.75 m^3/m^3)

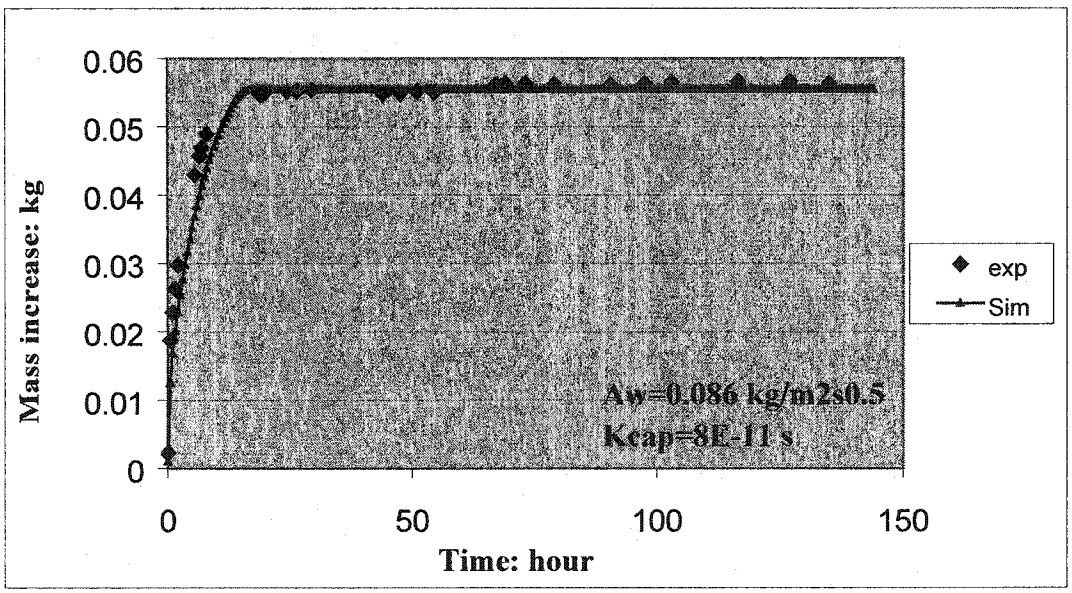

Figure 6-5. Case study on AAC with maximum Aw

(Specimen size: 55mm x 55mm x 55mm; Ocap=0.33 m^3/m^3, Opor=0.75 m^3/m^3)

It can be seen from the simulation with the increase of water absorption coefficient from 0.027 to 0.086 $kg/m^2s^{0.5}$, capillary liquid conductivity increases accordingly from 1.5E-11 to 8.0E-11s. Also noticeable is the time to reach the capillary saturation: a larger water absorption coefficient is accomplished by a larger capillary liquid conductivity, and a shorter time to pass the initial stage of water inflow to reach the capillary saturation. This is in agreement with conclusion from the parametric study on the capillary liquid conductivity.

6.5 Parametric study on material porosity

Since Engineering Model is related to material structure and its characteristic moisture content is associated with the pore size distribution, porosity is taken into account as one of the parameters that may influence the precision of model predictions. In this section, case studies are carried out in terms of two different situations: with constant capillary saturation; with capillary saturation proportional to the porosity change.

6.5.1 Case study with constant capillary saturation

In this series of simulation, capillary saturation is kept at constant value while porosity varies from 0.70 to 0.88 m^3/m^3, which represents the possible range of changes according to Annex24 Report on Material Properties for HAM Model Simulation. Values of three different levels are selected: 0.70, 0.77, and 0.88 respectively. The results of the simulation are given in Figure 6-6.

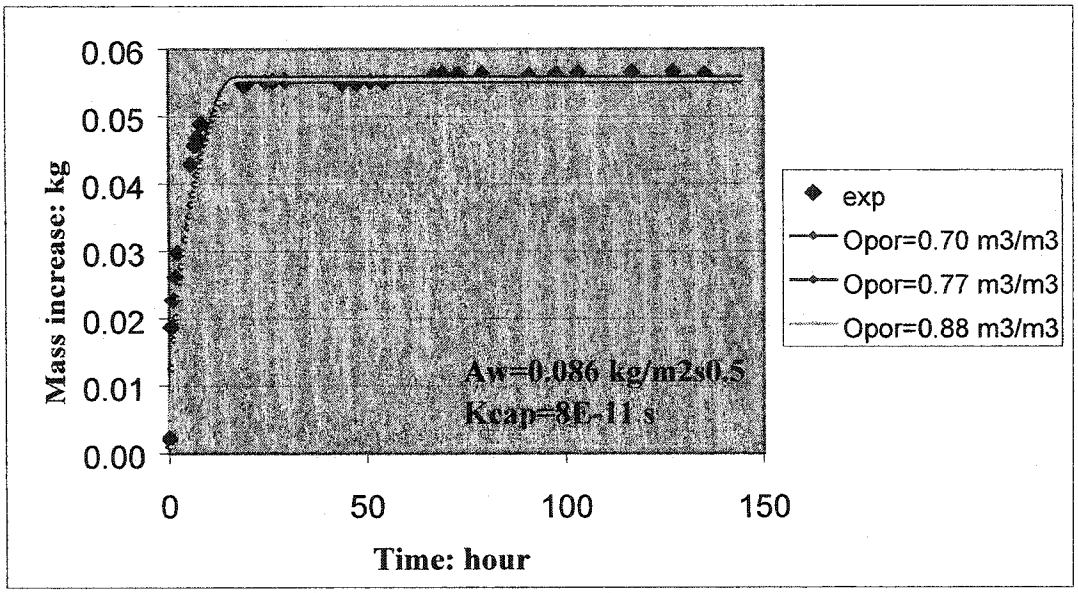

Figure 6-6. Parametric study on porosity with constant capillary saturation

(Specimen size: 55mm x 55mm x 55mm)

It can be noticed that the changes of material porosity alone without any change in capillary saturation shows no difference.

6.5.2 Case study with capillary saturation proportional to porosity change

In the second series of simulation, capillary saturation is proportional to the changes of material porosity. Different levels of capillary saturation match material porosity set at three values respectively (*Ocap1=0.26* m^3/m^3, *Opor1=0.70* m^3/m^3; *Ocap2=0.30* m^3/m^3, *Opor2=0.77* m^3/m^3; *Ocap3=0.33* m^3/m^3, *Opor3=0.88* m^3/m^3). Results of the simulation are given in Figure 6-7.

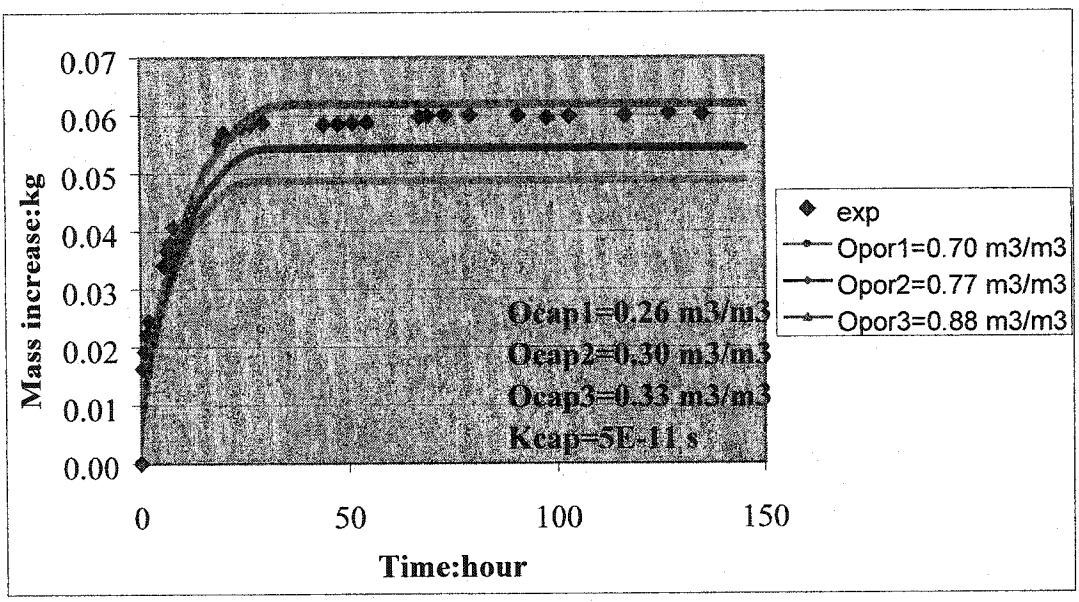

Figure 6-7. Parametric study on porosity with proportional capillary saturation changes

(Specimen size: 58mm x 57mm x 58mm)

The results of this series are noticeably different compared with previous calculations (6.5.1). The difference lies in the secondary stage of water inflow: the capillary saturation value varies from each other. Considering there's no obvious difference in the result of the previous simulation where capillary saturation is constant, the difference in the second series can be then explained in such a way that rather to say the proportional change of capillary saturation to the total porosity variation leads to the difference, it may be concluded that capillary saturation plays a more significant role in determining the model prediction than the material porosity. Yet, this does not mean that material porosity is not important, but material porosity, when compared with capillary saturation, does not have much influence on the control of model predictions.

It should also be noticed when comparing present calculations with the one, where Opor is constant, and Ocap is changing (6.2). In both cases, Ocap changes at three different levels: 0.26, 0.30, and 0.33 m^3/m^3, however, there exists clear difference in the transition area from the first stage to the second stage of water inflow. It can be observed that when Ocap changes proportional to the variations of Opor, the transition area is more flat, whereas when Opor is kept constant, the change of Ocap leads to a sharp transition between the first and the second stage (See Figure 6-1.). This indicates there's interaction between material porosity and capillary saturation, and this interaction has an impact on the precision of model predictions.

6.6 Drying-based parametric study for model control

The mechanism of drying is complicated: on the one hand, there's hysteresis involved between wetting and drying; on the other hand, it's difficult to precisely define the boundary conditions, i.e., surface resistance for vapor transfer. However, with the knowledge of the relationship between wetting and drying moisture storage factor, the simulation of drying can be calculated from that of wetting. In this section, parametric studies are carried out, based on the drying experiment of AAC, in terms of capillary liquid conductivity and moisture storage factor.

6.6.1 Drying rate to control model prediction

An AAC specimen with dimension of 58 mm x 53mm x 58mm was taken as benchmark. The specimen was sealed on its five surfaces with one side exposed to air. Temperature and relative humidity of the environment were recorded timely: they were measured 5

times a day, and were reported in the thesis appendix. The average value of temperature was 21.72 ± 0.98°C and that of relative humidity was 10.36 ± 2.6 %. Simulation of drying based on capillary liquid conductivity set at three different values is carried out. Results from calculation versus measurements are shown in Figure 6-8.

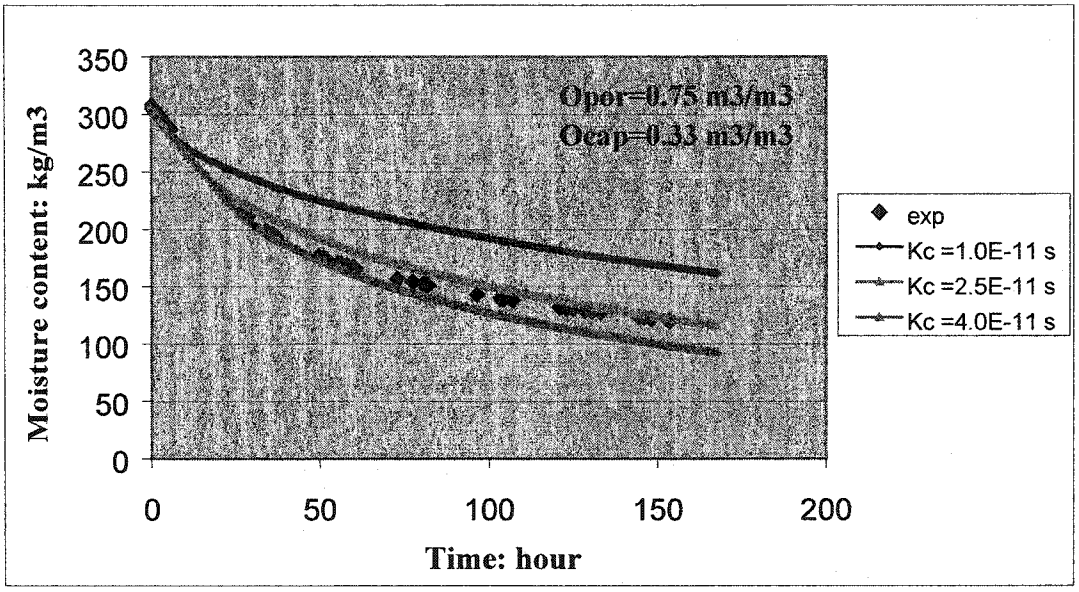

Figure 6-8. Parametric study on capillary liquid diffusivity for drying

It can be noticed that the rate of drying is strongly associated with the capillary liquid conductivity: an increase in the capillary liquid conductivity leads to a higher drying rate.

6.6.2 Parametric study on moisture storage factor

There's significant difference between wetting and drying moisture retention curve due to the different mechanisms involved. As a result, the moisture storage functions are not the same for both cases. The drying experiment is very sensitive on the moisture transfer coefficient in the middle moisture content region, therefore, the setup for drying

experiment can have an influence on the accuracy of the measurement in a very subtle way. This presents some practical difficulties for an accurate measurement of drying rate. However with the knowledge of MRC, this problem can be solved with ease: to find the change of storage factor between wetting and drying needed to get the same liquid diffusivity that is used to get the kcap to fit the drying calculations. Simulation results versus measurement for three specimens are given in Figure 6-9, 6-10, 6-11.

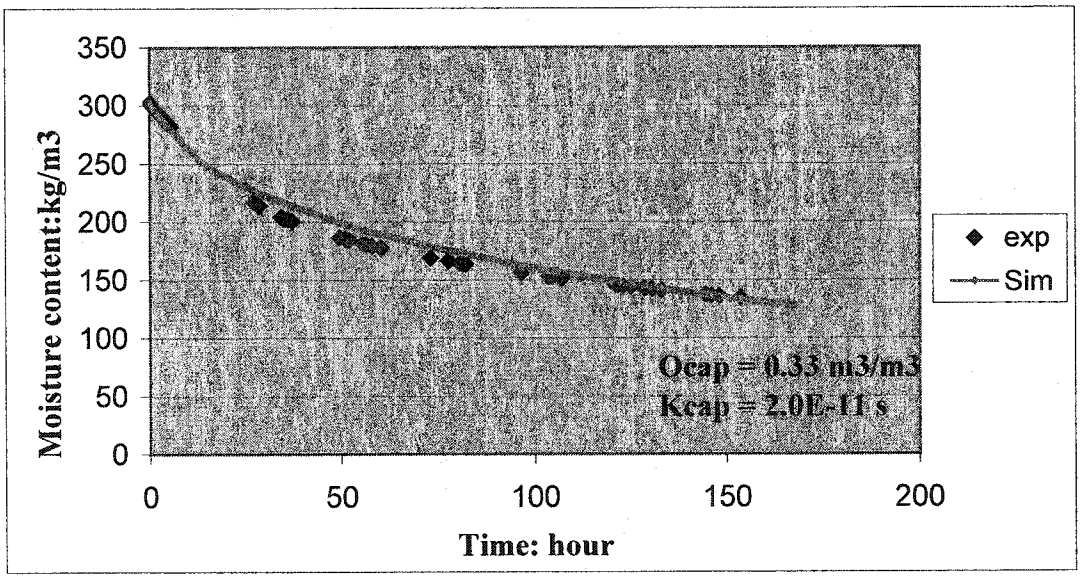

Figure 6-9. Parametric study on moisture storage factor

(Opor=0.75 m^3/m^3; specimen size: 54mm x 58mm x 54mm)

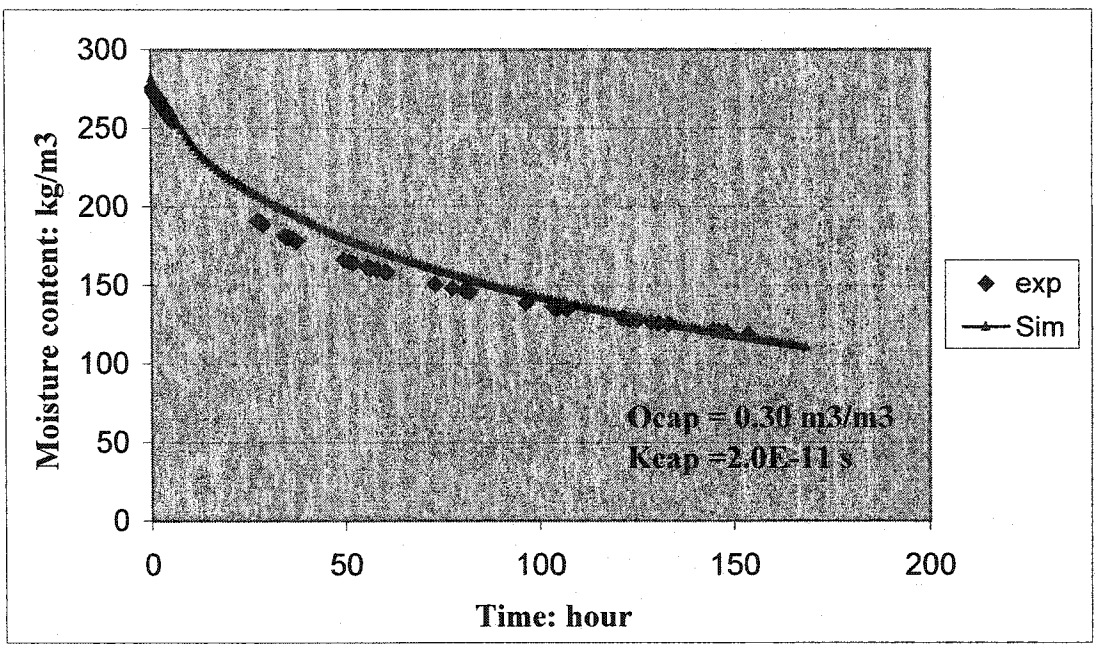

Figure 6-10. Parametric study on moisture storage factor

(Opor=0.75 m^3/ m^3; specimen size: 53mm x 57mm x 53mm)

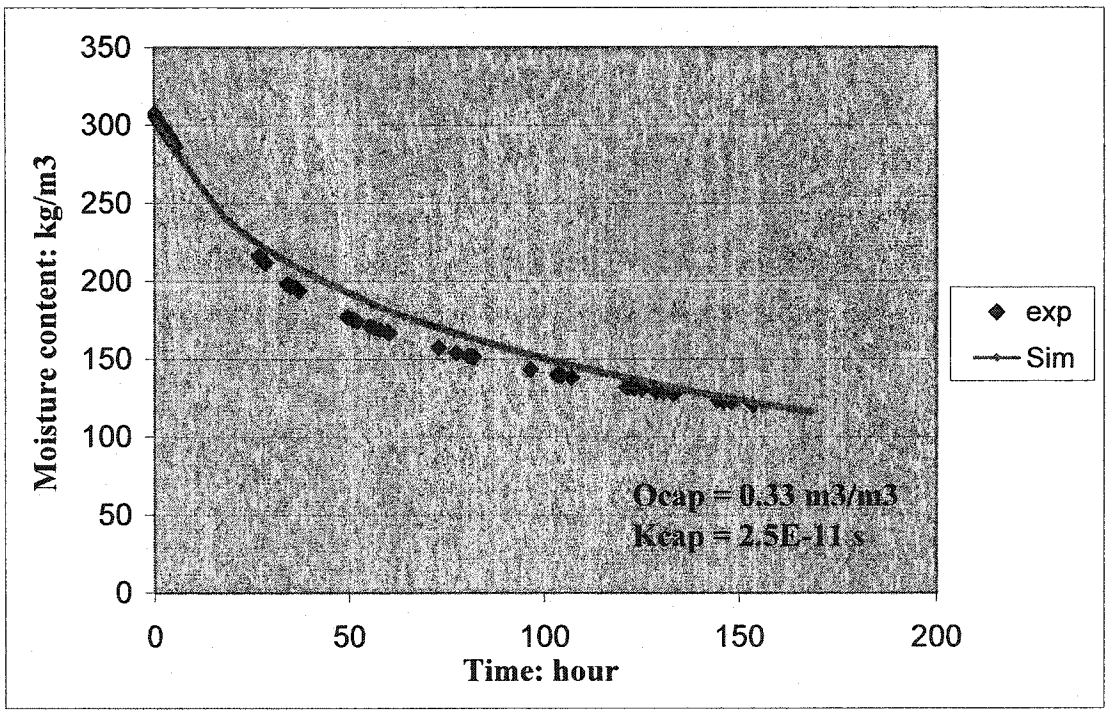

Figure 6-11. Parametric study on moisture storage factor

(Opor=0.75 m^3/ m^3; specimen size: 53mm x 58mm x 53mm)

Modification of storage factor to fit the drying calculations is given in Table 6-1.

Table 6-1.Results of drying calculation concerning the storage factor change

$Kcap_1$	2E-11	2E-11	2.5E-11
e_w	4.59E-03	4.59E-03	4.59E-03
D_L	4.36E-09	4.36E-09	5.45E-09
$Kcap_2$	1.72E-10	1.72E-10	1.72E-10
e	3.95E-02	3.95E-02	3.16E-02
e / e_w	8.60	8.60	6.88

Where $kcap_1$ is the capillary liquid conductivity that fits the drying curve;

e_w is the moisture storage factor determined by wetting;

D_L is the liquid diffusivity determined during the drying calculation;

$Kcap_2$ is the capillary liquid conductivity obtained from wetting calculation;

e is the changed storage factor that gives the same Dl as determined by drying.

It can be seen from Table 6-1 the wetting moisture retention curve of AAC has to be modified in such a way that e_w should be increase 8 times in order to fit the drying calculations.

6.7 Summary of the parametric studies

HAM model used for hygrothermal analysis requires a minimum of six parameters as initial input, which include material porosity (Opor), capillary saturation (Ocap), water vapor permeability at 25%RH (WVP), liquid diffusivity (D_L), two points from sorption curve with equilibrium moisture content at selected RH and another two points from over-hygroscopic region of MRC as well. Therefore, the application of HAM model depends on how well the material properties are known and presented. In this chapter, a parametric study was carried out to find the impacts of the input parameters and their interactions on the precision of the HAM model predictions. It was found that:

- Capillary saturation (Ocap) is responsible for the control of the secondary stage of the inflow curve, and determines the maximum value that can be reached during the water absorption process.
- Capillary liquid conductivity (Kcap) is responsible for the control of the initial stage of the inflow curve and determines the time for material to reach the capillary saturation. The larger the capillary liquid conductivity, the quicker the material passes through the initial stage of the water inflow.

- A larger water absorption coefficient (Aw) is accomplished by a larger capillary liquid conductivity, and a shorter time to pass the initial stage of water inflow to reach the capillary saturation.
- Material porosity (Opor) has minor effect on the control of model predictions. In comparison, capillary saturation plays a more significant role in determining the precisions of model control. There's interaction between material porosity and capillary saturation. This interaction has an impact on the control of model predictions.
- The drying rate is influenced by capillary liquid conductivity (Kcap): an increase in the capillary liquid conductivity leads to a higher drying rate.
- There's hysteresis effect involved between wetting and drying. With the knowledge of moisture storage factor change, the simulation of drying can be calculated from that of wetting. Study conducted on AAC indicates its wetting moisture retention curve has to be modified in such a way that e_w should be increased 8 times in order to fit the drying calculation.

CHAPTER 7 CONCLUSIONS AND RECOMMENDATIONS FOR THE FUTURE RESEARCH

While each chapter included discussion of findings and interim conclusions, the main conclusions from this work are listed below.

7.1 Main conclusions

Numerous models that describe moisture transfer have been developed for the hygrothermal analysis of building envelopes. A state-of-art review indicates, however, that the application of existing HAM models is restricted because of the lack of reliable material data. To this end, an engineering level material characterization based on the description of material porosity has been proposed and is examined in this thesis. Series of experiments were conducted on two commonly used building materials, AAC and stucco to provide a basis for an analysis of proposed method and examine to what extent the model benchmarking can help in improving precision of material characterization. The above discussed study leads to the following conclusions:

- The pore structure of two materials selected for the study namely AAC and stucco were very different. While AAC is a multi-phase system consisting of two distinctly different types of pores; stucco is more homogeneous in structure. It was not surprising that a 2-parameter model was found more precise and better describing the water intake process to the AAC than 1-parameter model.

- The knick point of water absorption vs. square root of time for stucco is clear, leading to an unambiguous determination of the capillary moisture content. Conversely, the knick point of similar curve determined on AAC shows a transition region and the capillary moisture content was found varying in a range of moisture content from 0.26 to 0.34 m^3/ m^3. Furthermore, the capillary moisture content for AAC obtained by gammy ray measurement by Qiu (2002) does not agree with the simulation results even though these tests were performed on the same specimens that were previously used by Qiu (2002).

- If liquid diffusivity coefficient is calculated from water absorption coefficient (Aw), then the Aw must be precisely determined. Ruggedness study was performed in this thesis to show that this was not the case for aerated autoclaved concrete: the A coefficient of AAC is influenced by a large number of factors. There is a need for improvement in the test method used for the determination of A-coefficient.

- Engineering Model helps bridge between practical and research application of HAM models. (Grunewald 2002). As a requirement for the proposed platform included

  1) Total open porosity of the material
  2) Capillary saturation
  3) Liquid water diffusivity
  4) Water vapor permeability

5) Two points from sorption curve (equilibrium MC at selected RH)

6) Two points from over-hygroscopic region of MRC

These material characteristics have been validated in HAM model simulations.

- Using material characteristics from the wetting benchmark to that of drying highlighted the effect of hysteresis between wetting and drying. It was also found in the present study, that the fitness of Engineering Model could be improved by applying both the wetting and drying benchmark tests and checking if the same liquid conductivity coefficient is achieved at the capillary moisture content.

7.2 Recommendations for future research

Based on the present study, some suggestions are made for future work. They can be summarized as follows:

- Precision of test method to determine water absorption coefficient should be improved. Based on the result of ruggedness study, an experimental factorial design is recommended to find out interactions between each factor, and how these interactions affect the test precisions.

- Capillary saturation may depend on the conditions applied during performing the test. This issue needs to be carefully examined and it is recommended to establish

the significance of factors affecting precision of a practical test method for the determination of the capillary moisture content.

- It is recommended that Engineering Model be used in developing a database for hygrothermal material properties of common building materials.

REFERENCES

- Annex24 Report on Material Properties. Building Performance Laboratory, Institute for Research in Construction, National Research Council, Canada

- ASTM standard (1994), "Standard Test Methods for Water Vapor Transmission of Materials. " Annual Book of ASTM Standards, Vol. 04.06.

- Arfvidsson J (1998), "Moisture transport in porous media." Ph.D. Thesis, Lund University.

- Bednar T (1998), "Influence of the variation of material properties and uncertainties of the material data model on the results of moisture performance calculations of constructions. " Institute for Building Materials, Building Physics and Fire Protection, University of Technology Vienna.

- Bednar T (2002), "Approximation of liquid moisture transport coefficient of porous materials by suction and drying experiments. Demands on determination of drying curve." Proceedings of Building Physics 2002—6th Nordic Symposium.Vol 2, pp493-500

- Bomberg M (1973), Moisture flow through porous building materials. Thesis. Lund University, Sweden.

- Bomberg M, Grunewald J (2002), "Issues for discussion of CIB W40 TG on material characterization and model benchmark. " www.cibw40.org.

- Bomberg M, Carmeliet J, et al (2002), "Position paper on material characterization and HAM model benchmarking." Nordic Building Physics Symposium 2002, Dresden Germany.

- Bomberg M (2002), "Unresolved issues in developing engineering model of material characteristics for input to HAM transport simulations. " Sep, 04, 2002. Submitted for discussion in 2003 Dresden meetings.

- Brocken H. J. P (1998), "Moisture transport in brick masonry: the grey area between bricks. " Ph.D. thesis at Technical U. of Eindhoven.

- Burch, D. M., Zarr, R. R., and Fanney, A. H (1995), "Experimental Validation of a Moisture and Heat Transfer Model in the Hygroscopic Regime." *Proceedings of Thermal Performance of the Exterior Envelopes of Buildings VI,* Clearwater Beach, FL, 4–8 pp. 273–281.

- Carmeliet J, Roels S (2000), "Determination of the Isothermal Moisture Transport Properties of Porous Building Materials." Journal of Thermal Envelope & Building Science. Vol 24-January 2001, pp183-210.

- Carmeliet J, Roels S (2002), "Description of moisture capacity of building materials." Proceedings of Building Physics 2002—6th Nordic Symposium. Vol 2, pp485-493

- Carmeliet J., Roels S (2002), "Optimal determination of the moisture capacity of porous building materials. " Journal of Thermal Envelope and Building. Science, January 2002, in press.

- Cunningham, M. J (1990), "Modeling of Moisture Transfer in Structures—I. A Description of a Finite-Difference Nodal Model. " Bldg. and Environ., Vol. 25, No. 1, 1990, pp. 55–61.

- Cunningham, M. J (1990), "Modeling of Moisture Transfer in Structures—II. A Comparison of a Numerical Model, an Analytical Model, and Some Experimental Results. " Bldg. and Environ., Vol. 25, No. 2, 1990, pp. 85–94

- Cunningham, M. J (1994), "Modeling of Moisture Transfer in Structures—I. A Comparison Between the Numerical Model SMAHT and Field Data." Bldg. and Environ., Vol. 29, No. 2, 1994, pp.191–196.

- Descamps F (1997), "Continuum and discrete modelling of isothermal water and air transfer in porous media. " PhD Thesis, Catholic University Leuven. Leuven, Belgium.

- Graham H. Galbraith, et al (1999), "Moisture permeability data presented as a mathematical function applicable to heat and moisture transport models." Glasgow Caledonian University.

- Grunewald J, Bomberg M (2000), "Towards an engineering model of material characteristics for input to HAM transports simulations, Part 1: An approach"

- Grunewald J, Bomberg M (2001), "An engineering approximation of material characteristics for input to Heat, Air and Moisture transport simulations." 7th International conference on Building Physics in Nordic Countries, Vol 1. Dresden Technology University Press, Germany.

- Grunewald J, Plagge R, Bomberg M (2001), "Introduction to material characterization for input to HAM models." ICBEST 2001 Conference, Ottawa, Canada.

- Grunewald J, Plagge R, Bomberg M (2001), "Advantages and disadvantages of lumped parameter or phase-dividing HAM-models." ICBEST 2001 Conference, Ottawa, Canada.

- Grunewald J, Plagge R, Häupl P (2001), "Numerical and experimental investigation of Coupled Heat, Air, Moisture and Salt Transport Problems." ASHRAE 2001 Conference, Oak Ridge, USA.

- Grunewald J, Houvenaghel G (1998), "Final report of Task 2: Modeling. European ProjectBE96-3290--Development of a new methodology to analyse the durability of facade repair and retrofitting systems. "

- Grunewald J (1998), "Final report of Task 5:Numerical simulation and program development. European Project BE96-3290--Development of a new methodology to analyse the durability of facade repair and retrofitting systems."

- Grunewald J, Funk M, Scheffler G (2002), "Engineering Model of the numerical Heat and Moisture Transport Simulation Program DELPHIN4." Institute of Building Climatology, Faculty of Architecture, Technology University of Dresden, Zellescher Weg 17, 01069 Dresden.

- Grunewald J, Bomberg M (2002), "An engineering approximation of material characteristics for input to Heat, Air and Moisture Transport Simulations." Institute of Building Climatology, Faculty of Architecture, Technology University of Dresden, Zellescher Weg 17, 01069 Dresden.

- Hall C and Hoff W.D (2002), "Water Transport in Brick, Stone and Concrete." Spon Press, London and New York, 2002, ISBN 0-419-22890-X.

- Holm A, Kunzel H.M (1996), "Non-isothermal Moisture Transfer in Porous Building Materials." Fraunhofer-Institut for Building Physics, Holzkirchen, Germany.

- Huang Y, Zhang GQ, Haghighat F (2001), "Modeling of moisture transfer in porous building materials: a literature review." Proceedings of the Fourth International Conference on Indoor Air Quality, Ventilation and Energy Conservation in Buildings, pp.807-814, Vol 2.

- Janz M (2000), "Moisture transport and fixation in porous materials at high moisture levels." Doctoral Dissertation, October 2000, Division of Building Materials, Faculty of Technology, Lund University, Sweden.

- Krus M and Holm A (2002), "Simple methods to approximate the liquid transport coefficients describing the absorption and drying." Nordic Building Physics Symposium 2002, Dresden Germany.

- Mukhopadhyaya P, et al. (2002), "Effect of surface temperature on water absorption coefficient of building materials. " Journal of Thermal Envelope & Building Science. Vol 26, No.2 -October 2002, pp179-195.

- Paule, R.C., George M, Melissa K (1986), "Ruggedness Testing—Part I: Ignoring Interactions. " *J. Res. Natl. Bur. Stand.*, vol. 91, NO. 1 pp. 3–8.

- Plagge R., Grunewald J., Häupl P (1999), "Application of Time Domain Reflectometry to Determine Water Content and Electrical Conductivity of Capillary Porous Media." 5th Symposium on Building Physics in the Nordic Countries, Chalmers University of Technology, Sweden.

- Qiu X, Haghighat F, et al. (2002), "Modeling moisture accumulation in multi-layered building materials." Proceedings of eSim, pp.147-154, September 11-13th, 2002, Montreal, Quebec, Canada.

- Roels S (2000), "Modeling unsaturated moisture transport in heterogeneous limestone. " Ph.D. Thesis at Kat. University of Leuven.

- Standard Guide for Conducting Ruggedness Tests (1994), "ASTM Designation: E1169-89. " Volume 14.02 of *1994 Annual Book of ASTM Standards*, pp. 692–697.

- Straube J, Burnett E (2002), "Review of Modeling Methods for Building Enclosure Design." Civil Engineering Dept. and School of Architecture, University of Waterloo, Ontario, Canada.

- Straube J, Burnett E (2002), "Overview of Hygrothermal (HAM) Analysis Methods. " Civil Engineering Dept. and School of Architecture, University of Waterloo, Ontario, Canada.

- Wernimont, Grant (1977), "Ruggedness Evaluation of Test Procedures. " *ASTM Stand. News*, pp. 13–16.

APPENDIX A

Detailed Results of Ruggedness Study on Water Absorption Coefficient of AAC: the first series

Graphic presentations of water intake process for all the specimens in the first series of test are given below:

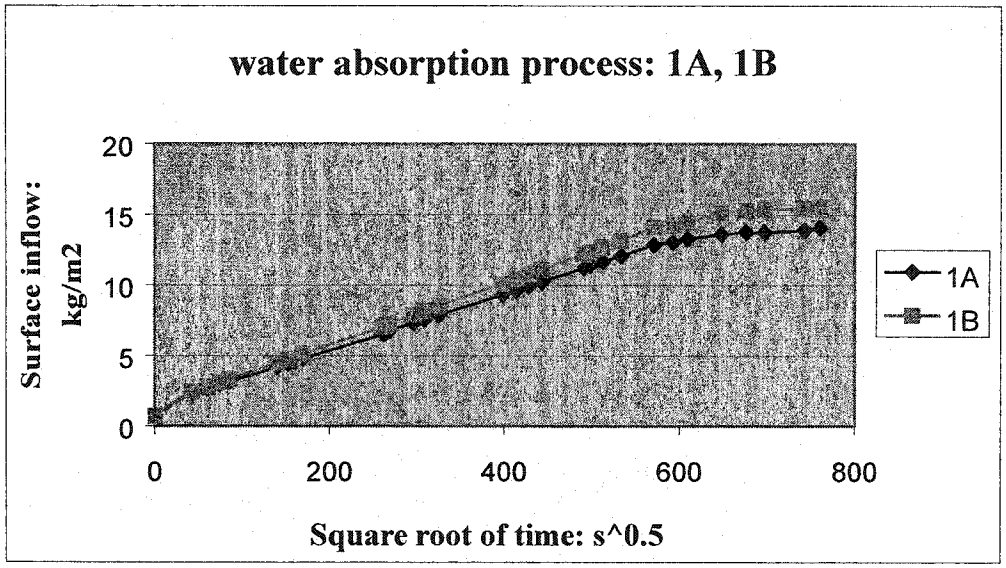

Figure A-1. Water absorption process of 1A, 1B in the first series

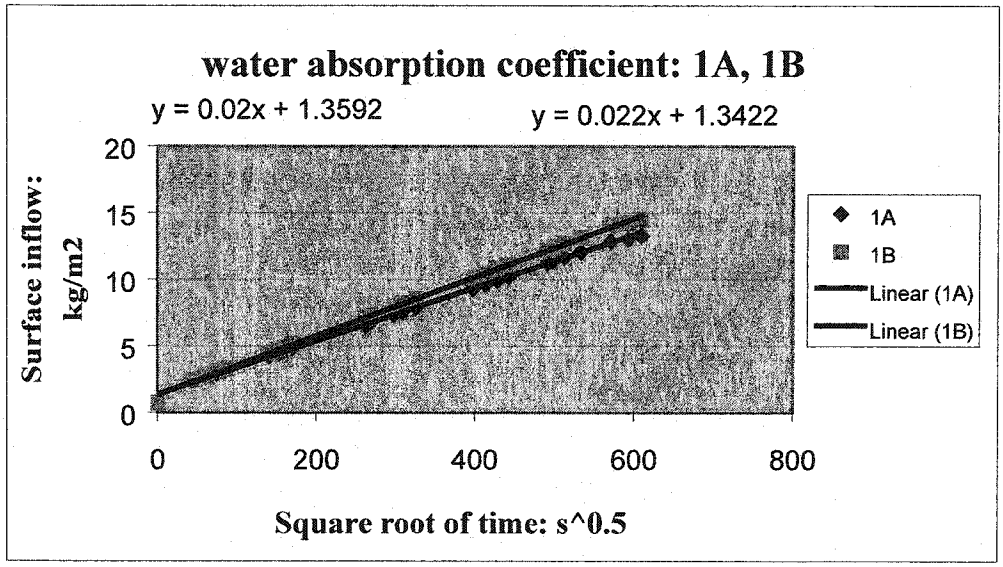

Figure A-2. Water absorption coefficient of 1A, 1B in the first series

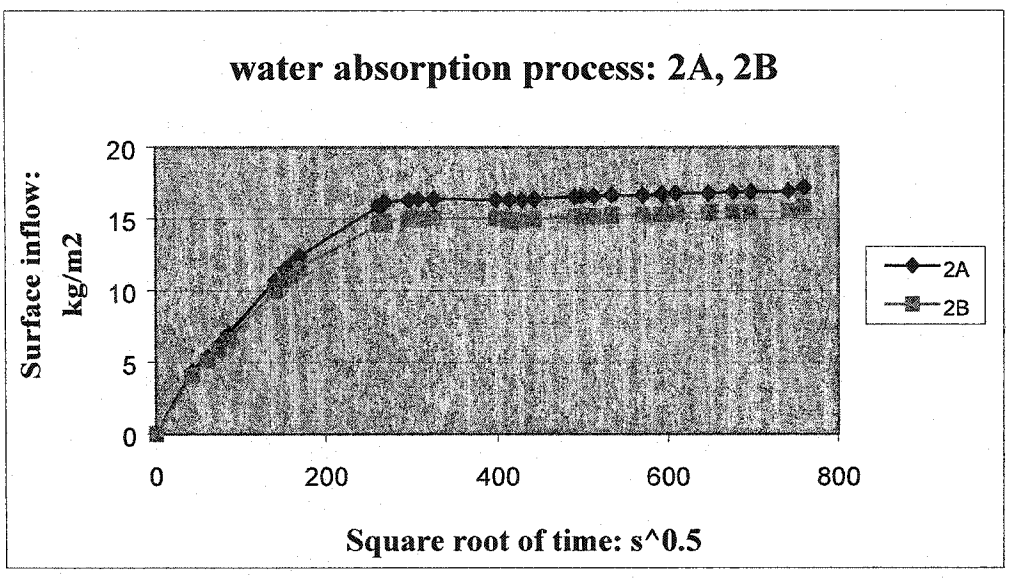

Figure A-3. Water absorption process of 2A, 2B in the first series

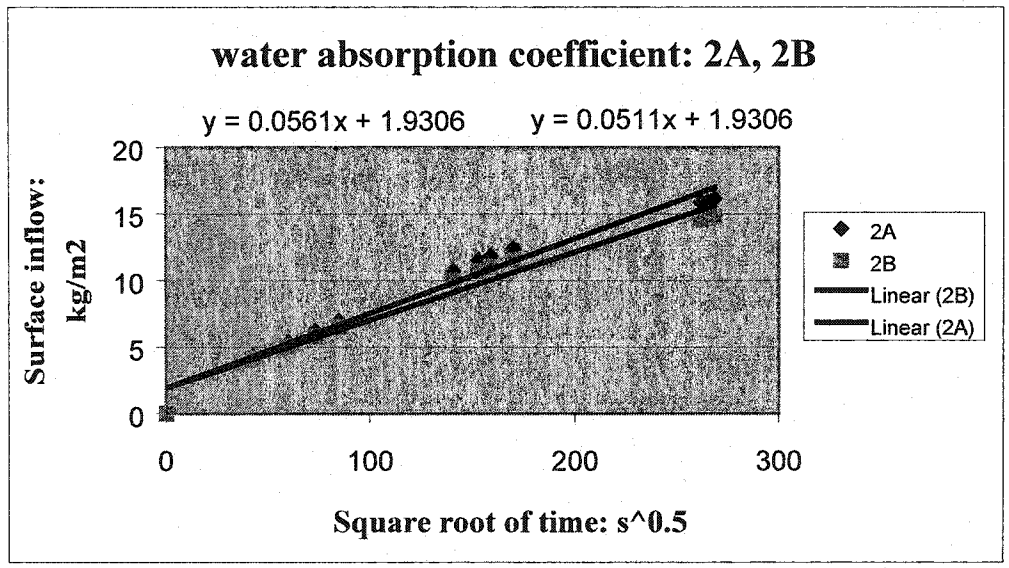

Figure A-4. Water absorption coefficient of 2A, 2B in the first series

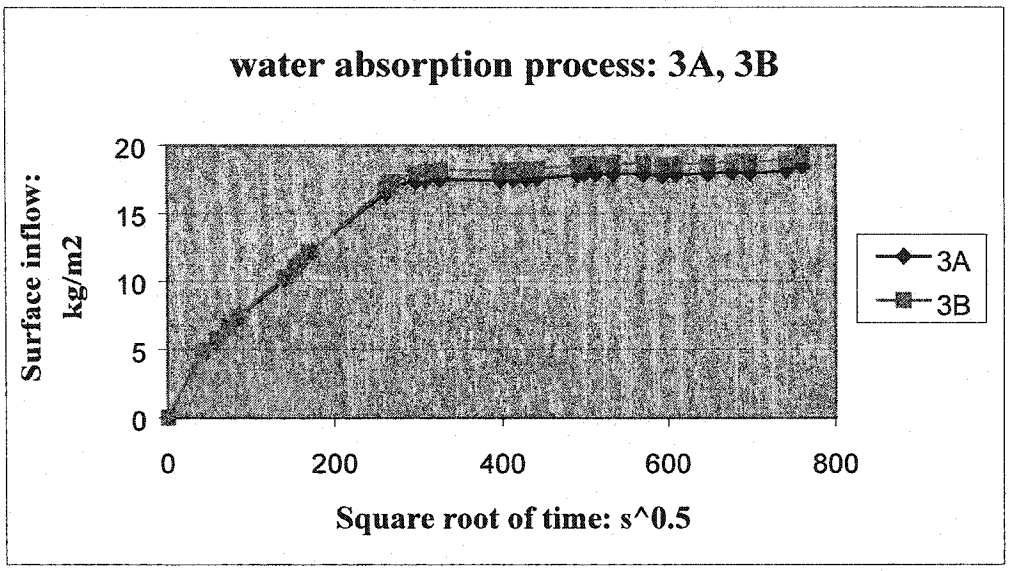

Figure A-5. Water absorption process of 3A, 3B in the first series

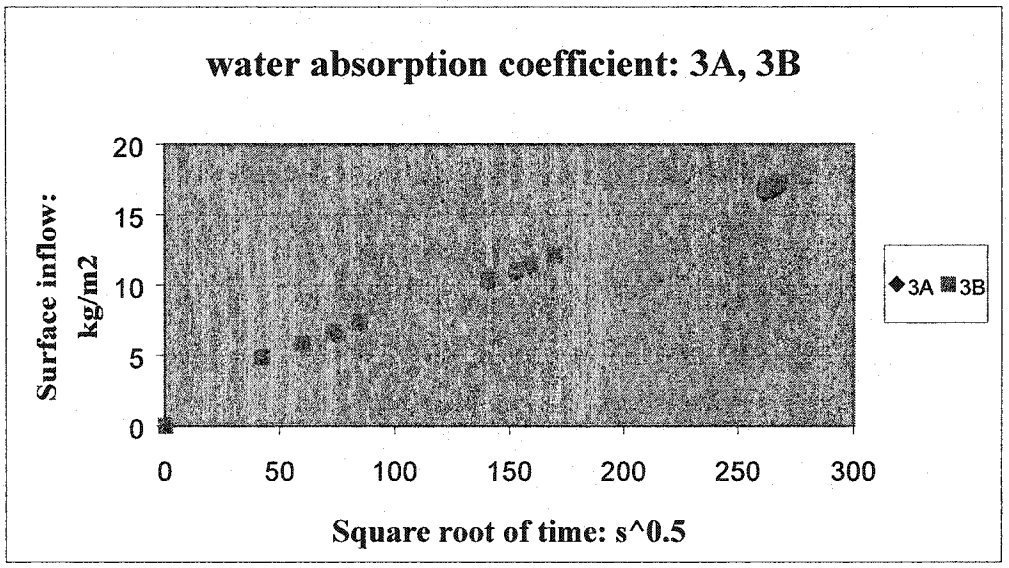

Figure A-6. Water absorption coefficient of 3A, 3B in the first series

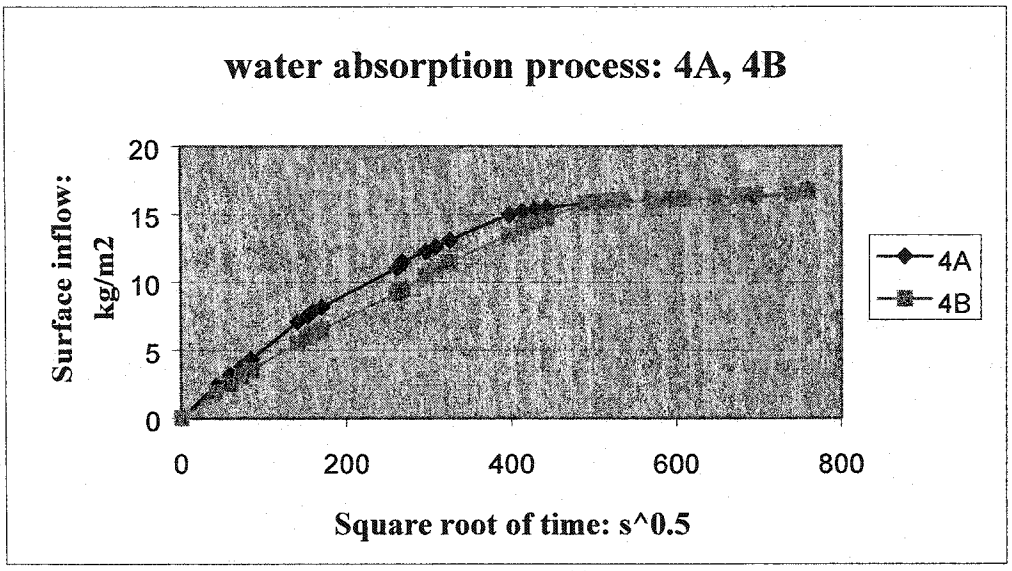

Figure A-7. Water absorption process of 4A, 4B in the first series

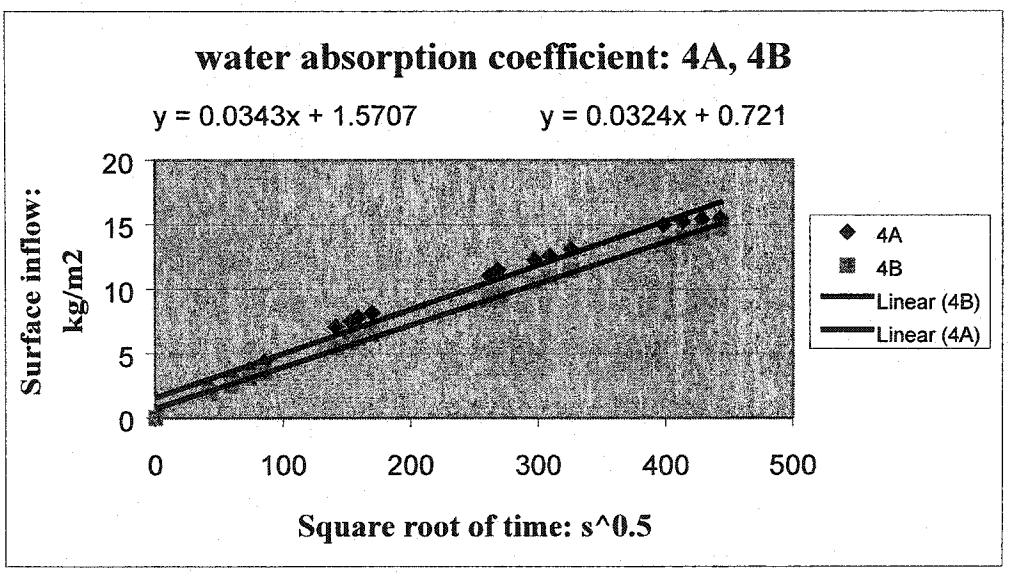

Figure A-8. Water absorption coefficient of 4A, 4B in the first series

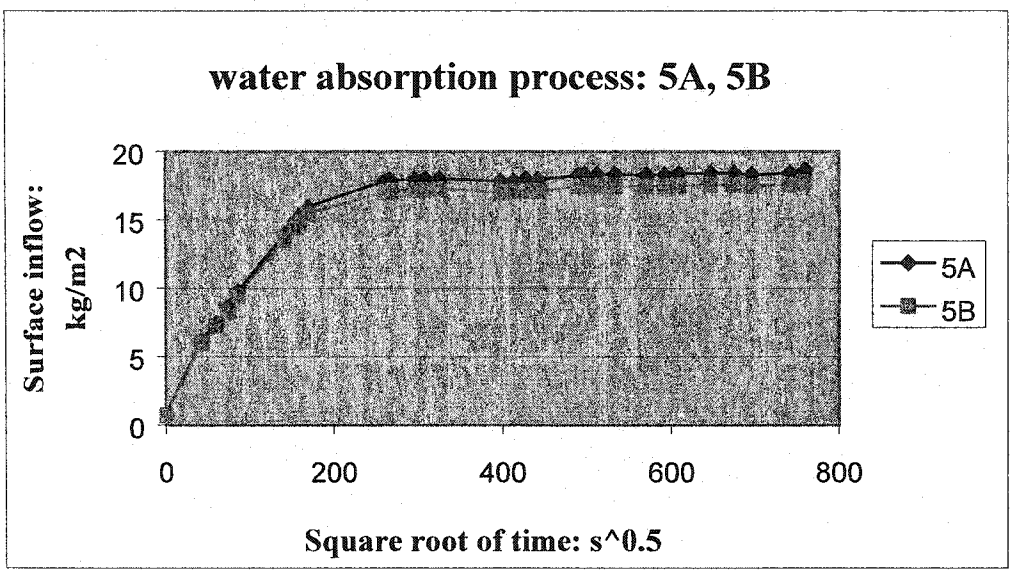

Figure A-9. Water absorption process of 5A, 5B in the first series

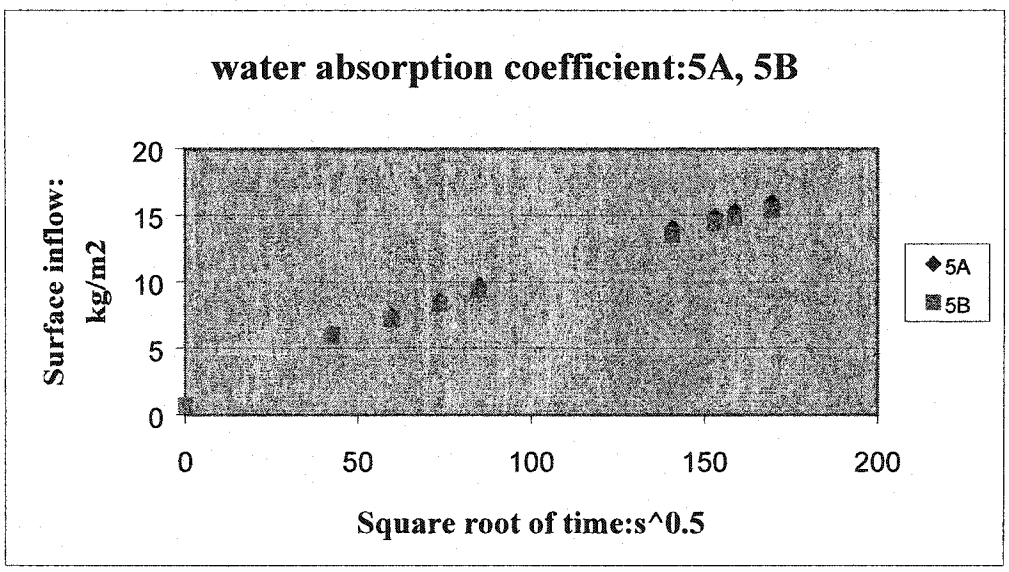

Figure A-10. Water absorption coefficient of 5A, 5B in the first series

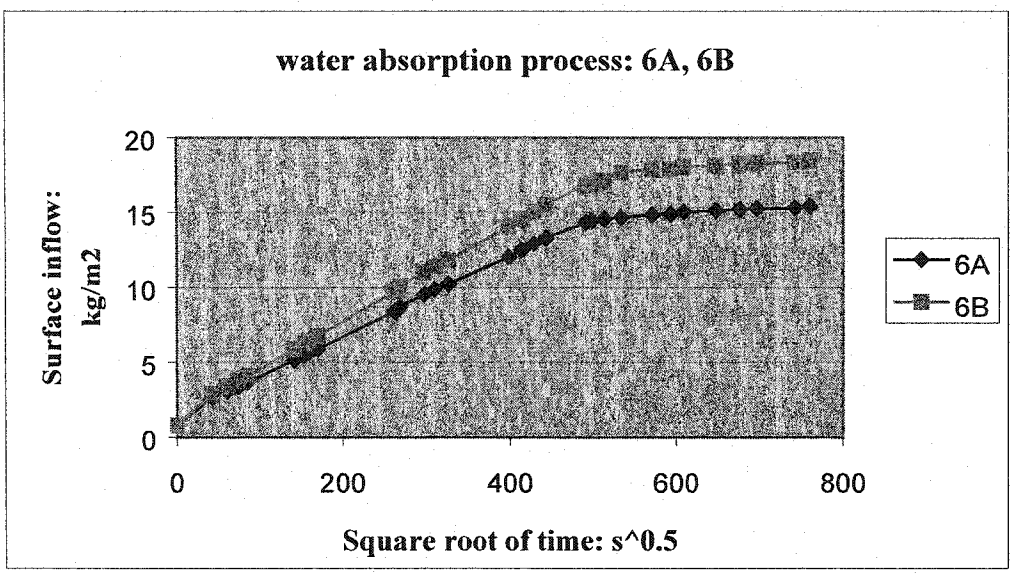

Figure A-11. Water absorption process of 6A, 6B in the first series

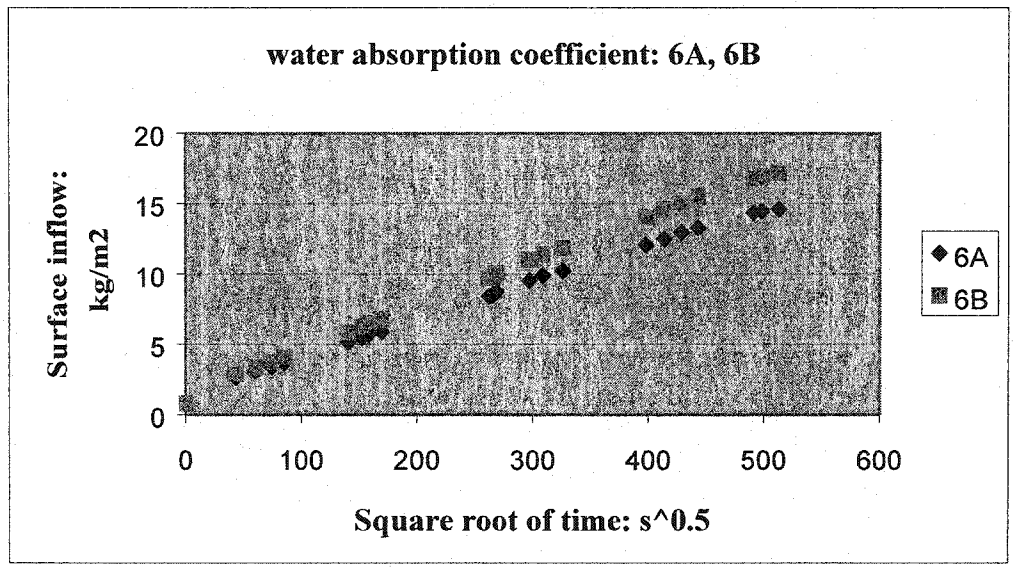

Figure A-12. Water absorption coefficient of 6A, 6B in the first series

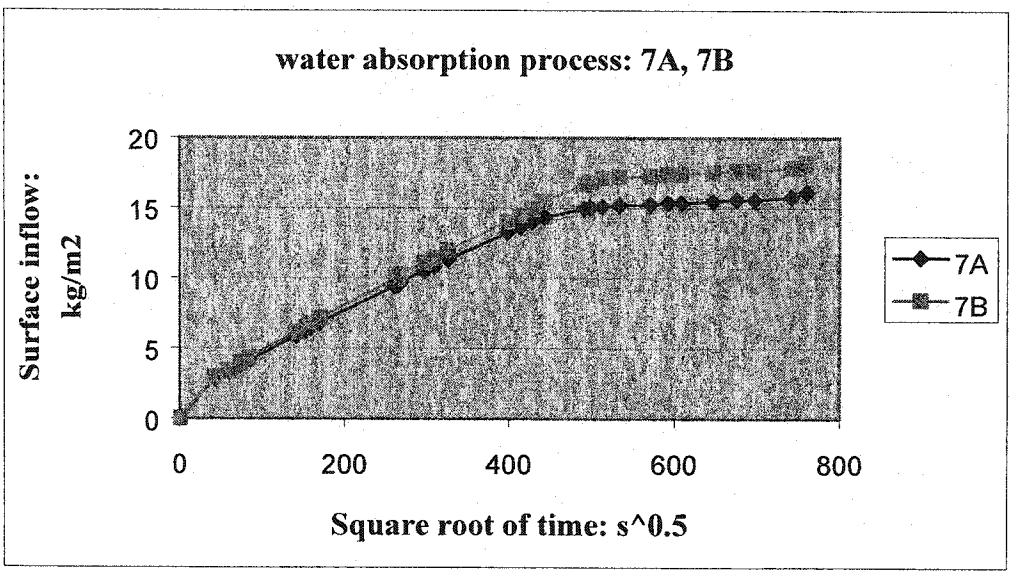

Figure A-13. Water absorption process of 7A, 7B in the first series

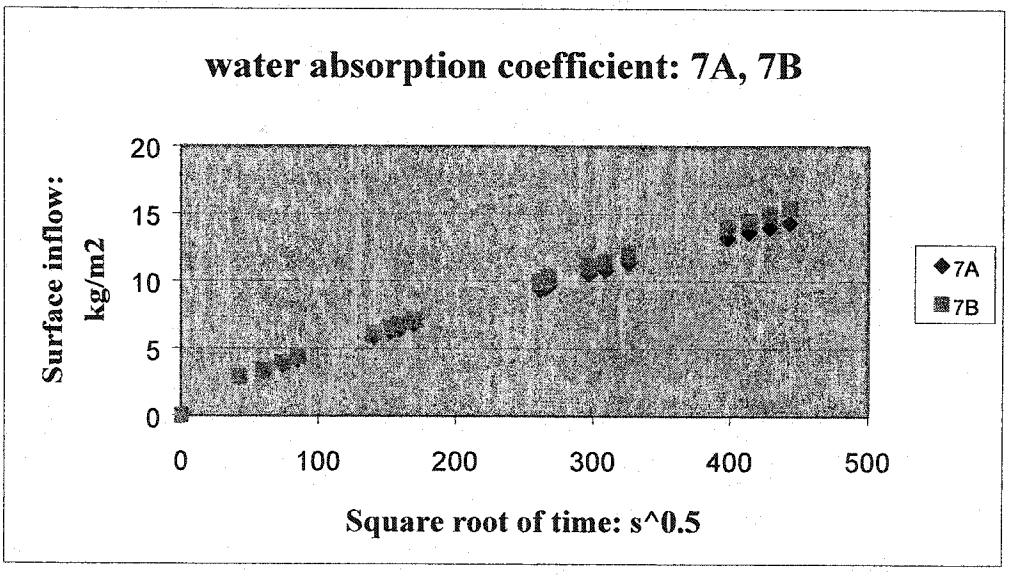

Figure A-14. Water absorption coefficient of 7A, 7B in the first series

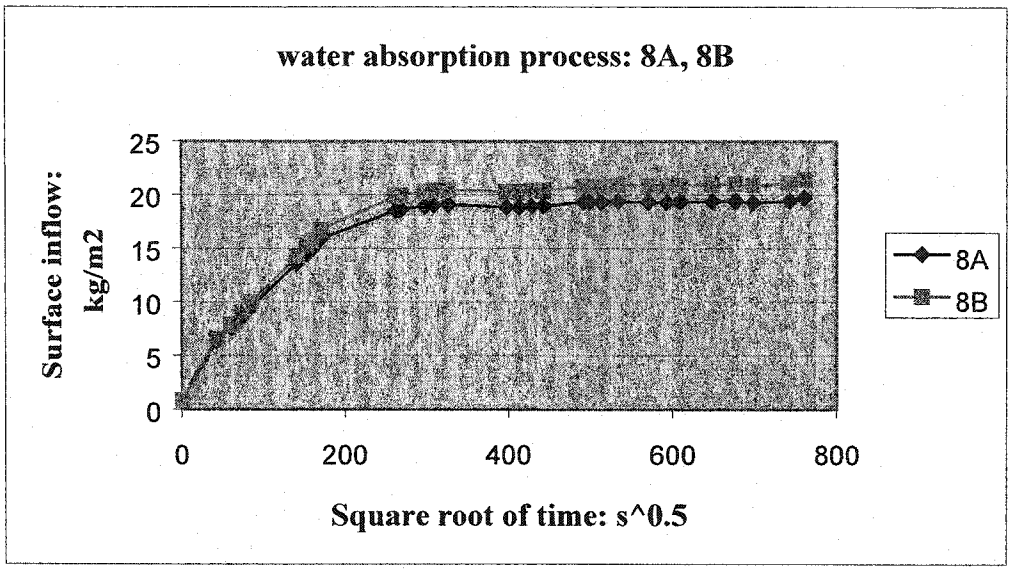

Figure A-15. Water absorption process of 8A, 8B in the first series

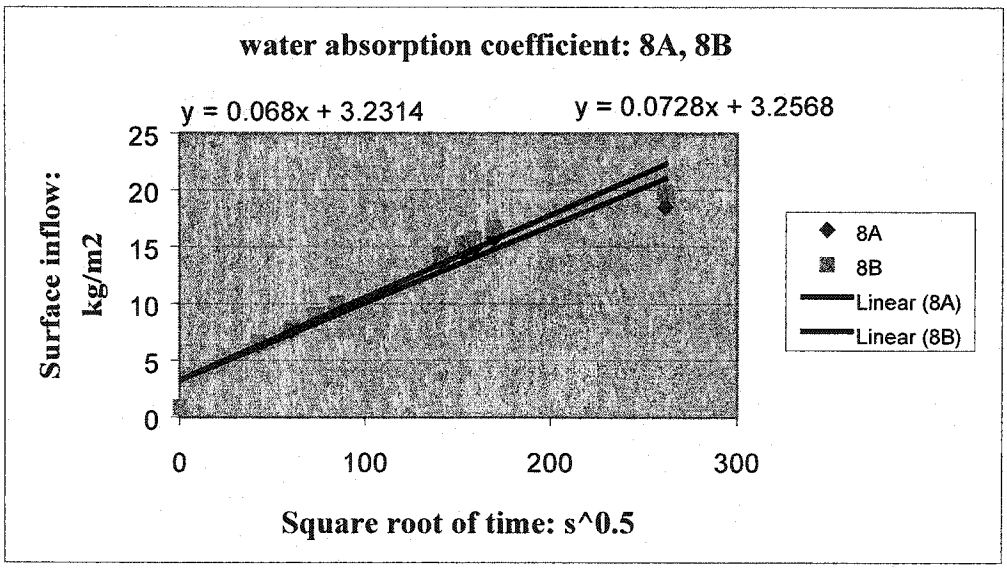

Figure A-16. Water absorption coefficient of 8A, 8B in the first series

Given below is the timely record of temperature and relative humidity during the whole process of measurement for the first series of ruggedness study.

Table A-1. Timely record of temperature and relative humidity

Time: hr	**RH: %**	**T: C**
0	27%	20.80
0.5	26%	21.00
1	24%	21.50
1.5	25%	21.20
2	24%	21.40
5.5	26%	20.80
6.5	24%	21.60
7	26%	21.70
8	25%	21.20
19	22%	21.80
19.5	22%	21.90
20	22%	22.10
24.5	22%	22.10
26.5	22%	22.30
29.5	22%	22.30
44	25%	22.10
47.5	27%	22.30
51	27%	22.40
54.5	24%	22.10
67	22%	22.00
69	22%	22.10
73	25%	22.10
79	26%	21.90
90.5	24%	21.60
97.5	27%	21.60
103	22%	21.00
116.5	28%	23.10
127	27%	23.00
135	23%	23.40
153	25%	23.50
160.5	24%	22.50
Average	**24%**	**21.95**

APPENDIX B

Detailed Results of Ruggedness Study on Water Absorption Coefficient of AAC: the second series

Graphic presentations of water intake process for all the specimens in the first series of test are given below:

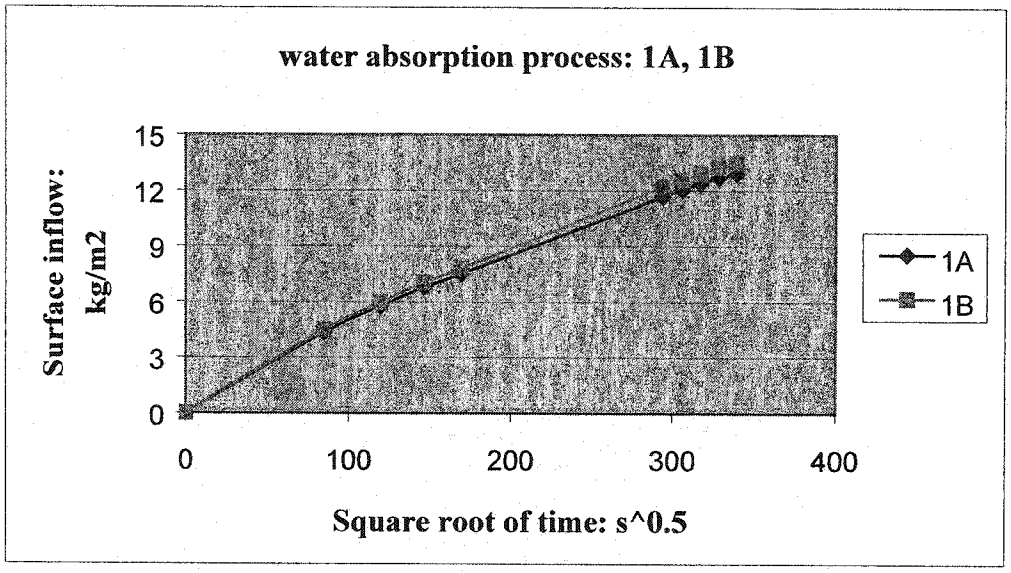

Figure B-1. Water absorption process of 1A, 1B in the second series

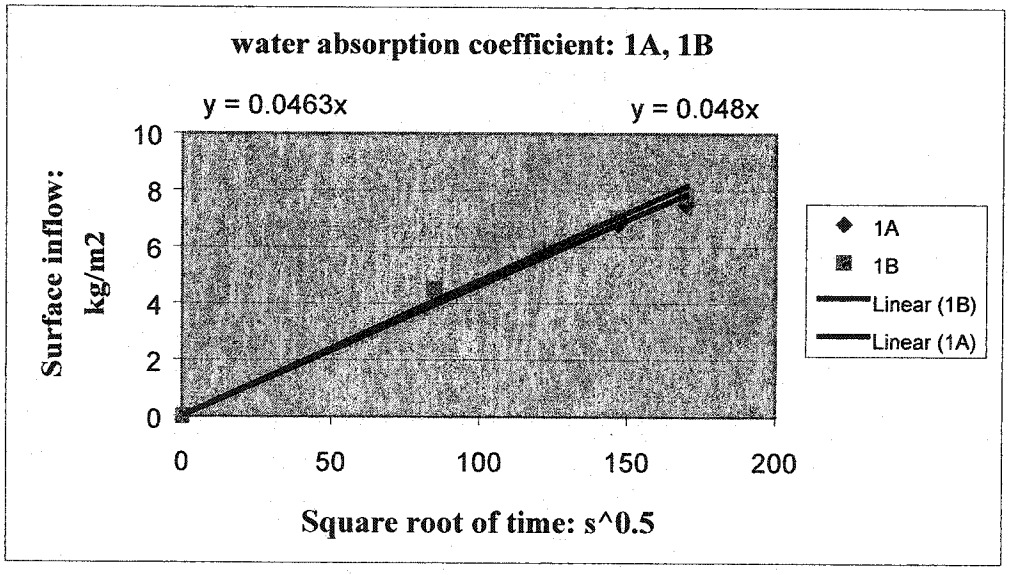

Figure B-2. Water absorption coefficient of 1A, 1B in the second series

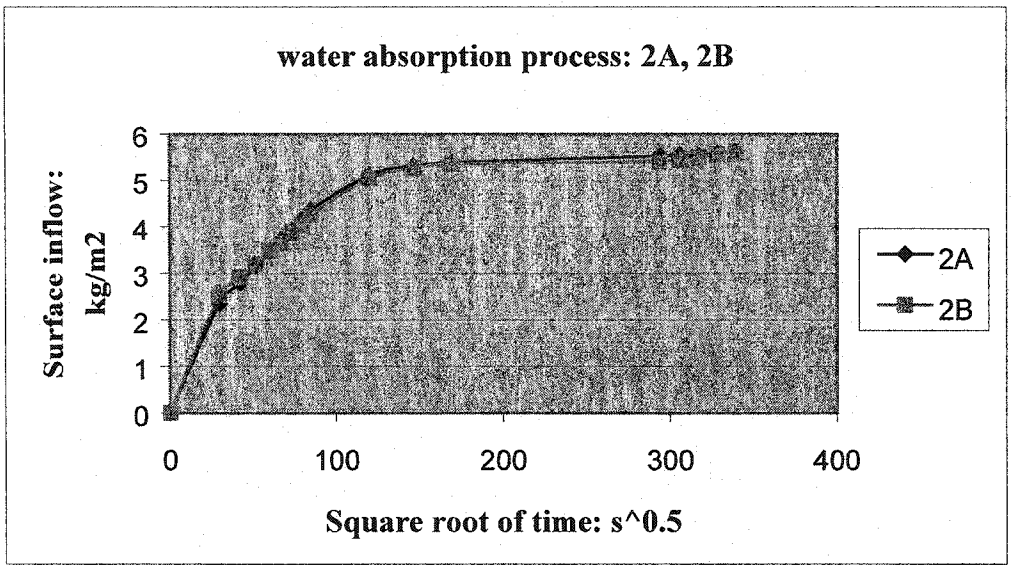

Figure B-3. Water absorption process of 2A, 2B in the second series

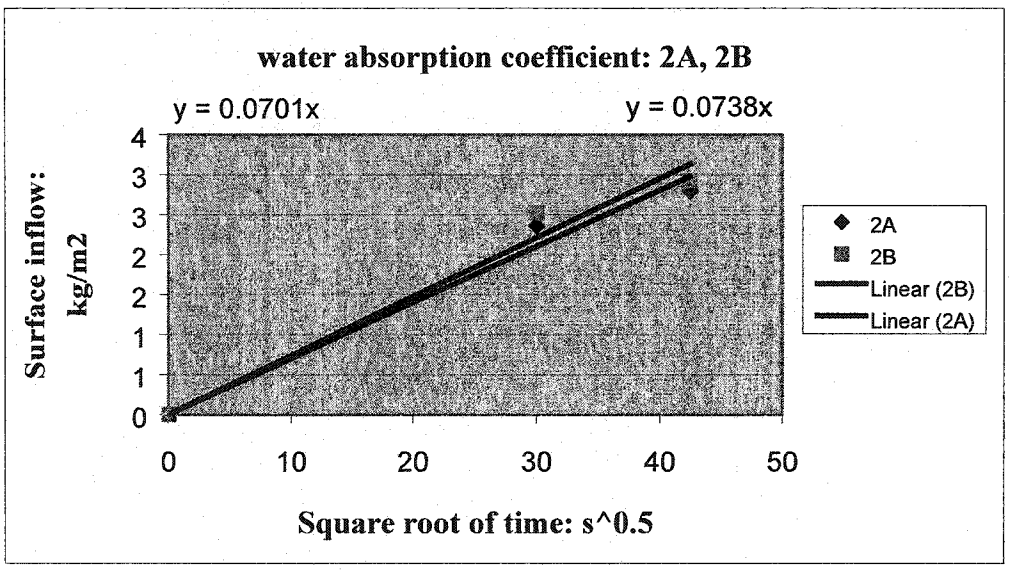

Figure B-4. Water absorption coefficient of 2A, 2B in the second series

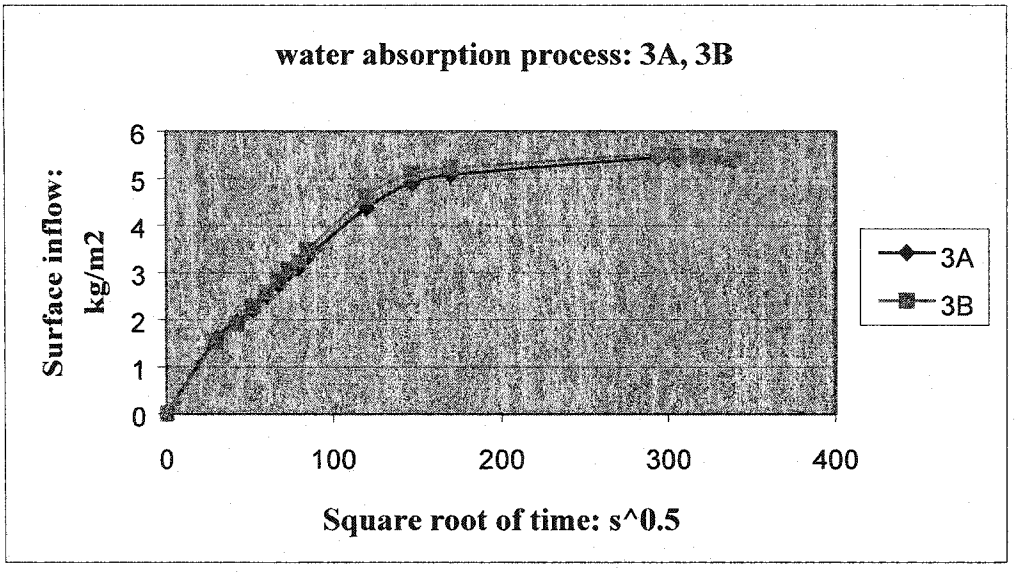

Figure B-5. Water absorption process of 3A, 3B in the second series

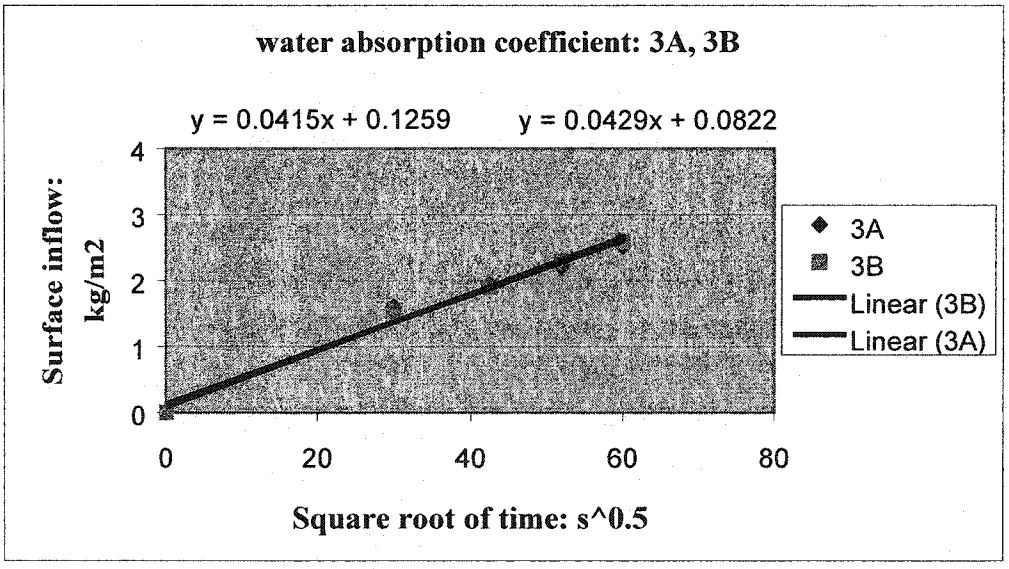

Figure B-6. Water absorption coefficient of 3A, 3B in the second series

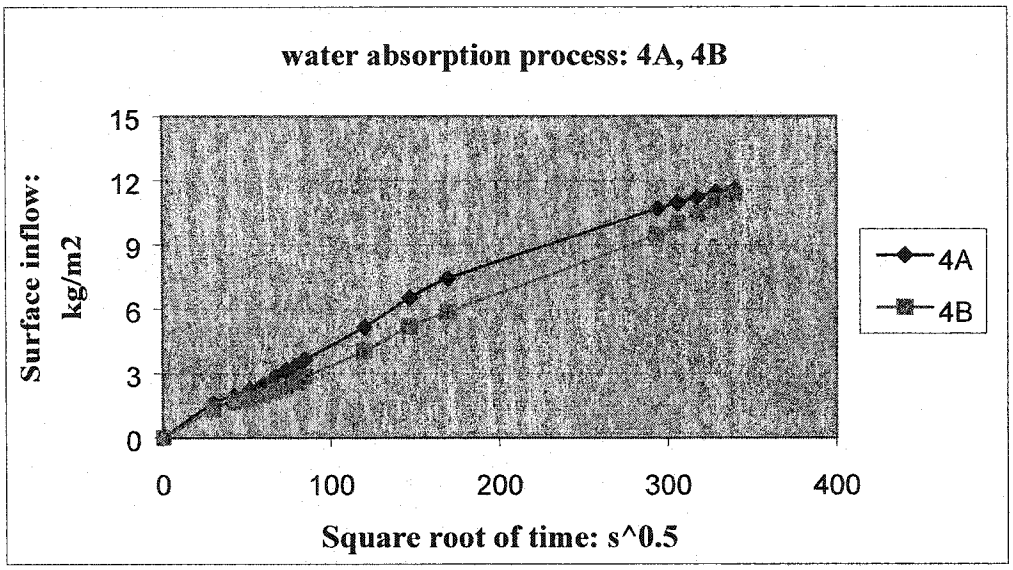

Figure B-7. Water absorption process of 4A, 4B in the second series

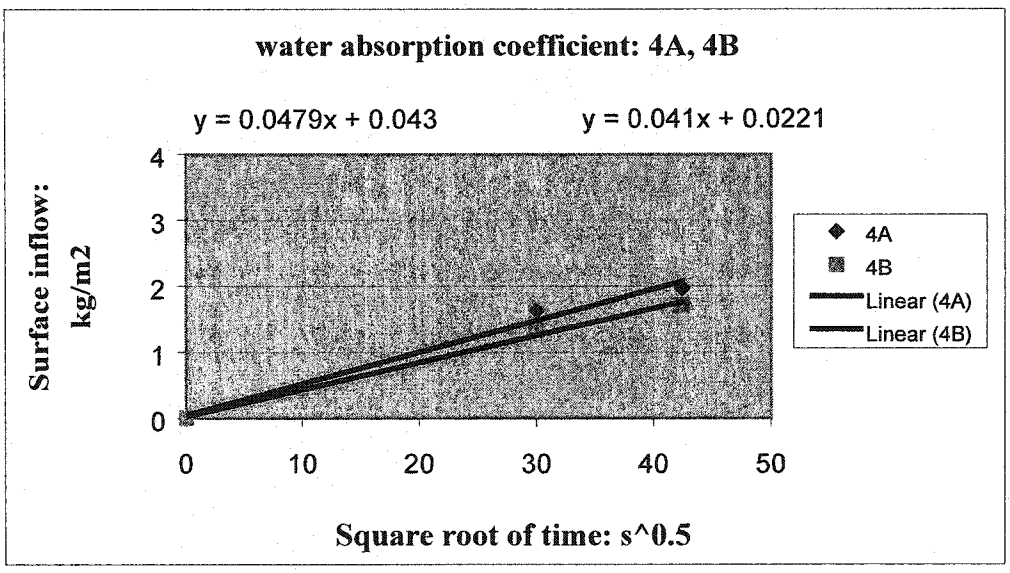

Figure B-8. Water absorption coefficient of 4A, 4B in the second series

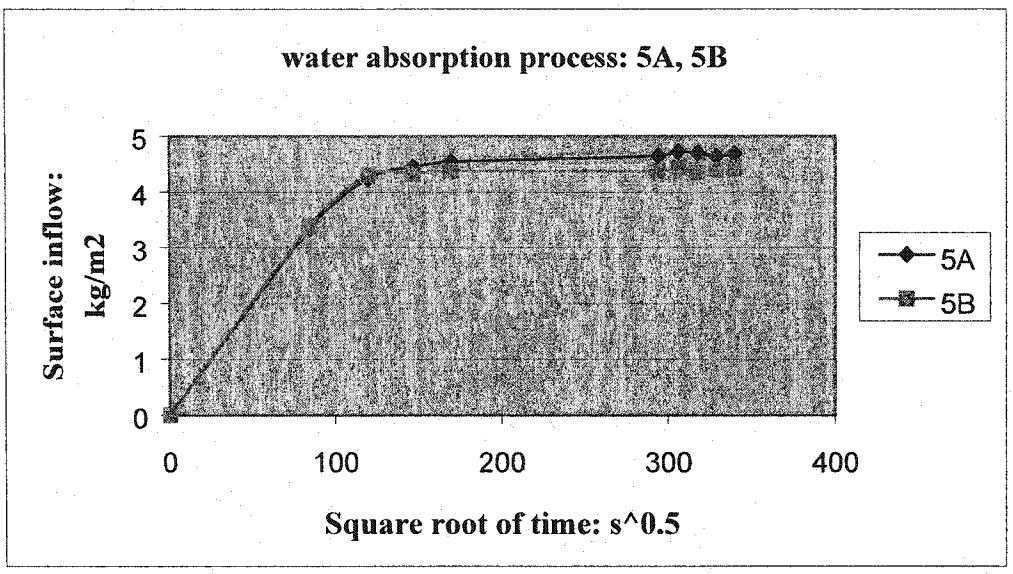

Figure B-9. Water absorption process of 5A, 5B in the second series

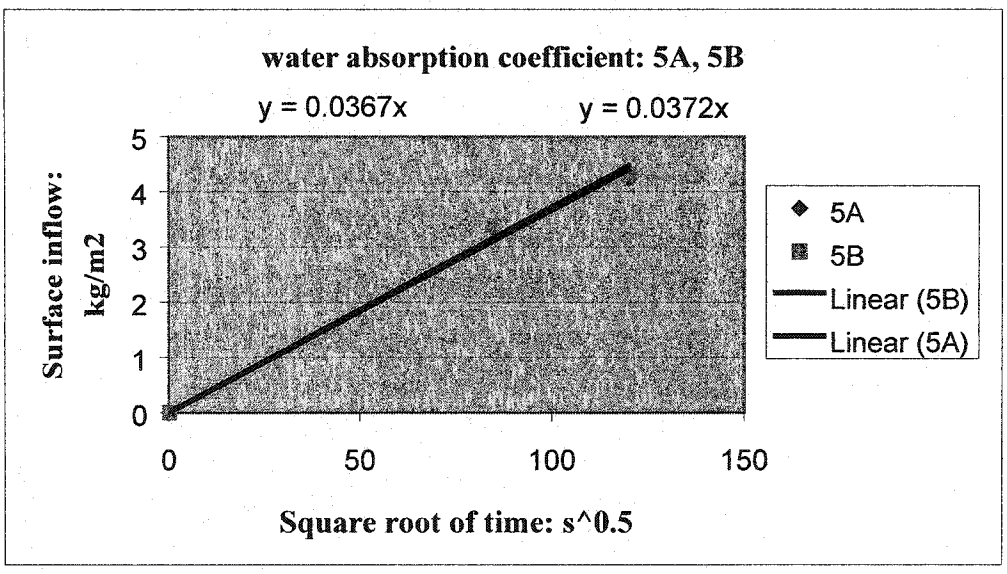

Figure B-10. Water absorption coefficient of 5A, 5B in the second series

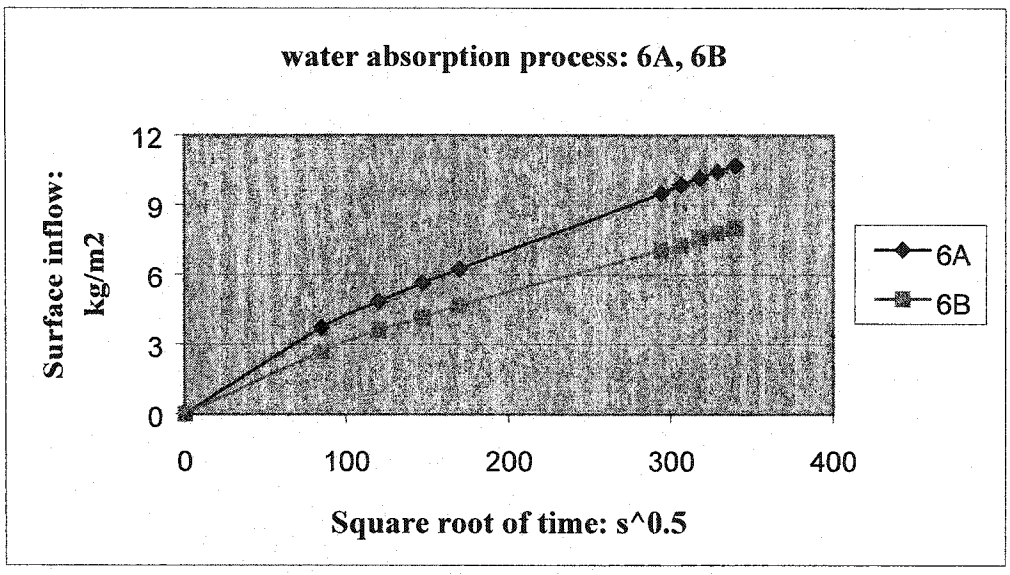

Figure B-11. Water absorption process of 6A, 6B in the second series

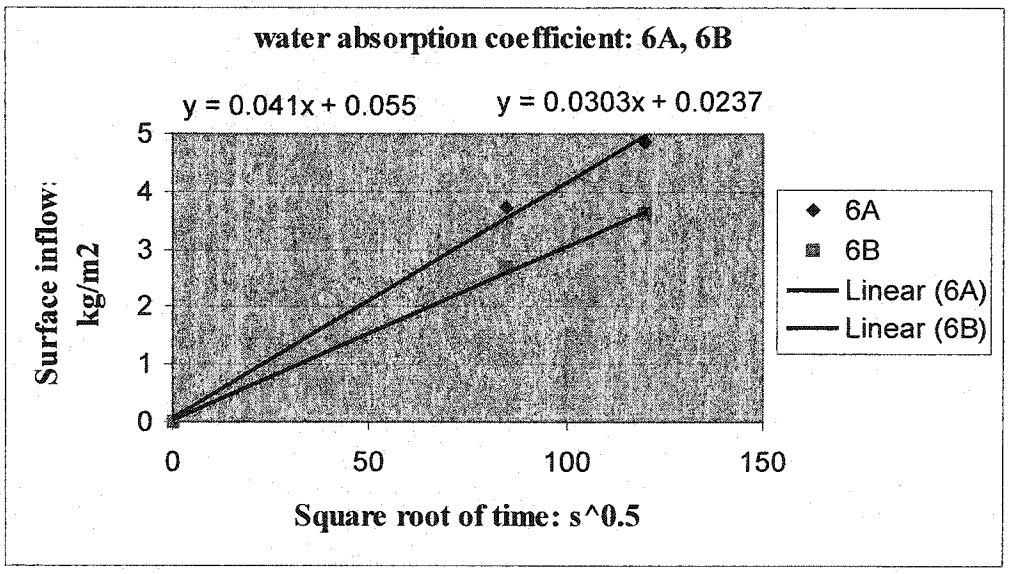

Figure B-12. Water absorption coefficient of 6A, 6B in the second series

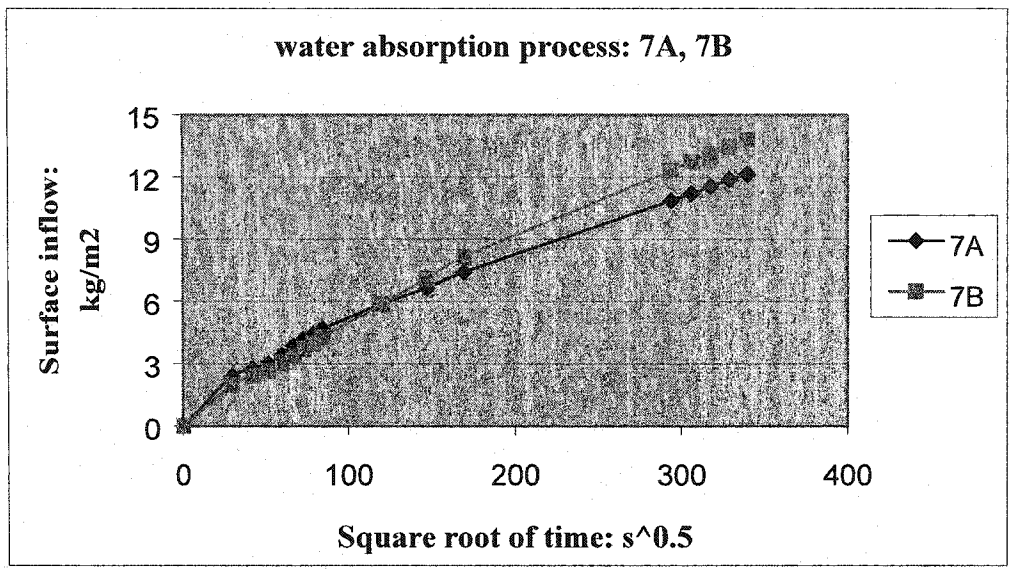

Figure B-13. Water absorption process of 7A, 7B in the second series

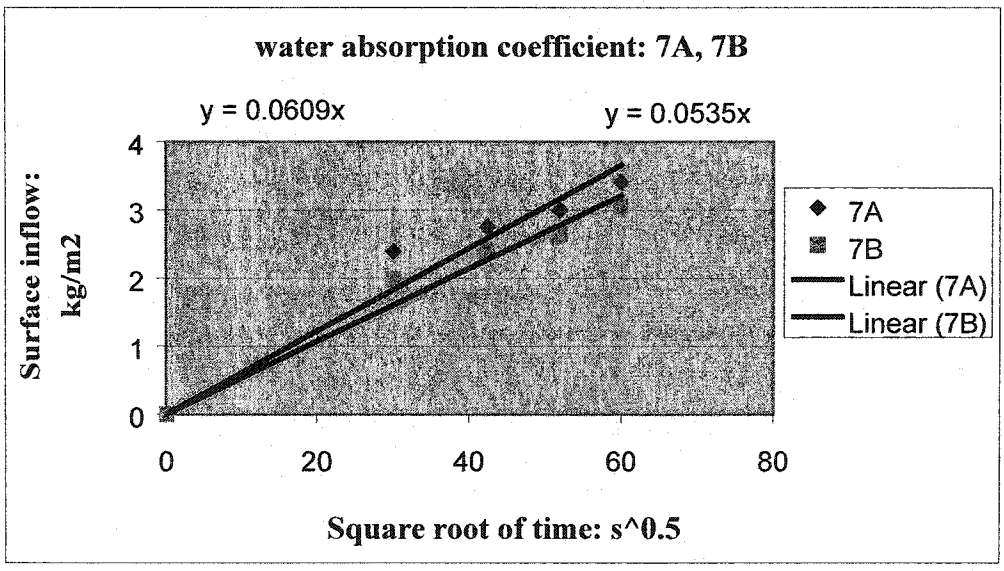

Figure B-14. Water absorption coefficient of 7A, 7B in the second series

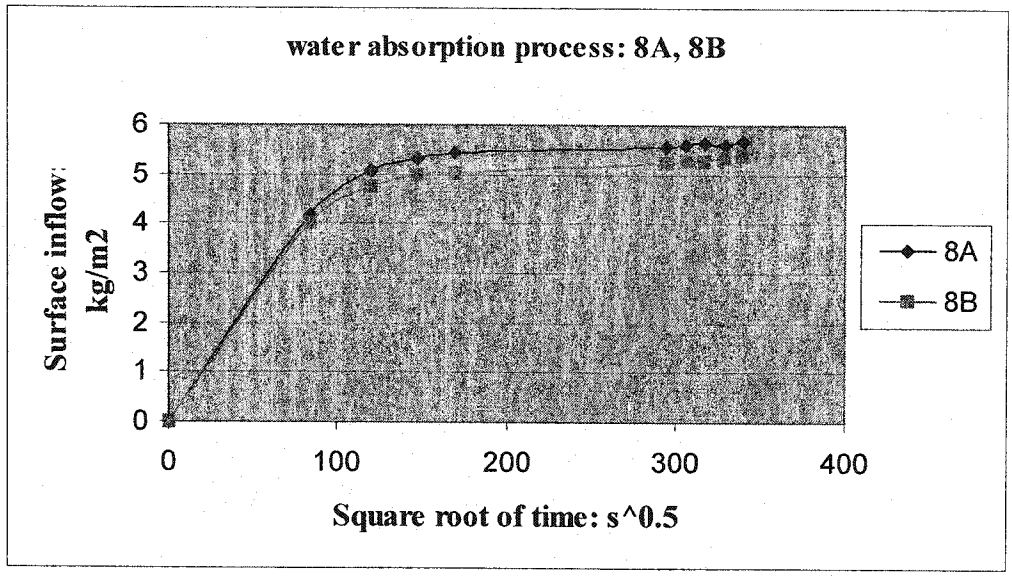

Figure B-15. Water absorption process of 8A, 8B in the second series

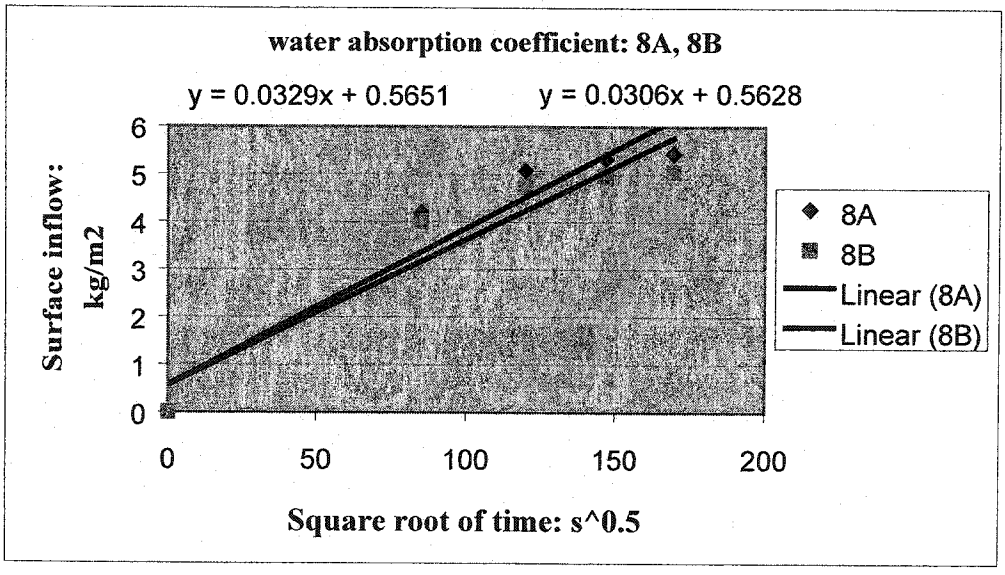

Figure B-16. Water absorption coefficient of 8A, 8B in the second series

Given below is the timely record of temperature and relative humidity during the whole process of measurement for the second series of ruggedness study.

Table B-1. Timely record of temperature and relative humidity

Time: hr	**RH: %**	**T: C**
0	11%	21.40
0.5	11%	21.50
2.5	10%	21.70
4.5	11%	21.20
8.5	10%	21.80
9.5	10%	22.00
24	9%	21.20
24.5	9%	21.30
25	9%	21.40
25.5	9%	21.40
28.5	9%	22.50
34	10%	22.60
36	10%	22.50
48	11%	21.70
50.5	12%	21.60
56	13%	22.10
61	12%	22.00
71.5	11%	21.10
80.5	12%	22.60
85	12%	22.50
96	12%	22.00
103.5	12%	22.20
119	13%	22.70
122.5	13%	22.10
142.5	17%	22.20
151.5	18%	23.10
166	14%	23.00
169.5	14%	23.10
174	14%	23.00
Average	**12%**	**22.05**

APPENDIX C

Measurement of AAC Drying Curve

Graphic presentations of AAC drying curve measured in three different environmental conditions are given below:

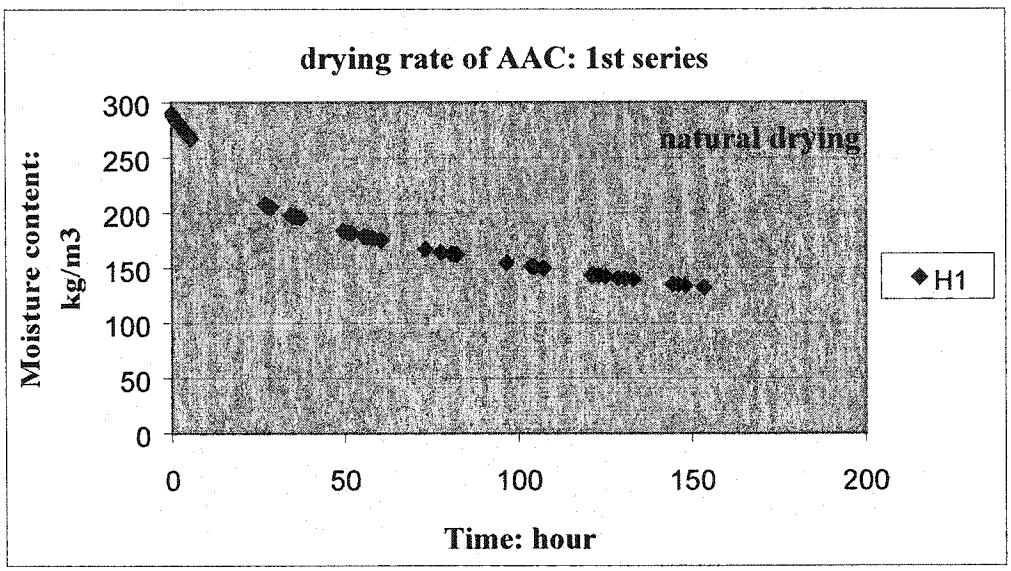

Figure C-1. Drying of AAC in the natural environment: specimen H1

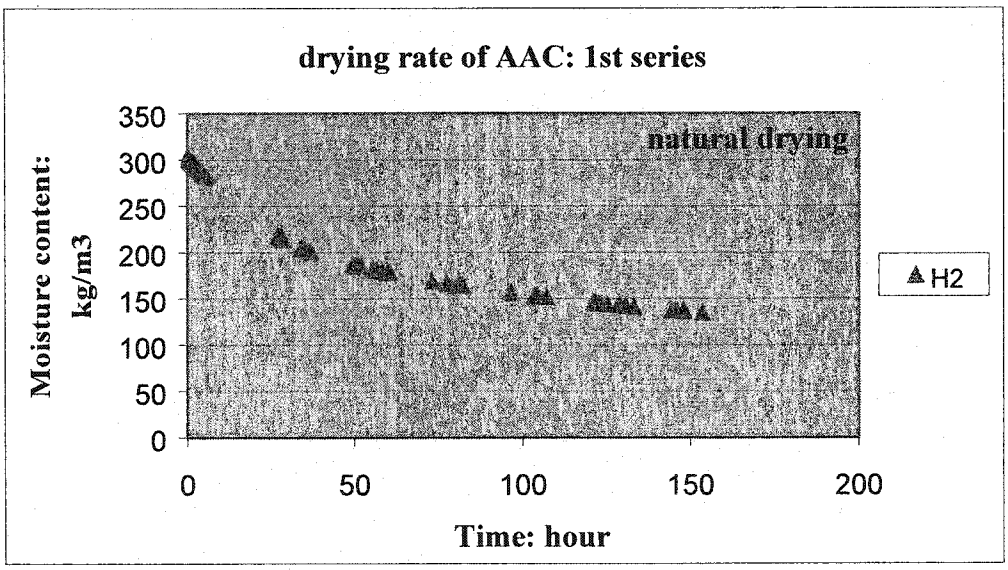

Figure C-2. Drying of AAC in the natural environment: specimen H2

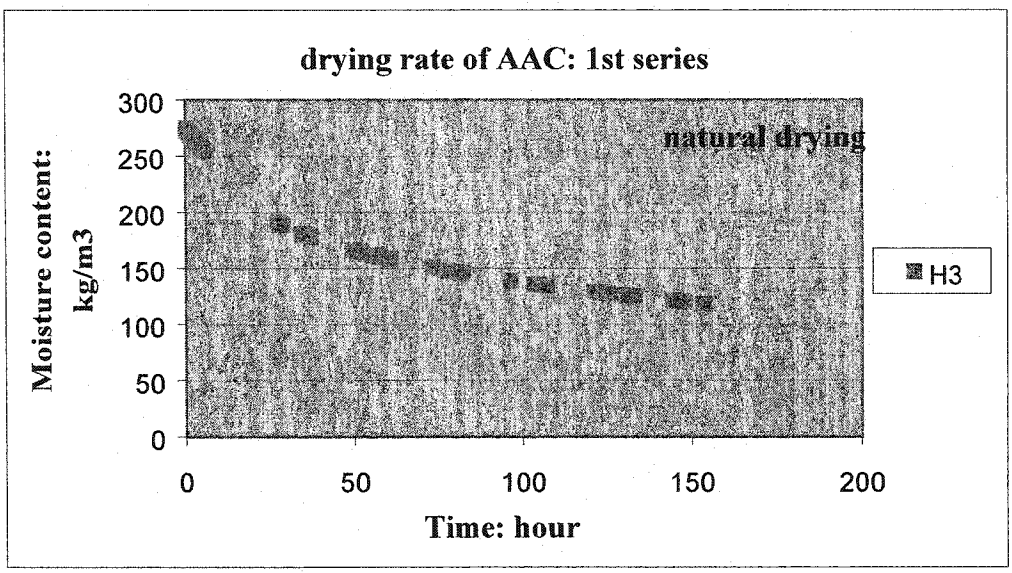

Figure C-3. Drying of AAC in the natural environment: specimen H3

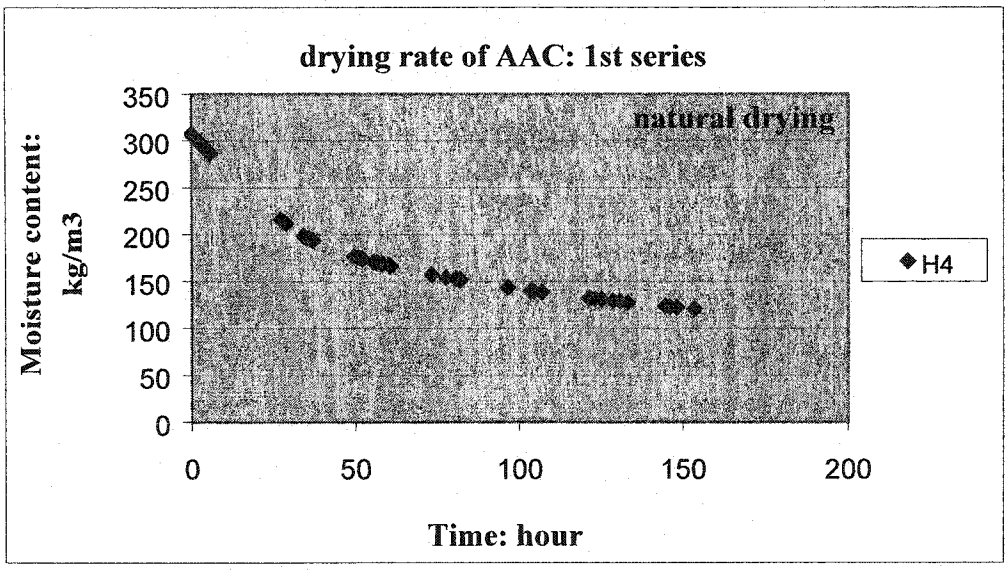

Figure C-4. Drying of AAC in the natural environment: specimen H4

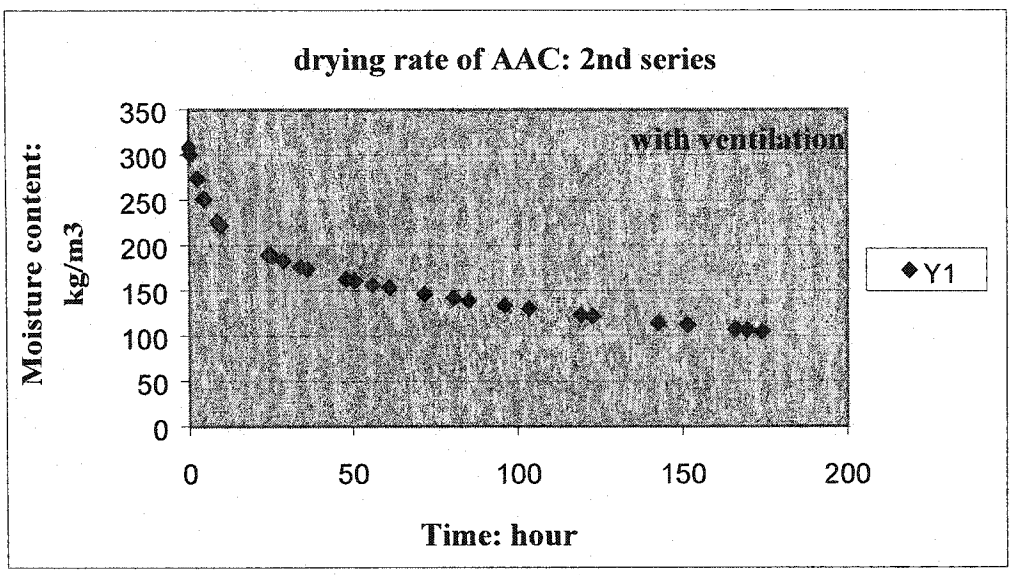

Figure C-5. Drying of AAC with mechanical ventilation: specimen Y1

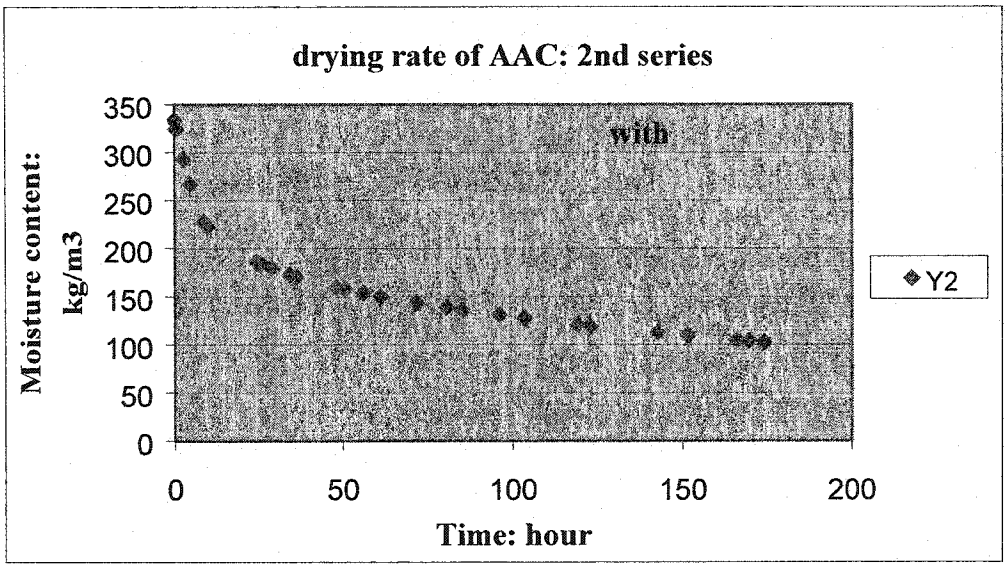

Figure C-6. Drying of AAC with mechanical ventilation: specimen Y2

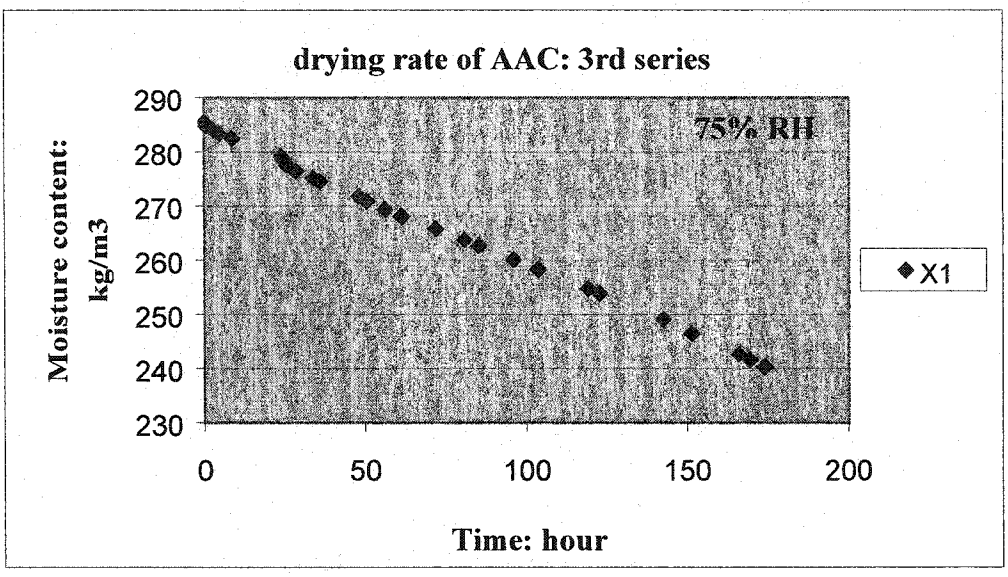

Figure C-7. Drying of AAC in a desiccator with 75%RH: specimen X1

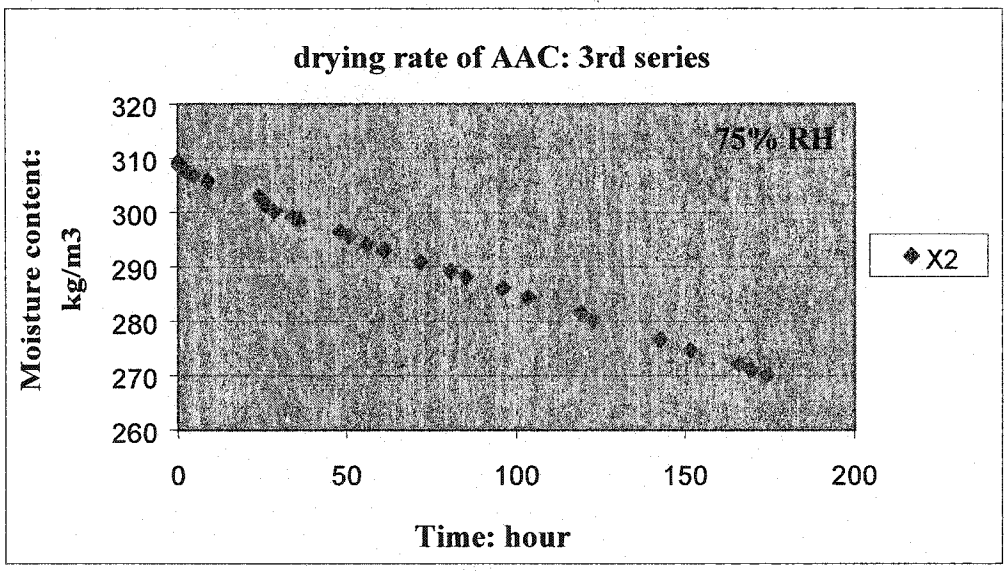

Figure C-8. Drying of AAC in a desiccator with 75%RH: specimen X2

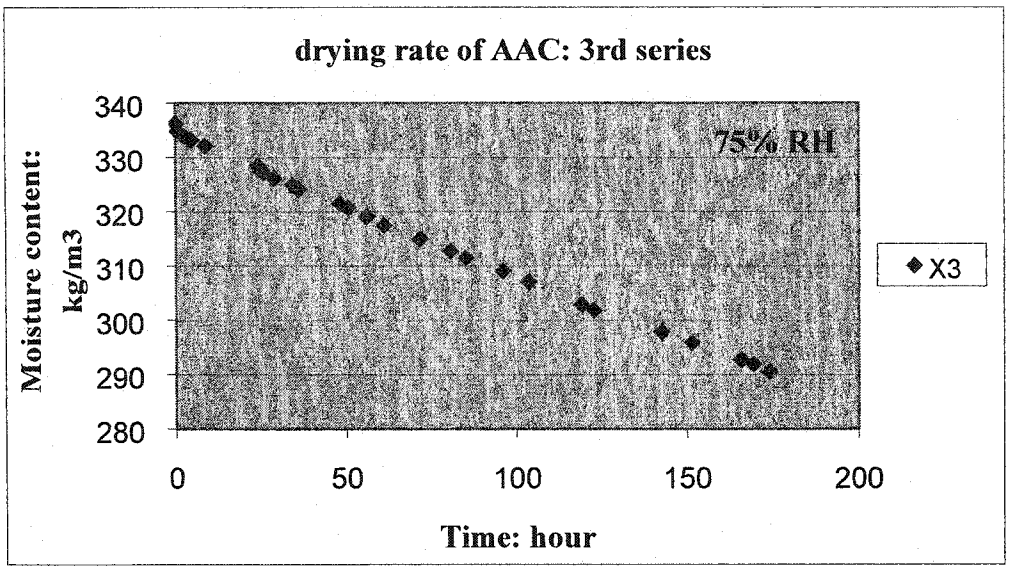

Figure C-9. Drying of AAC in a desiccator with 75%RH: specimen X3

Note

The three series of drying curves were measured in different environment. For the first series, specimens were exposed to a laboratory environment, drying naturally. For the second series, mechanical ventilation was applied: an electronic fan was kept operating, providing airflow above the unsealed surface of the specimens. For the third series, specimens were put in desiccator, in which relative humidity was controlled to be 75% by providing over-saturated salt solution.

Timely record of temperature and relative humidity for each series are given below:

Table C-1. Timely record of temperature and relative humidity for the first series: natural drying

Time: hr	**RH: %**	**T: C**	56.5	12%	22.00
0	11%	22.10	58	12%	22.10
0.5	11%	22.40	60	12%	21.90
1	11%	22.30	60.5	12%	22.00
1.5	11%	22.30	73	12%	22.00
2	12%	22.30	77.5	12%	22.30
2.5	11%	22.40	80.5	12%	22.50
3	11%	22.50	81.5	12%	22.40
3.5	11%	22.60	82	12%	22.40
4	12%	22.70	96.5	8.9%	20.80
4.5	13%	22.20	103.5	8.9%	21.40
5	11%	22.20	104	8.9%	21.40
5.5	12%	22.60	104.5	8.9%	21.40
27	11%	21.70	107	8.8%	21.30
27.5	12%	21.20	121	7.9%	20.40
28	11%	21.60	121.5	7.8%	20.40
28.5	10%	21.70	123	7.8%	20.40
34	10%	21.50	125	8.6%	20.60
34.5	11%	21.80	128.5	9.0%	20.90
35	10%	21.90	130.5	8.6%	21.10
36	10%	22.00	133	8.9%	21.20
37	10%	21.90	144.5	8.4%	20.60
49.5	10%	21.90	146	8.4%	20.70
51	10%	22.00	148	9.0%	20.60
52	11%	22.00	153.5	9.2%	21.30
55.5	11%	22.00	**Average**	**10.36%**	**21.72**

Table C-2. Timely record of temperature and relative humidity for the second series: drying with mechanical ventilation

Time: hr	RH: %	T: C	56	12.7%	22.1
0	10.6%	21.4	61	12.1%	22.0
0.5	10.8%	21.5	71.5	11.4%	21.1
2.5	10.2%	21.7	80.5	11.6%	22.6
4.5	10.6%	21.2	85	11.8%	22.5
8.5	9.8%	21.8	96	12.0%	22.0
24	9.3%	21.2	103.5	12.4%	22.2
24.5	9.4%	21.3	119	12.9%	22.7
25	9.4%	21.4	122.5	13.2%	22.1
25.5	9.2%	21.4	142.5	16.9%	22.2
28.5	9.0%	22.5	151.5	18.2%	23.1
34	9.9%	22.6	166	14.0%	23.0
36	10.1%	22.5	169.5	13.6%	23.1
48	10.8%	21.7	174	13.7%	23.0
50.5	11.7%	21.6	**Average**	**11.69%**	**22.05**

Table C-3. Timely record of temperature and relative humidity for the third series: drying in a desiccator with salt solution

Time: hr	RH: %	T: C	Time: hr	RH: %	T: C
0	75%	21.4	56	72%	22.1
0.5	74%	21.5	61	76%	22
2.5	72%	21.7	71.5	71%	21.1
4.5	74%	21.2	80.5	75%	22.6
8.5	70%	21.8	85	73%	22.5
9.5	75%	22	96	72%	22
24	74%	21.2	103.5	74%	22.2
24.5	72%	21.3	119	72%	22.7
25	73%	21.4	122.5	74%	22.1
25.5	71%	21.4	142.5	72%	22.2
28.5	72%	22.5	151.5	75%	23.1
34	74%	22.6	166	73%	23
36	70%	22.5	169.5	74%	23.1
48	72%	21.7	174	75%	23
50.5	74%	21.6	**Average**	**73.10%**	**22.05**